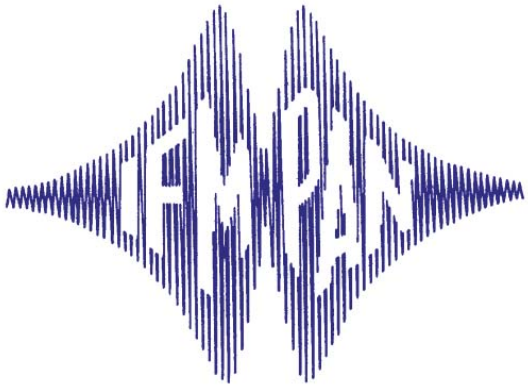

Helium: properties, liquefaction

Zbigniew Trybuła

Institute of Molecular Physics, Polish Academy of Sciences, Poznań, Poland

Division of Low Temperature Physics in Odolanów

1. Introduction.
2. Helium 4.
3. Helium 3.


INSTYTUT FIZYKI MOLEKULARNEJ PAN
Poznań
Warszawa
Ostrów Wlkp.
Odolanów

Odolanów

small town in Wielkopolska (80 km from Wroclaw) is a special place in Europe where by the use of the cryogenic method, liquid helium is obtained from the natural gas on the industrial scale.

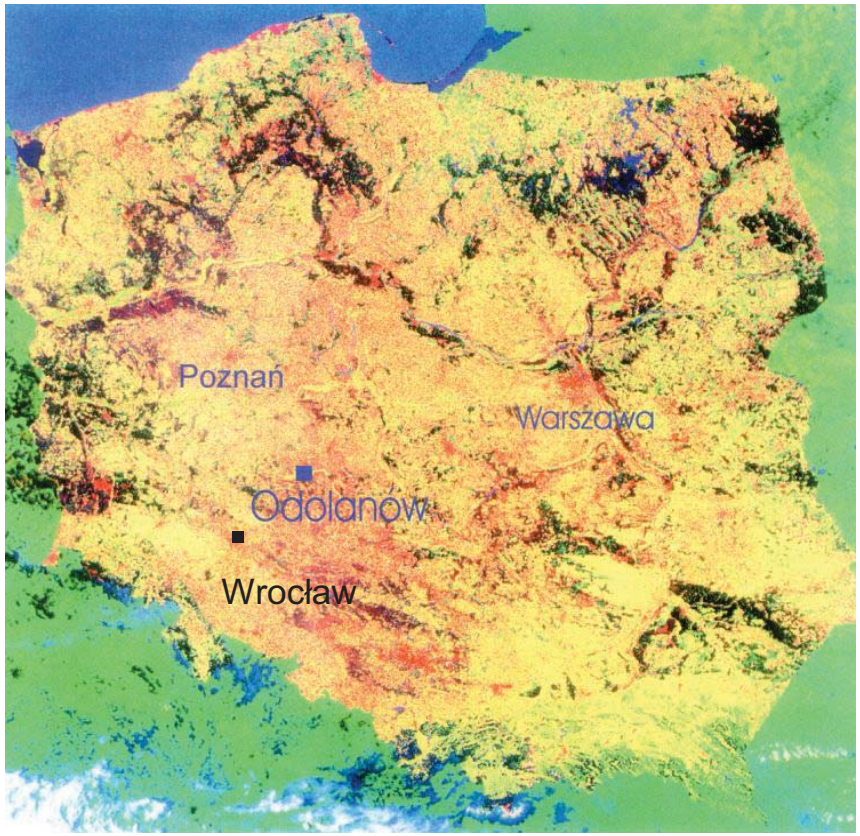

In 1977 Prof. Jan Stankowski developed in Odolanów the Division of Low Temperature Physics of the Institute of Molecular Physics Polish Academy of Sciences in Poznań, which has been using liquid helium to the low temperature scientific research up till now.

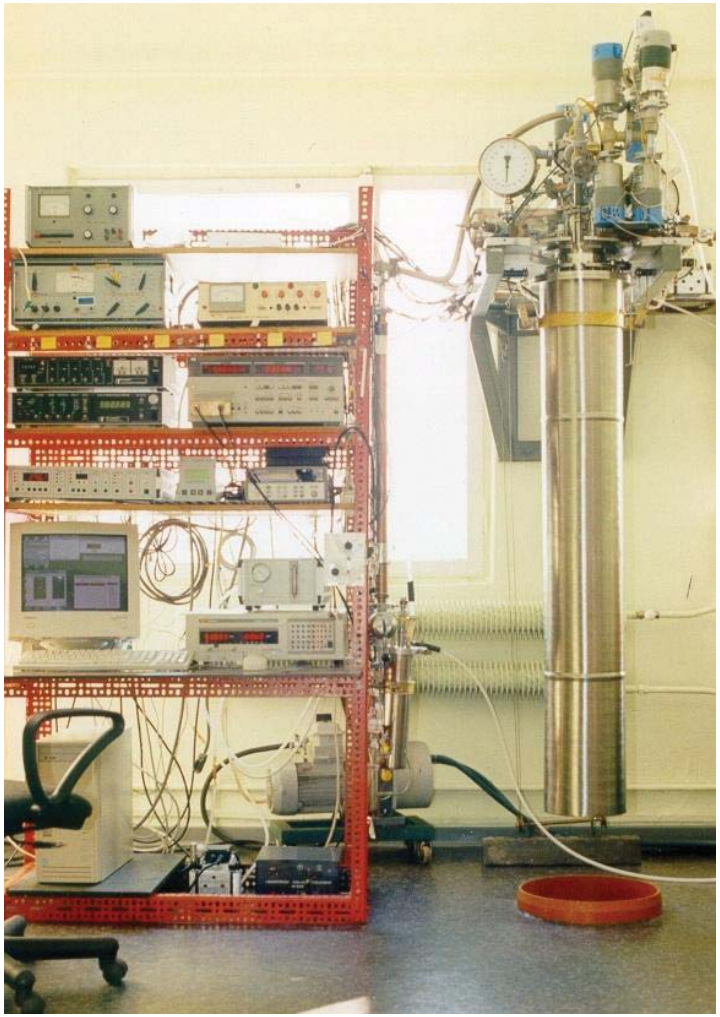

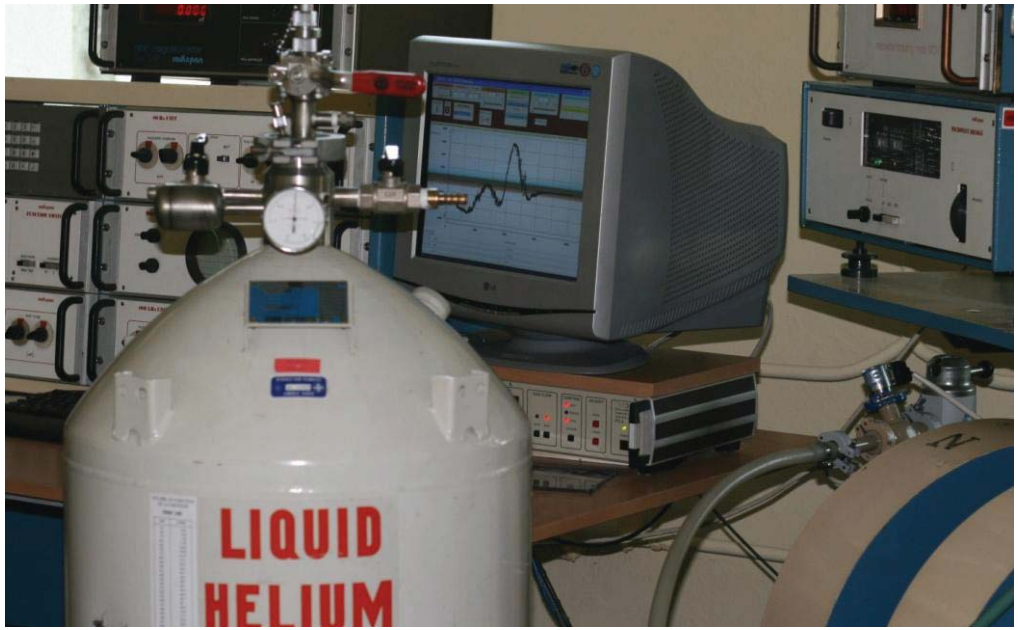

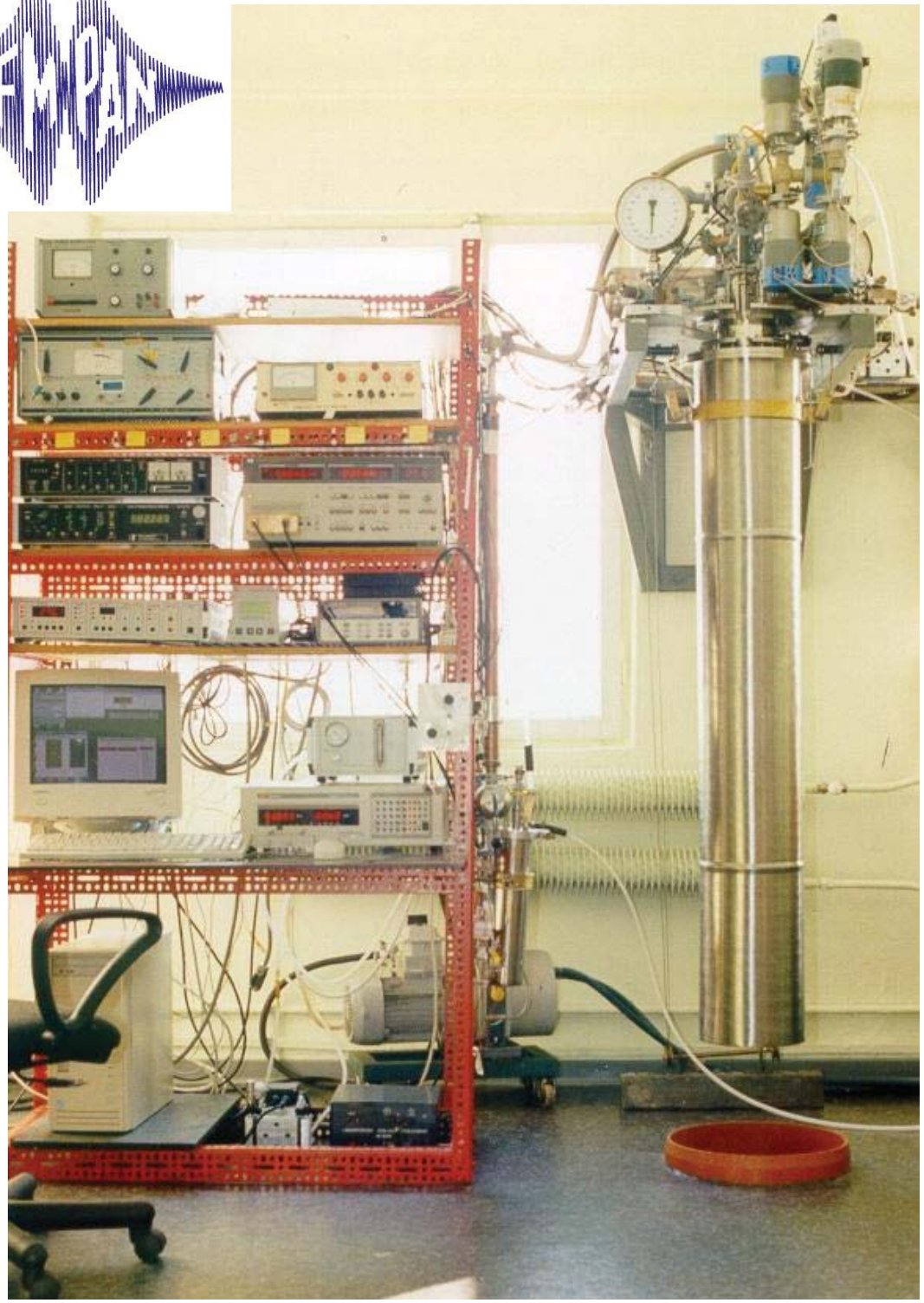

Equipment with helium 3 cryostat to transport properties, electric permittivity and magnetic susceptibility measurements in the temperature range 300 K to 0.3 K.

Division of Low Temperature Physics in Odolanów.

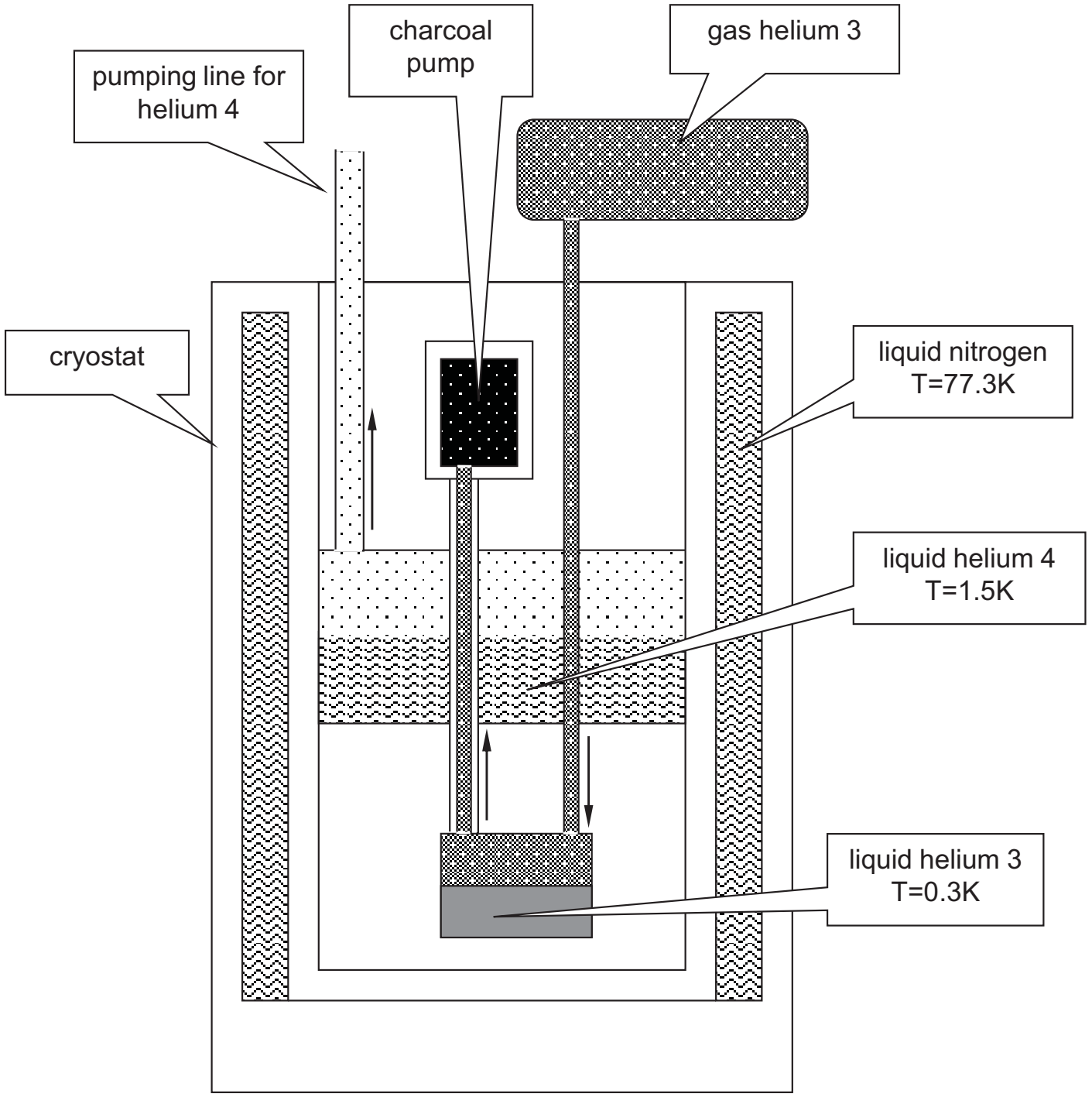
charcoal pump
gas helium 3
pumping line for helium 4
cryostat
liquid nitrogen T=77.3K
liquid helium 4 T=1.5K
liquid helium 3 T=0.3K

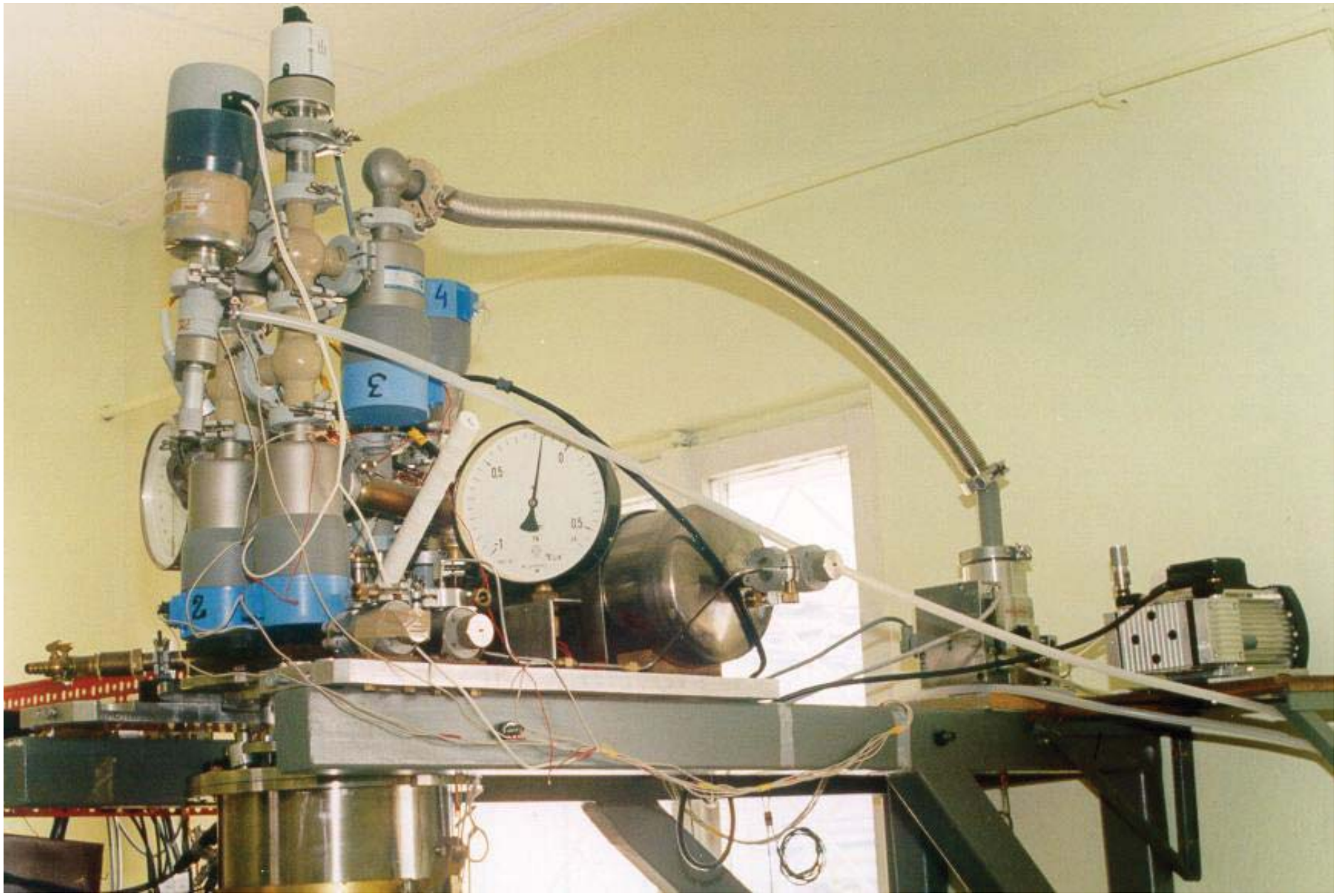
4
3
2

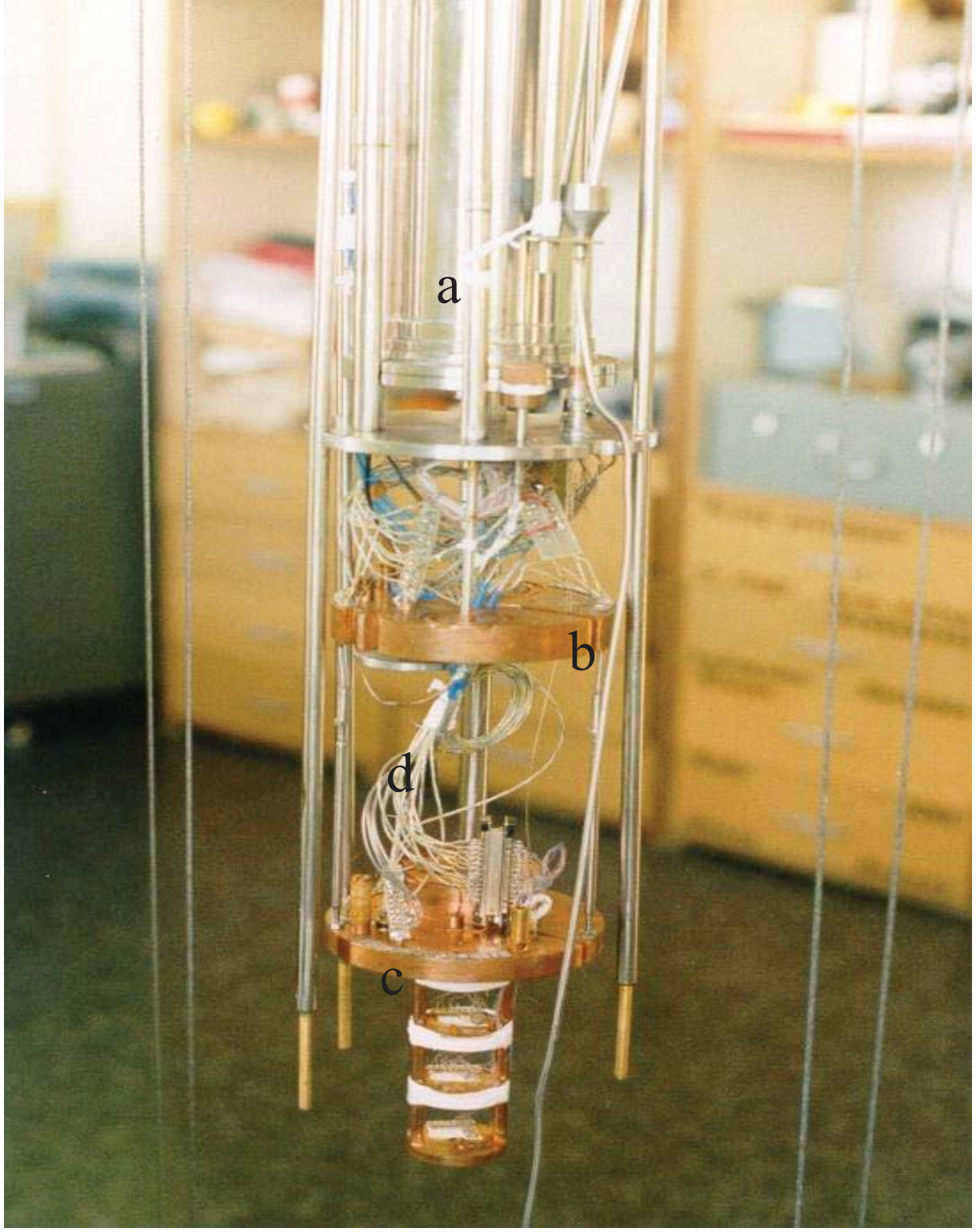

a) charcoal pump

b) 1.5K plate

c) 0.3K plate

d) NbTi superconducting wires (58)

1.5K plate

RuO_2 (2200-ohm ruthenium oxide resistance thermometer)

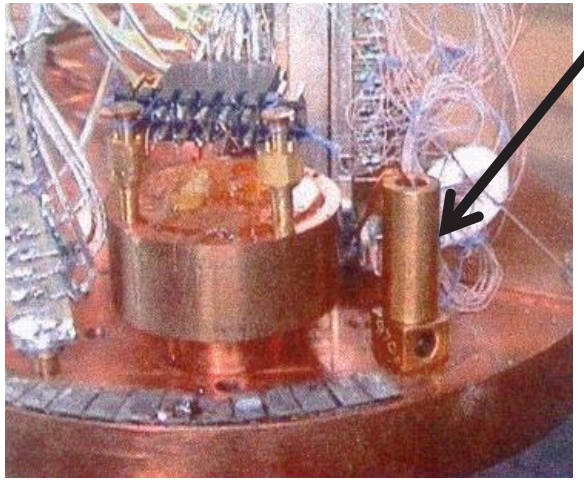

$T(R)=exp[a\ ln(R-R_o)+b]$

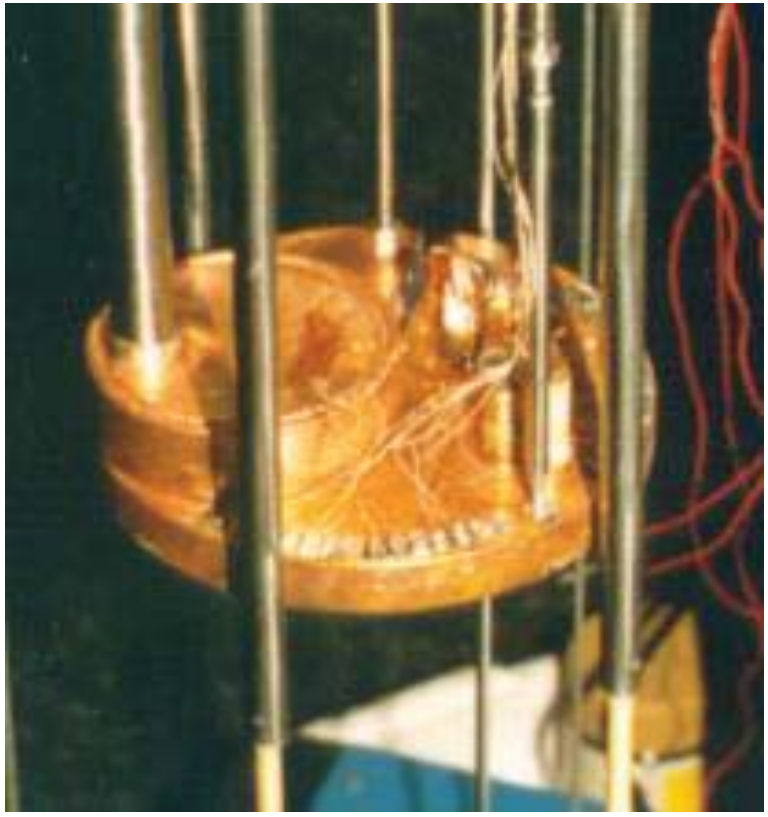

0.3K plate

Low temperature
TS-530A

AVS-47 bridge

RV-Elektroniikka Oy PICOWATT
Finland

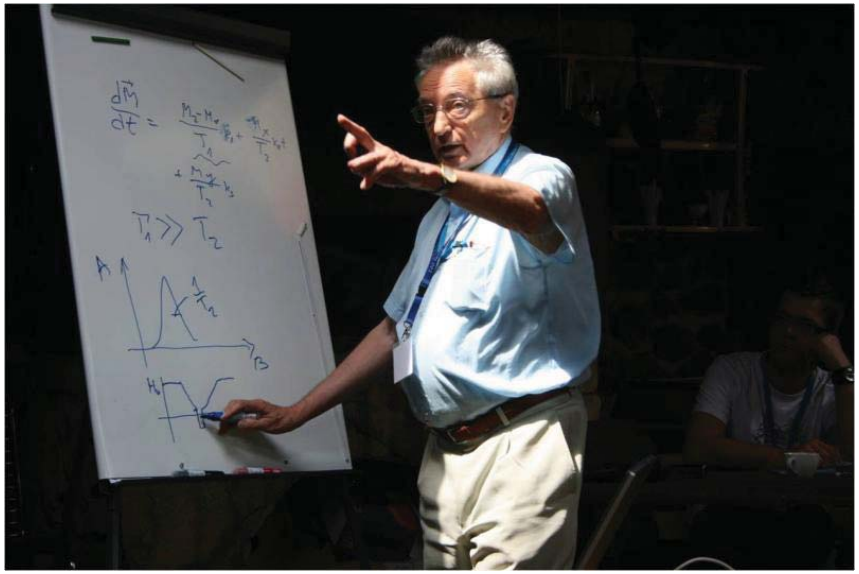

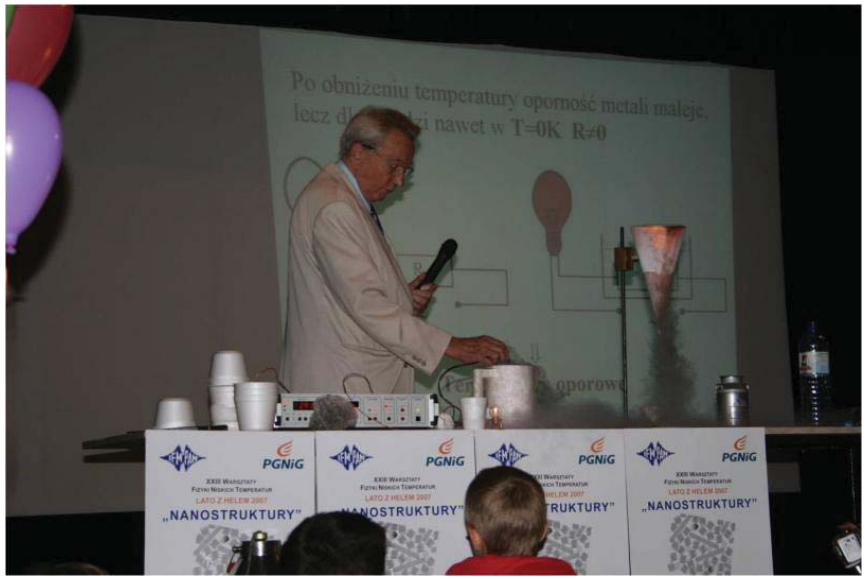

•Professor Stankowski was the initiator of annual academic workshops *"Lato z Helem – Summer with Helium"* organized by the Division of Low Temperature Physics in Odolanów.

•For the last 26 years these workshops gave high school students a unique chance to participate in experiments and lectures covering such topics as, e.g. the low temperature studies, cryogenics, and superconductor research, delivered by eminent Polish physicists.

.

XXIV Academic Workshops „Summer with Helium" 2008

CRYOGENICS

The branches of physics and engineering that involve the study of temperatures below 111 K, how to produce them, and how materials behave at those temperatures.

(T_b =111 K - temperatute of boiling point of methane - CH_4)

κρυοζ – cold

γενοζ – generate

Heike Kamerlingh-Onnes 1908

The Cryogenics Temperature Range

„low” - below 273.15K (0°C)

„very low” - around 100K

„deep low” - around 4K

„ultra low” - less than 0.3K

The French had only two terms:

„basse” and *„très basse”*

- Low-temperature physics has surpassed nature by several orders of magnitude, because the lowest temperature in nature and in the universe is 2.73 K.

- This background temperature exists everywhere in the universe because of the photon energy which is still being radiated from the “big bang”.

- Low-temperature physics is actually one of the very few branches of science where mankind has surpassed nature.

„An experimentalist wishing to pursue research at low temperatures faces four technical difficulties:

1. *how to reach the low temperature,*
2. *how to measure it,*
3. *how to reduce the external heat leak so that the low temperature can be maintained for a sufficiently long time,*
4. *how to transfer cold from one place to another.*

Many experimental methods have been developed to provide a satisfactory solution to these problems.”

O.V. Lounasmaa: *Experimental Principles and Methods Below 1 K*
(Academic, London 1974)

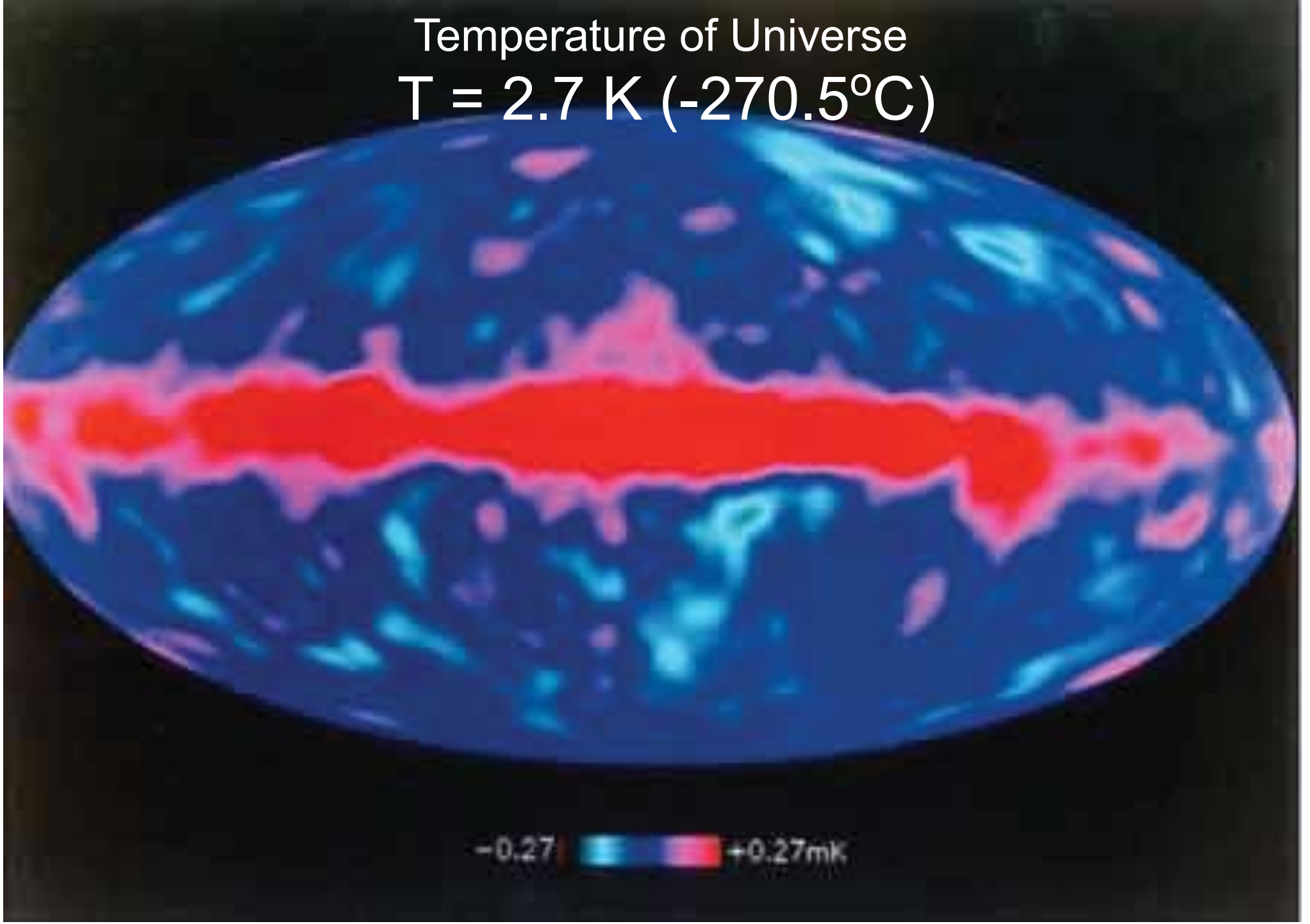
Temperature of Universe
T = 2.7 K (-270.5°C)
−0.27
+0.27mK

0°C = 273.15 K

LOGARITHMIC TEMPERATURE SCALE

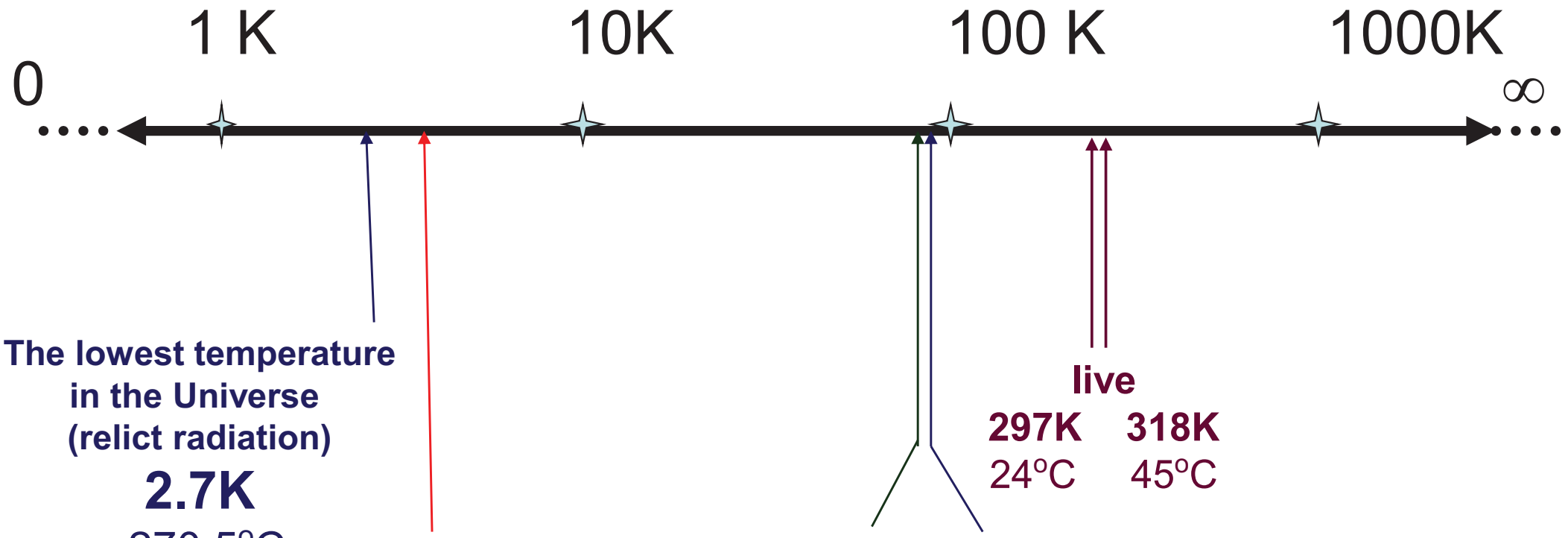

VOLUME 70, NUMBER 18 PHYSICAL REVIEW LETTERS 3 MAY 1993

Nuclear Antiferromagnetism in Rhodium Metal at Positive and Negative Nanokelvin Temperatures

P. J. Hakonen, R. T. Vuorinen, and J. E. Martikainen
Low Temperature Laboratory, Helsinki University of Technology, 02150 Espoo, Finland
(Received 1 February 1993)

We have measured the dynamic susceptibility of polycrystalline rhodium foils down to 280 pK and up to −750 pK. These record-low and -high nuclear spin temperatures were reached by adiabatic demagnetization using initial polarizations of 83% and −60%. At $T>0$, the static susceptibility, integrated from NMR spectra, displays an antiferromagnetic Curie-Weiss law, with $\theta=-1.8\pm0.3$ nK. At $T<0$, a crossover from ferro- to antiferromagnetic tendency is found around −6 nK. We obtain $J_{nn}/h=-17\pm3$ Hz and $J_{nnn}/h=10\pm3$ Hz if only nearest and next nearest neighbor interactions are assumed.

PACS numbers: 75.30.Kz, 75.90.+w

The record – low spin temperature

T= 280 pK (10^{-12} K) !

0,000000000028 K

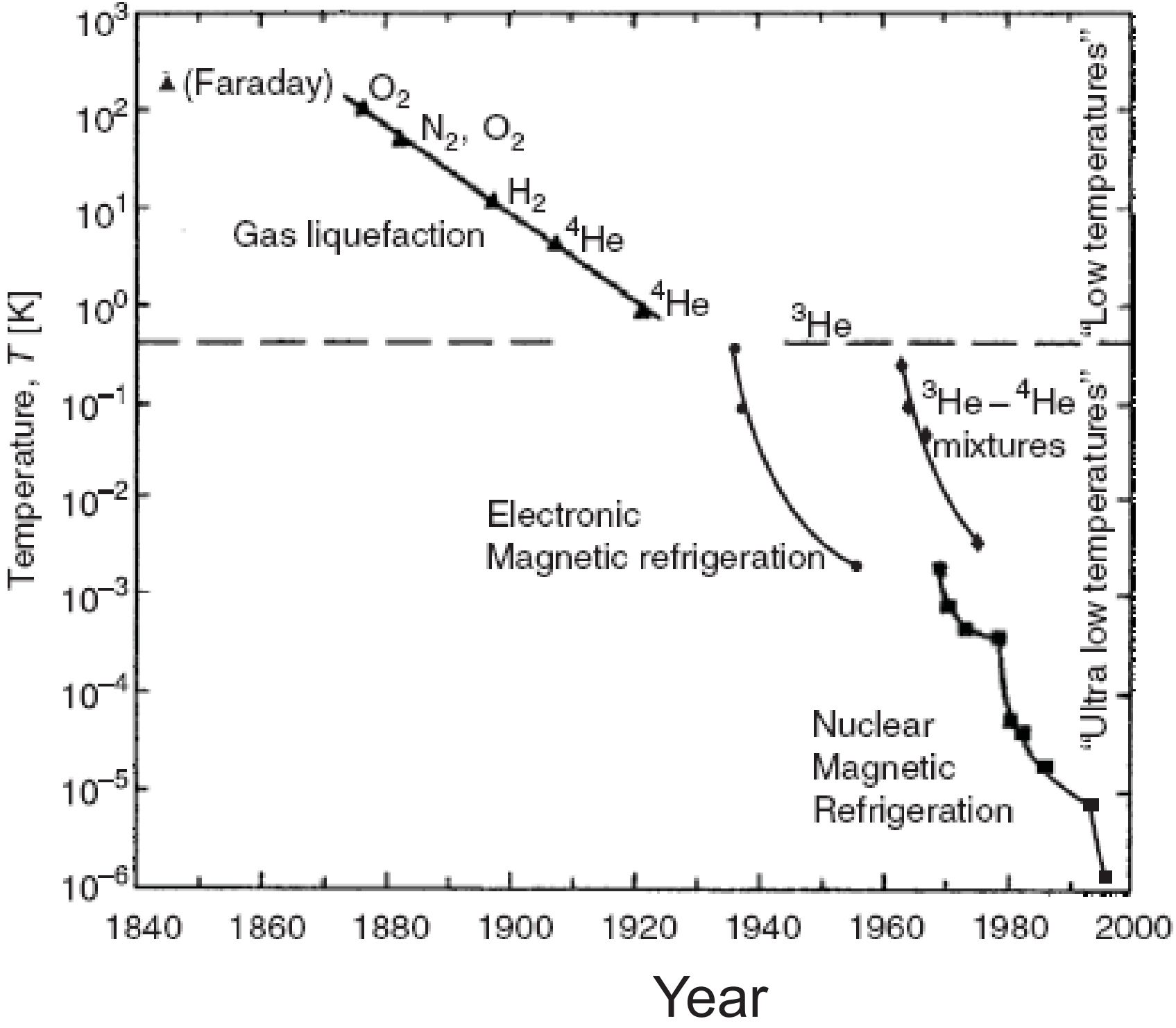
Temperature, T [K]
10^3
10^2
10^1
10^0
10^-1
10^-2
10^-3
10^-4
10^-5
10^-6
(Faraday)
O2
N2, O2
H2
4He
4He
Gas liquefaction
3He
3He – 4He mixtures
Electronic Magnetic refrigeration
Nuclear Magnetic Refrigeration
"Low temperatures"
"Ultra low temperatures"
1840
1860
1880
1900
1920
1940
1960
1980
2000
Year

Table 1.1. Refrigeration techniques. The methods which dominate in the three temperature ranges are in italics

Temperature range		Refrigeration technique	Available since	Typical $T_{\min}$	Record $T_{\min}$
I	Kelvin	Universe			2.73 K
		Helium-4 evaporation	1908	1.3 K	0.7 K
		Helium-3 evaporation	1950	0.3 K	0.23 K
II	Millikelvin	**^{3}He–^{4}He dilution**	1965	10 mK	2 mK
		Pomeranchuk cooling	1965	3 mK	2 mK
		Electronic magnetic refrigeration	1934	3 mK	1 mK
III	Microkelvin	**Nuclear magnetic refrigeration**	1956	100 μK	1.5 μK[a]

[a]The given minimum temperature for the microkelvin temperature range is the *lattice* (*electronic*) *equilibrium* temperature. *Nuclear spin* temperatures as low as 0.3 nK have been reached (Table 10.2)

Table 10.2. Minimum temperatures to which the given materials have been cooled by nuclear magnetic refrigeration

Refrigerated material	Minimum temperature	Reference
Liquid ^{3}He; liquid ^{3}He–^{4}He	0.10 mK	[10.78, 10.86–10.88]
Solid ^{3}He	34 μK	[10.89]
Massive Cu nuclear refr. stage	10 μK	[10.30]
Metals	1.5 μK	[10.67]
Nuclear moments in metals	0.28 nK	[10.24]

[10.24] T.A. Knuuttila, J.T. Tuoriniemi, K. Lefmann, K.I. Juntunen, F.B. Rasmussen, K.K. Nummila: J. Low Temp. Phys. **123,** 65 (2001)

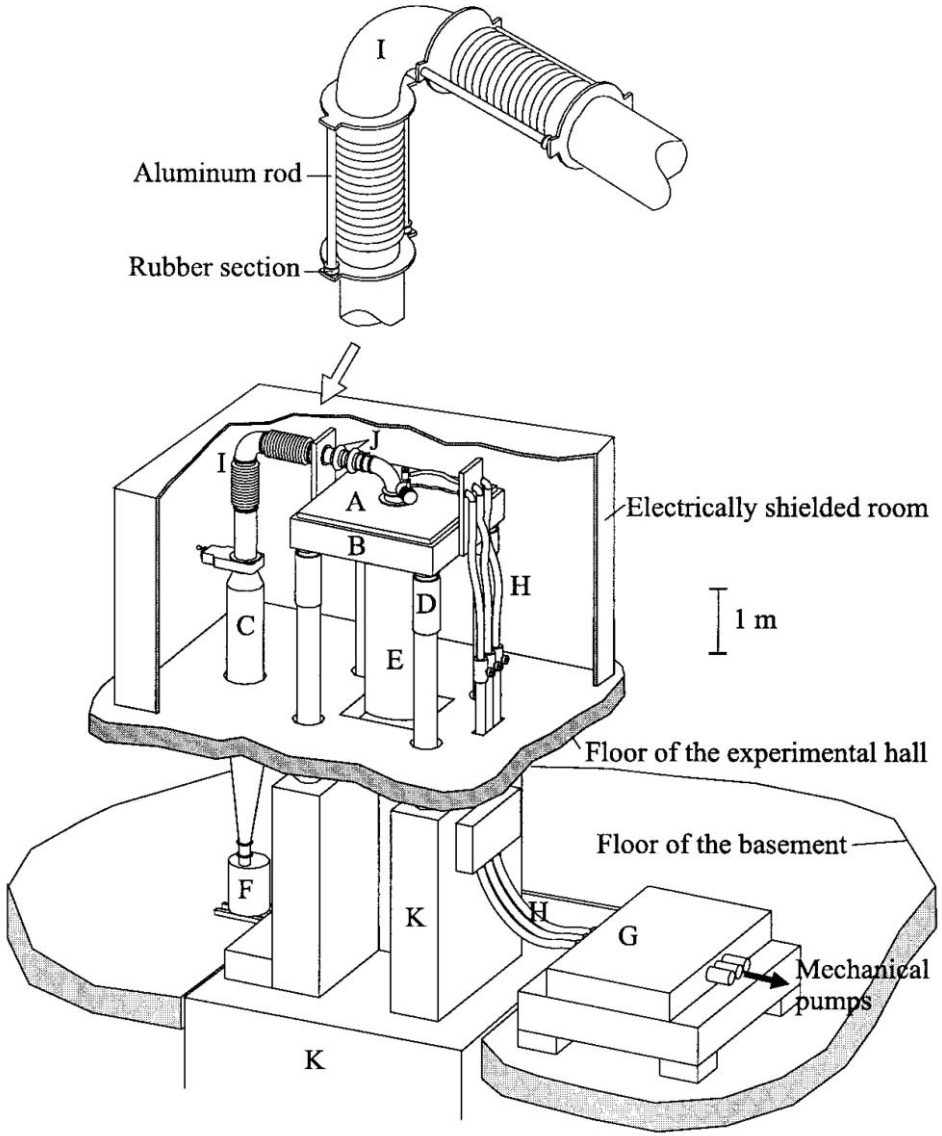

Fig. 2. Cryostat with its supporting structure. For further explanations, see text.

Journal of Low Temperature Physics, Vol. 120, Nos. 1/2, 2000

W. Yao,[1] T. A. Knuuttila, K. K. Nummila,[2] J. E. Martikainen, A. S. Oja,[2] and O. V. Lounasmaa

Low Temperature Laboratory, Helsinki University of Technology, P.O. Box 2200, FIN-02015 HUT, Finland
(e-mail: tauno.knuuttila@hut.fi)

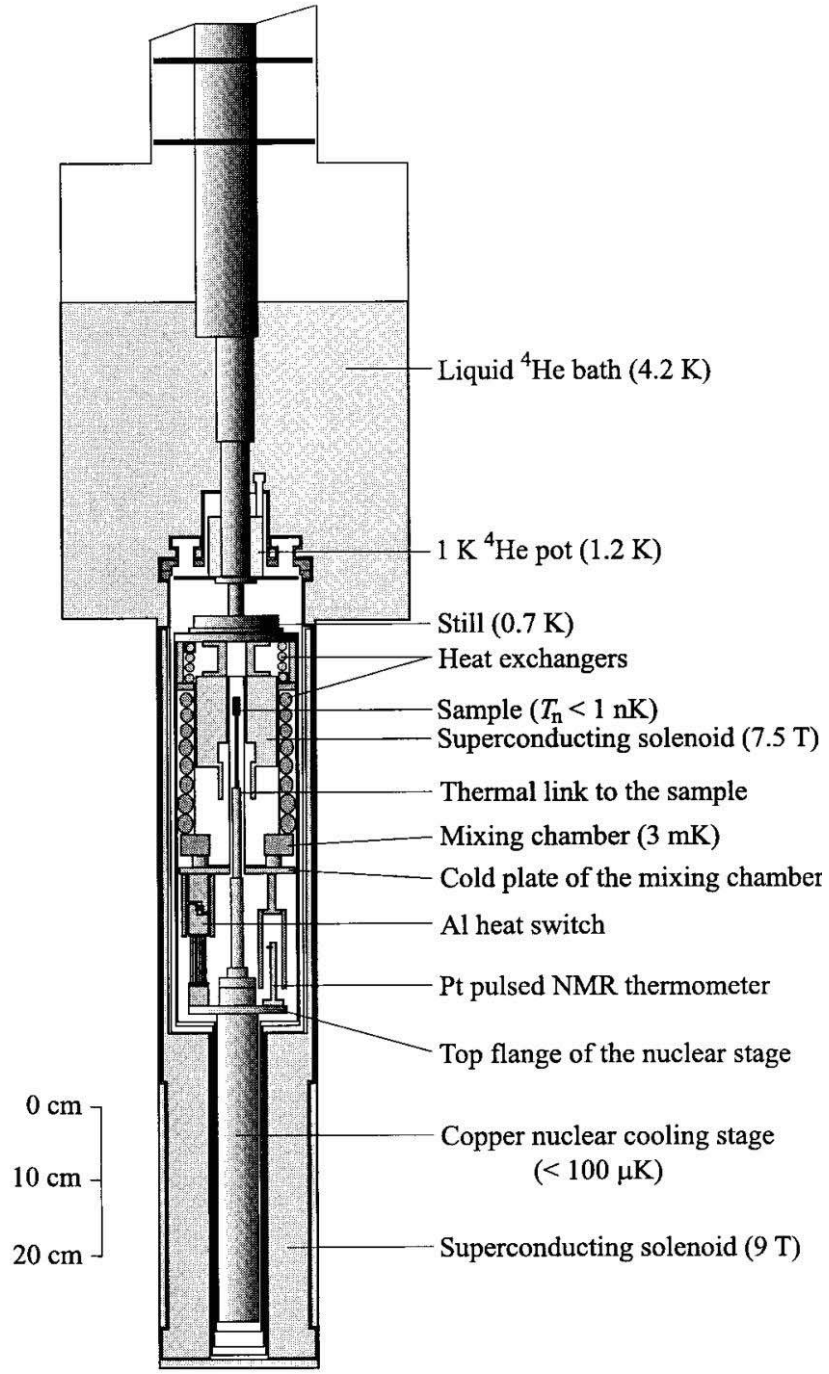

Fig. 1. Layout of the cryostat.

Jagiellonian University in Cracow, POLAND

Zygmunt Wróblewski

Karol Olszewski

1883

On 5th of April they managed to achieve

liquefaction of oxygen T_b= 90,2K (-182,95°C)

On April 13 they had achieved

the liquefaction of nitrogen T_b= 77,3K (-195,8°C)

Museum of the Jagiellonian University in Cracow

The room and instruments employed by Karol Olszewski and Zygmunt Wróblewski in bringing about the liquifaction of oxygen in 1883

liquifaction vessel

cryostat

Collegium Maius - its history goes back to the year 1400

In 1927 W. Keesom with **M. Wolfke** discovered, that there is a change in the form of liquid helium at 2.17 K

Mieczysław Wolfke ***Willem Hendrik Keesom***

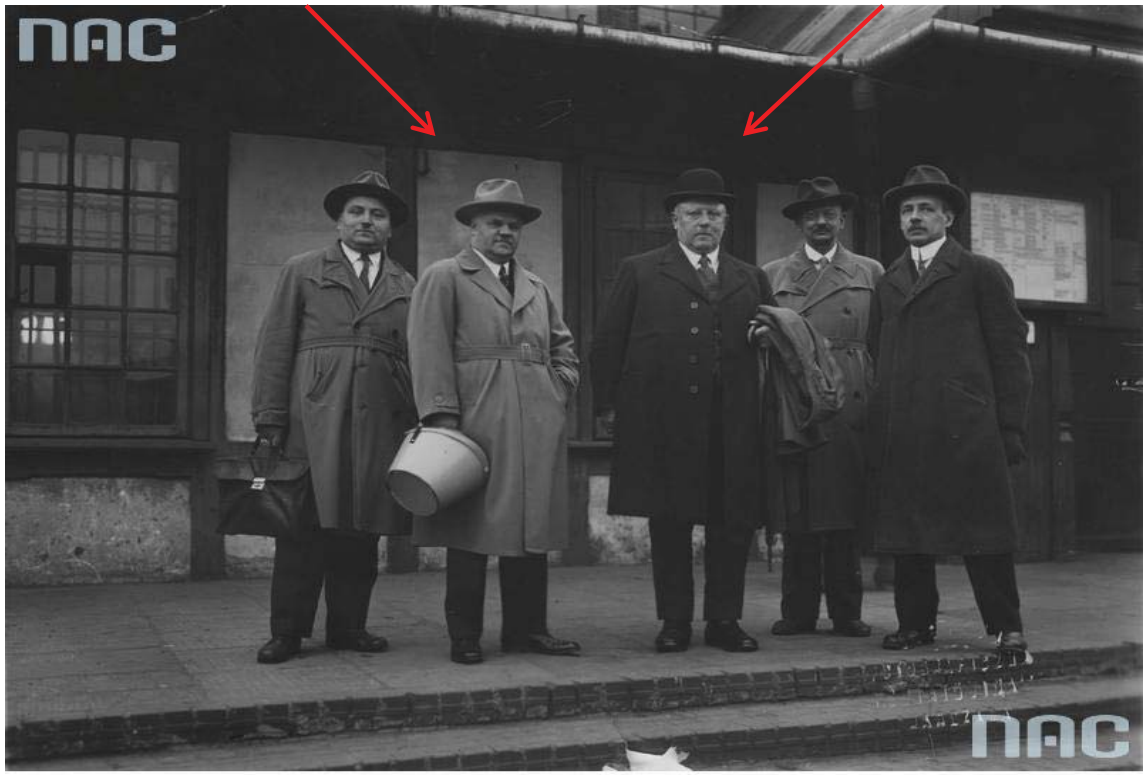

Narodowe Archiwum Cyfrowe, sygn. 1-N-1120-1

History of Helium

- The first evidence of helium was observed on August 18, 1868 as a bright yellow line with a wavelength of 587.49 nanometers in the spectrum of the chromosphere of the Sun. The line was detected by French astronomer *Pierre Janssen* during a total solar eclipse in Guntur, India.

- On October 20 of the same year, English astronomer *Norman Lockyer* observed a yellow line in the solar spectrum.

- He concluded that it was caused by an element in the Sun unknown on Earth. *Lockyer* and English chemist *Edward Frankland* named the element with the Greek word for the Sun, helios.

- In 1882, Italian physicist *Luigi Palmieri* detected helium on Earth, for the first time, through its D_3 spectral line, when he analyzed the lava of Mount Vesuvius.

- On March 26, 1895, Scottish chemist *Sir William Ramsay* isolated helium on Earth by treating the mineral *cleveite*.

- In 1907, *Ernest Rutherford* and *Thomas Royds* demonstrated that alpha particles are helium nuclei by allowing the particles to penetrate the thin glass wall of an evacuated tube, then creating a discharge in the tube to study the spectra of the new gas inside.

Spectral lines of:

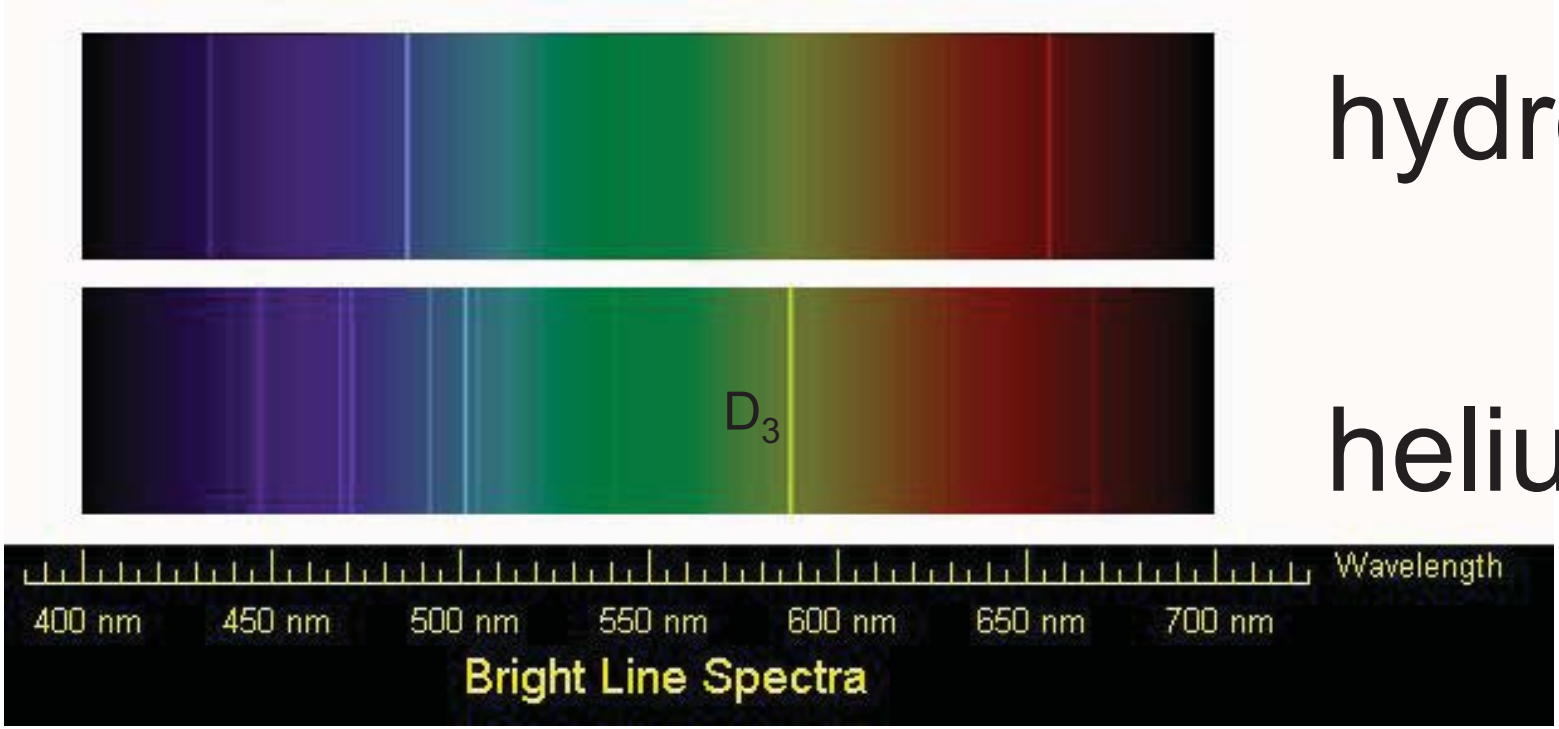

hydrogen

helium

sourcs:
http://imagine.gsfc.nasa.gov/docs/teachers/lessons/xray_spectra/worksheet-specgraph2-sol.html

- Stable helium isotopes:

helium 4 $^{4}_{2}He$

atomic mass - 4,0038

helium 3 $^{3}_{2}He$

atomic mass - 3,0169

helium 3 constitutes a fraction $1 \div 2 \times 10^{-7}$ of helium gas from natural gas sources, and about 1.3×10^{-6} of the helium gas in the atmosphere.

Not-stable helium isotopes:

- helium 5 - half – live 7.6×10^{-22} s
- helium 6 - half – live 0.8 s
- helium 7 - half – live $2.9(5)\times10^{-21}$ s
- helium 8 - half – live 0.12 s
- helium 9 - half – live $7(4)\times10^{-21}$ s
- helium 10 - half – live $2.7(18)\times10^{-21}$ s

STARS

$$4_1^1H \rightarrow {}_2^4He + 2_1^0e + 2\nu + 26{,}7\,MeV$$

Earth

Helium is present today has been mostly created by the natural radioactive decay of heavy radioactive elements thorium and uranium as the alpha particles that are emitted by such decays consist of helium-4 nuclei.

^{238}U -	half – live	4,5 x10^9 years
^{235}U -	half – live	707 x10^9 years
^{232}Th -	half – live	13,9 x10^9 years

Helium 3

STARS

$$ {}_{1}^{2}H + {}_{1}^{2}H \rightarrow {}_{2}^{3}He + {}_{0}^{1}n $$

Helium 3

$$^{6}_{3}Li + ^{1}_{0}n \rightarrow ^{3}_{1}H + ^{4}_{2}He$$

$$^{3}_{1}H \xrightarrow{12{,}3\ years} ^{3}_{2}He + ^{0}_{-1}e + \bar{\nu}$$

10th of July 1908 H. Kamerlingh – Onnes condensed helium for the first time
Leiden University 4,2K (-269 °C)

100-lecie skroplenia helu przez Heike Kamerlingha-Onnesa
30-lecie skroplenia helu w instalacji w Odolanowie PGNiG S.A.
30-lecie działalności Instytutu Fizyki Molekularnej PAN w Odolanowie
LHe Sympozjum z okazji 100-lecia skroplenia helu

Odolanów
July 10, 2008

Sympozjum

10 lipca 2008 Odolanów

z okazji 100-lecia skroplenia helu

impreza towarzysząca

XXIV Warsztaty Naukowe „Lato z Helem”

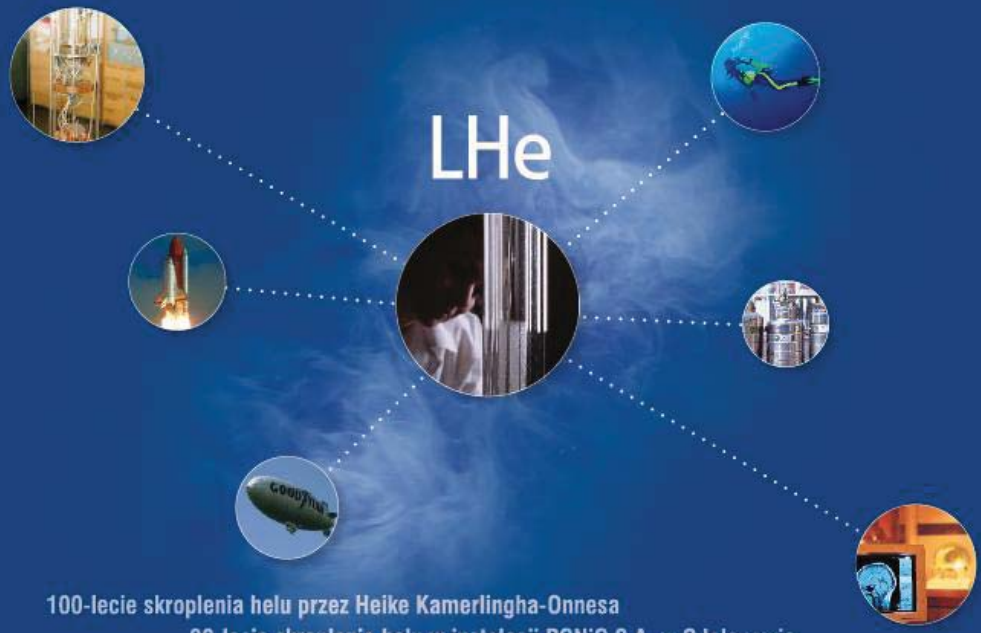

100-lecie skroplenia helu przez Heike Kamerlingha-Onnesa

30-lecie skroplenia helu w instalacji PGNiG S.A. w Odolanowie

30-lecie działalności Instytutu Fizyki Molekularnej PAN w Odolanowie

Komitet Honorowy Sympozjum

Prof. dr hab. Janusz Jurczak
Przewodniczący Wydziału Nauk Matem.-Fiz.-Chem. PAN Warszawa

Prof. dr hab. Stanisław Lorenc
Rektor Uniwersytetu im. Adama Mickiewicza Poznań

Prof. dr hab. Tadeusz Luty
Rektor Politechniki Wrocławskiej, Przewodniczący Konferencji Rektorów Akademickich Szkół Polskich

Prof. dr hab. Andrzej Jeziorski
Dyrektor Instytutu Fizyki Molekularnej PAN Poznań

Prof. dr hab. Henryk Szymczak
Instytut Fizyki PAN Warszawa

Prof. dr hab. Józef Szmajd
Dyrektor Instytutu Niskich Temperatur i Badań Strukturalnych PAN Wrocław

Prof. dr hab. inż. Stanisław Rychliski
Przewodniczący Rady Nadzorczej PGNiG S.A.

Michał Szubski
Prezes Zarządu PGNiG S.A.

Mirosław Dobrut
Wiceprezes Zarządu PGNiG S.A. ds. Techniczno-Inwestycyjnych

Prof. dr hab. Jan Kłamut
Dyrektor Międzynarodowego Laboratorium Silnych Pól Magnetycznych i Niskich Temperatur Wrocław

Prof. dr hab. Stefan Jurga
Dyrektor Centrum Integracji Europejskiej, Kierownik Zakładu Fizyki Makromolekularnej UAM Poznań

Prof. dr hab. Jan Stankowski
Przewodniczący Rady Naukowej Instytutu Fizyki Molekularnej PAN Poznań

Sesja wykładowa

- **Otwarcie**
  prof. dr hab. Jan Stankowski - IFM PAN Poznań
- **Badania niskotemperaturowe w Odolanowie**
  doc. dr hab. Zbigniew Trybuła - Kierownik Zakładu Fizyki Niskich Temperatur Odolanów, IFM PAN Poznań
- **Bethego - cykl Słońca**
  prof. dr hab. Piotr Pieranski - Politechnika Poznańska
- **Technologia odzysku, oczyszczania i skraplania helu w instalacji przemysłowej w Odolanowie**
  Dyrektor Oddz. w Odolanowie PGNiG S.A. - Tomasz Jaskólski
- **Przemiany fazowe w helu**
  prof. dr hab. Józef Szmajd - INTiBS Wrocław
- **Temperatura spinowa**
  prof. dr hab. Stefan Jurga - IF UAM Poznań
- **Kondensacja Bosego-Einsteina magnonów**
  prof. dr hab. Henryk Szymczak - IF PAN Warszawa
- **Kondensacja Bosego-Einsteina w nadprzewodnikach**
  prof. dr hab. Roman Micnas - IF UAM Poznań
- **Najzimniejsze atomy**
  doc. dr hab. Tadeusz Domański - UMCS Lublin
- **Nadpłynność helu - pokaz**
  doc. dr hab. Wojciech Kempiński - ZFNT Odolanów IFM PAN Poznań

www.ifmpan.poznan.pl

PGNiG www.pgnig.pl

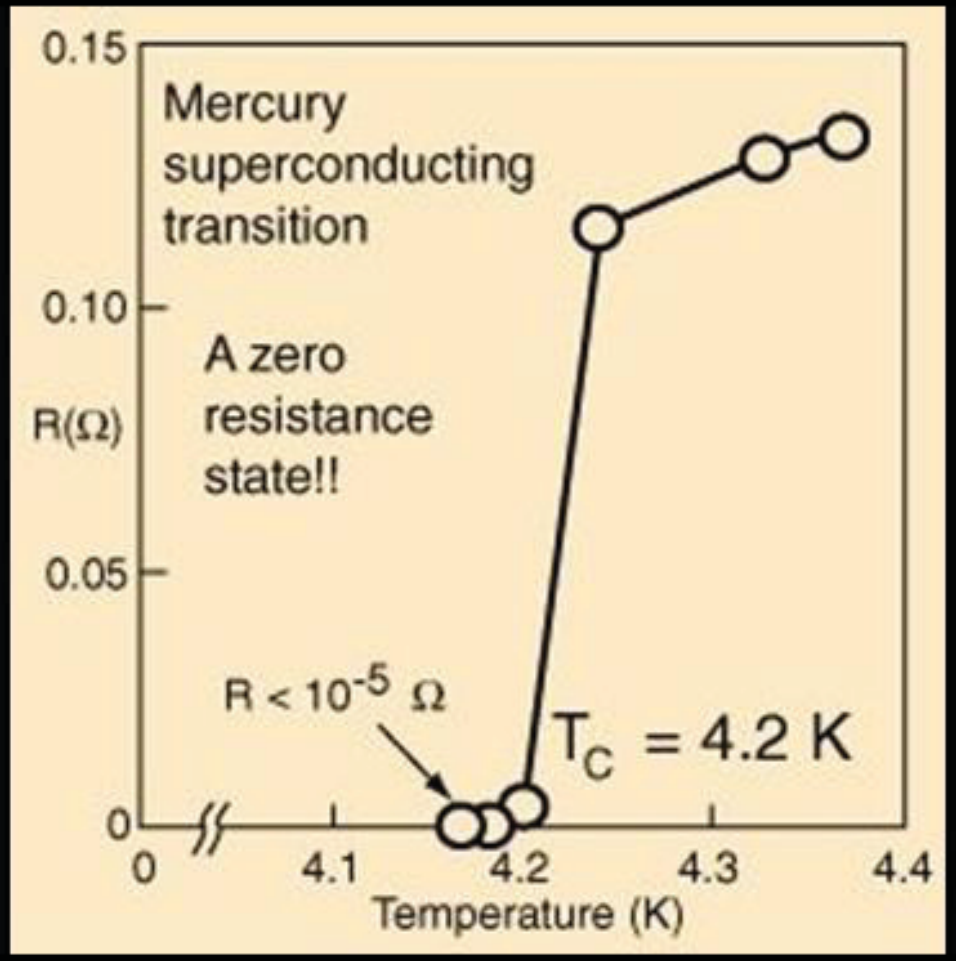

1911
H. Kamerlingh-Onnes
discovered
superconductivity

H. Kamerlingh-Onnes
1911

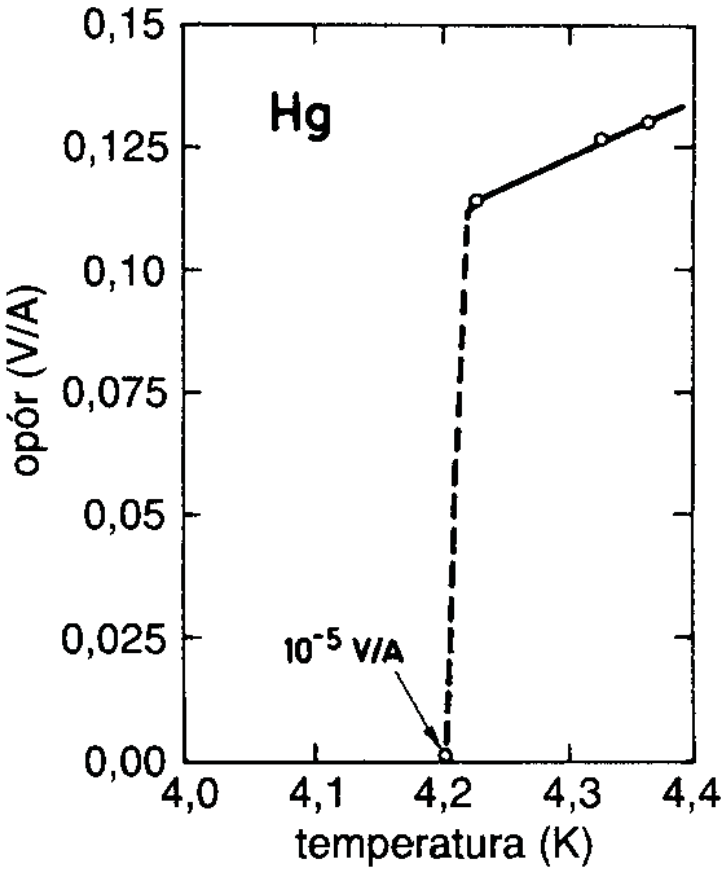

Nobel Prizes:

1. H. Kamerlingh-Onnes - 1913
2. J. Bardeen, L. N. Cooper, J. R. Schrieffer - 1972
3. B. D. Josephson - 1973
4. J. G. Bednorz, A. K. Müller - 1987
5. V. L. Ginzburg, A. Abrikosov A. J. Legget - 2003

Oil and natural gas

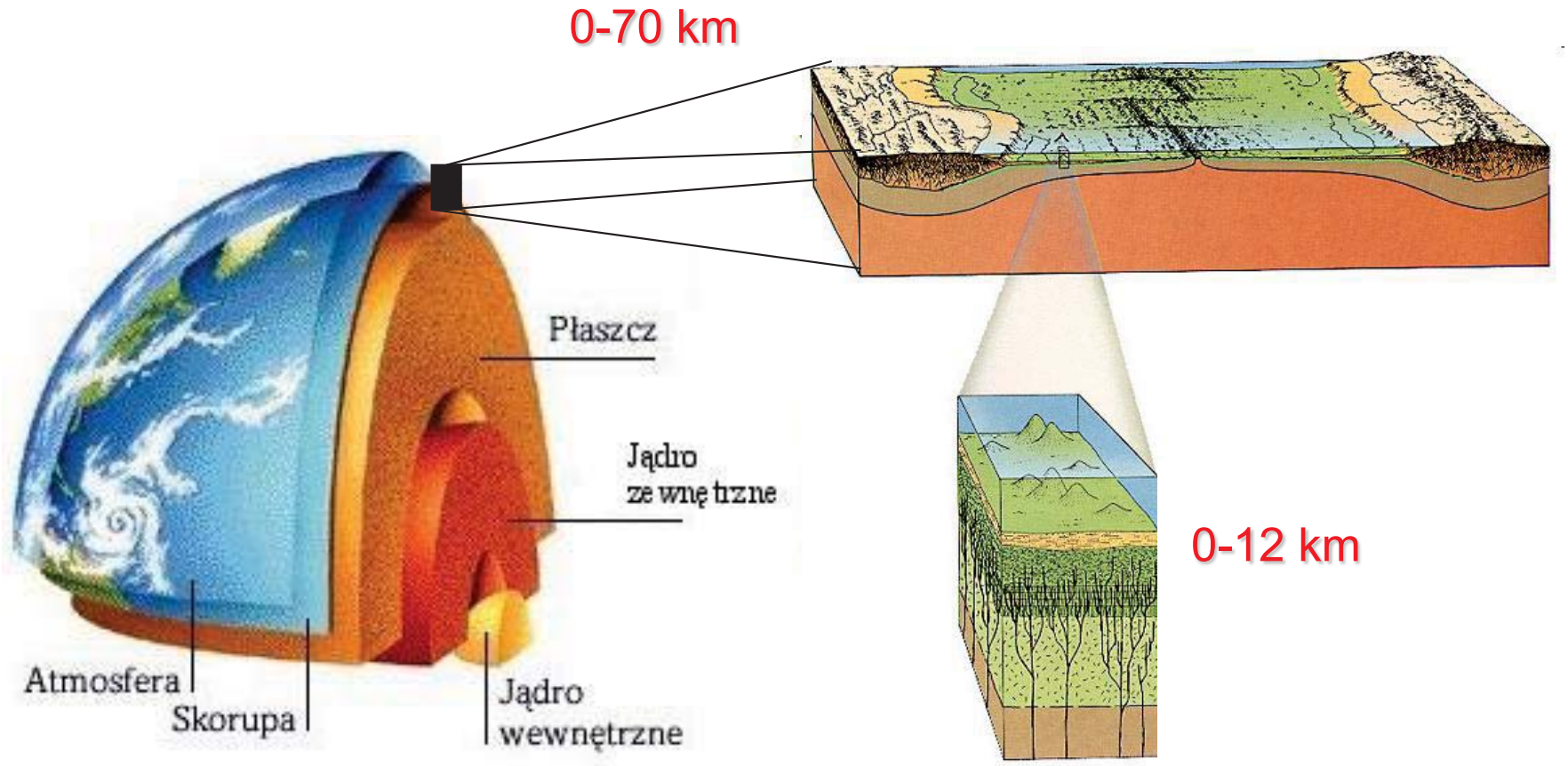

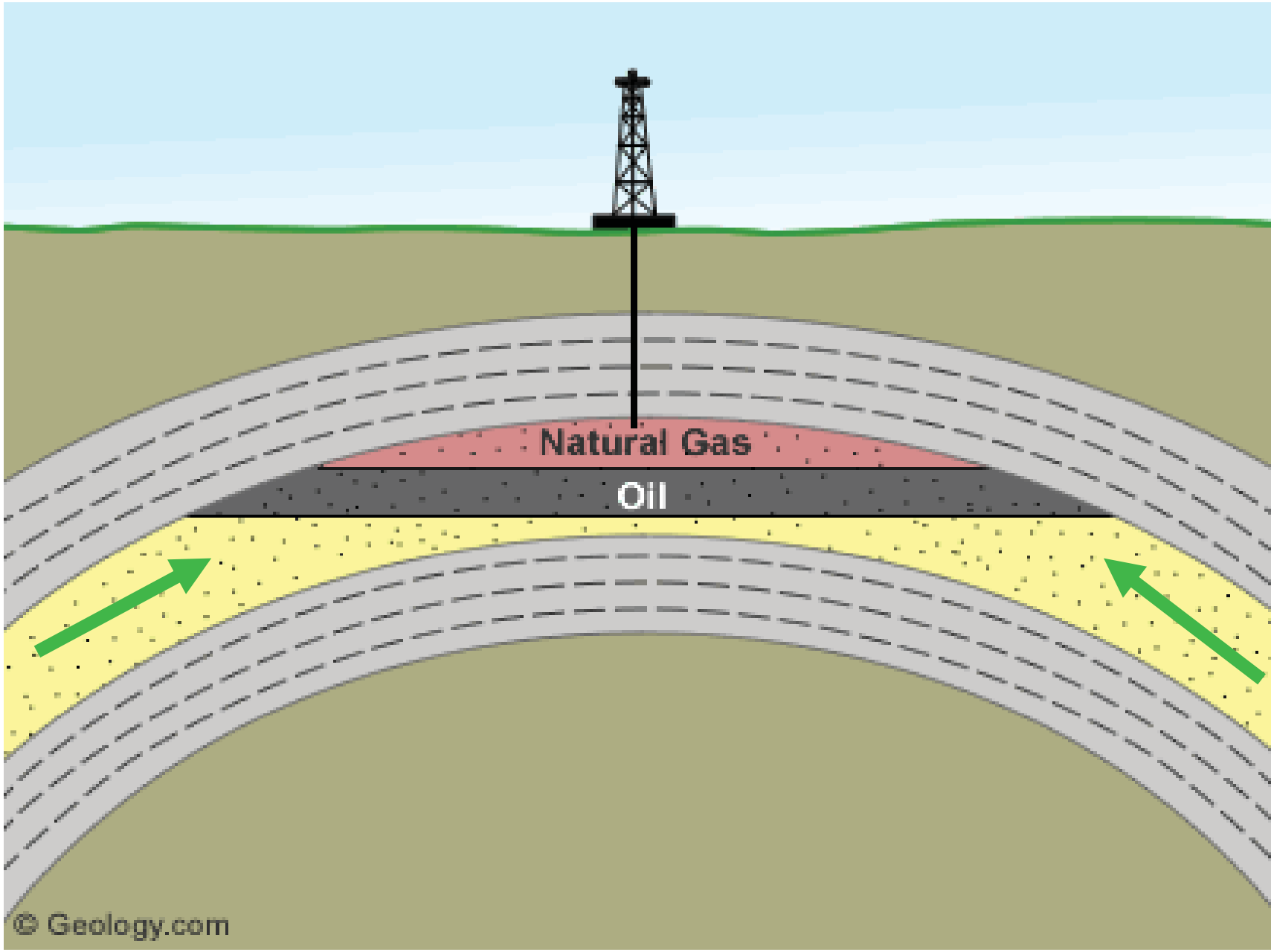
Natural Gas
Oil
© Geology.com

Oil or gas rig

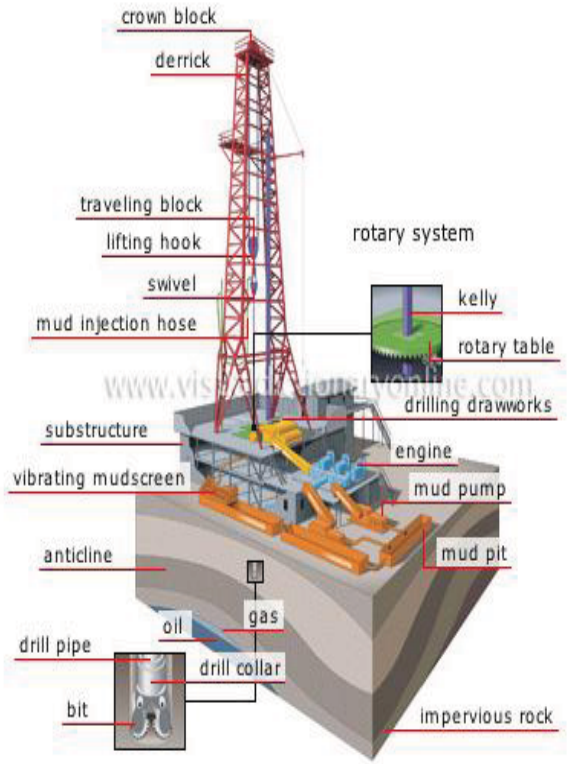

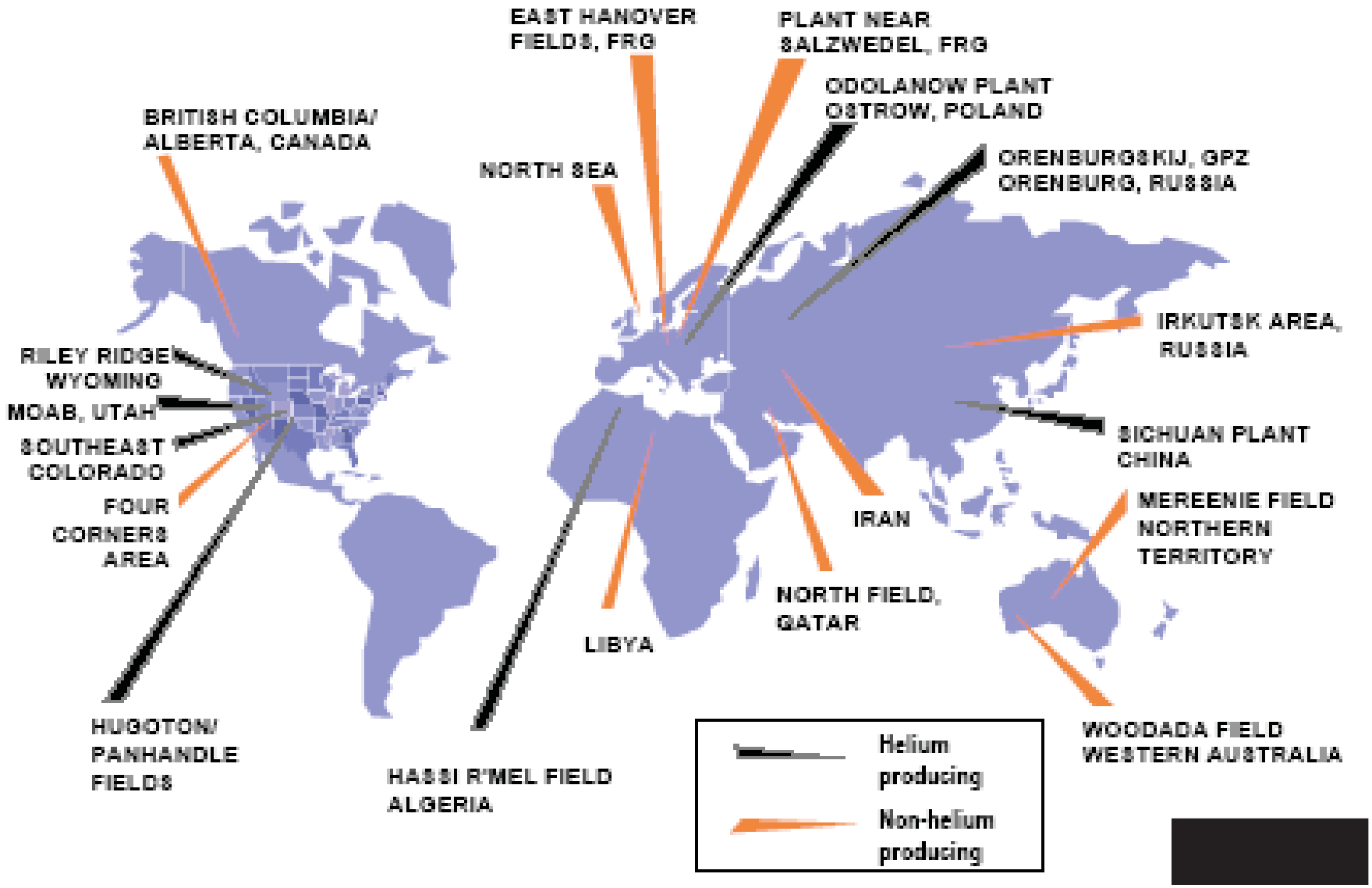
EAST HANOVER FIELDS, FRG
PLANT NEAR SALZWEDEL, FRG
ODOLANOW PLANT OSTROW, POLAND
BRITISH COLUMBIA/ ALBERTA, CANADA
NORTH SEA
ORENBURGSKIJ, GPZ ORENBURG, RUSSIA
IRKUTSK AREA, RUSSIA
RILEY RIDGE WYOMING
MOAB, UTAH
SOUTHEAST COLORADO
FOUR CORNERS AREA
SICHUAN PLANT CHINA
IRAN
MEREENIE FIELD NORTHERN TERRITORY
NORTH FIELD, QATAR
LIBYA
HUGOTON/ PANHANDLE FIELDS
HASSI R'MEL FIELD ALGERIA
WOODADA FIELD WESTERN AUSTRALIA
Helium producing
Non-helium producing

The helium plant, built in 1974 in Odolanów

the branch of the Polish Oil & Gas Company in Warsaw
(Polskie Górnictwo Naftowe i Gazownictwo S.A.)
the largest Polish oil and gas exploration and production company)

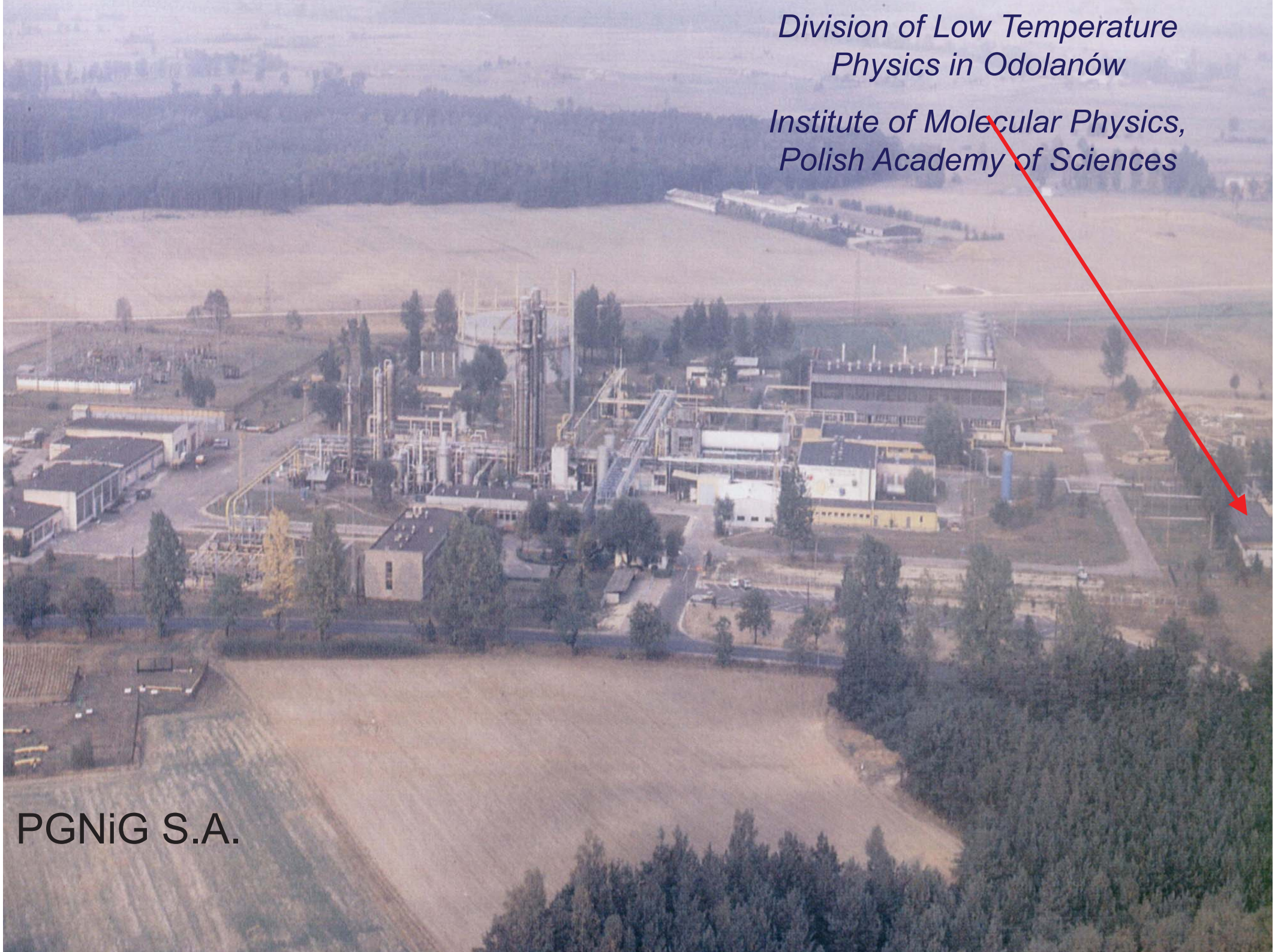
Division of Low Temperature
Physics in Odolanów
Institute of Molecular Physics,
Polish Academy of Sciences
PGNiG S.A.


ZAKŁAD ODAZOTOWANIA GAZU
"KRIO" W ODOLANOWIE
KRIO
ODOLANÓW
CH_4
GAZ ZIEMNY
N_2
LN_2
He
LHe
POLSKIE
GÓRNICTWO
NAFTOWE

magazyny i ekspedycja LNG

sprężanie gazu wysokometanowego

napełnianie i ekspedycja helu ciekłego

sekcja oczyszczania gazu zaazotowanego

sekcja niskotemperaturowej destylacji gazu ziemnego

instalacja oczyszczania, skraplania i magazynowania helu

napełnianie i ekspedycja helu gazowego

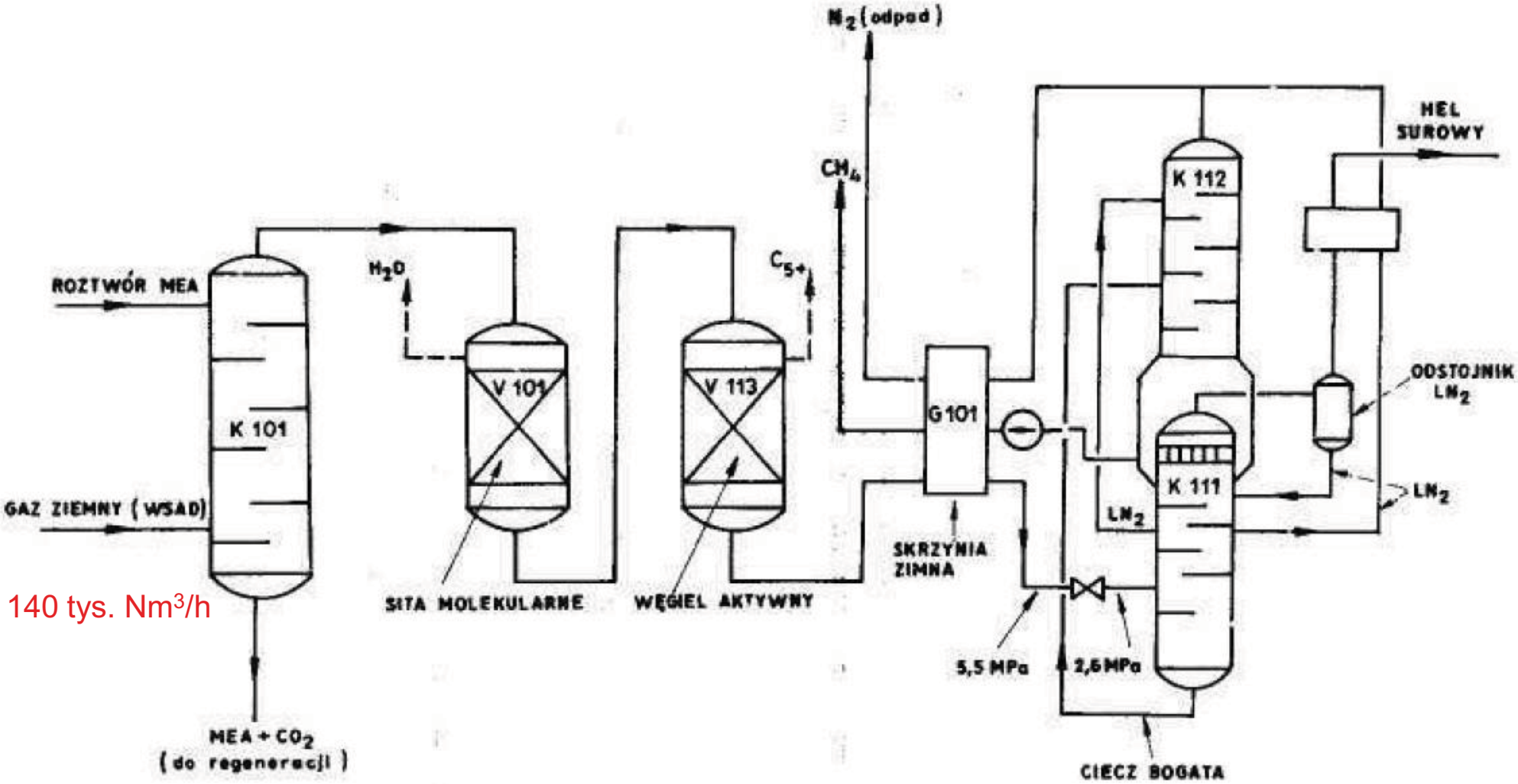

Flow diagram of KRIO plant in Odolanów

600 Nm^3/h

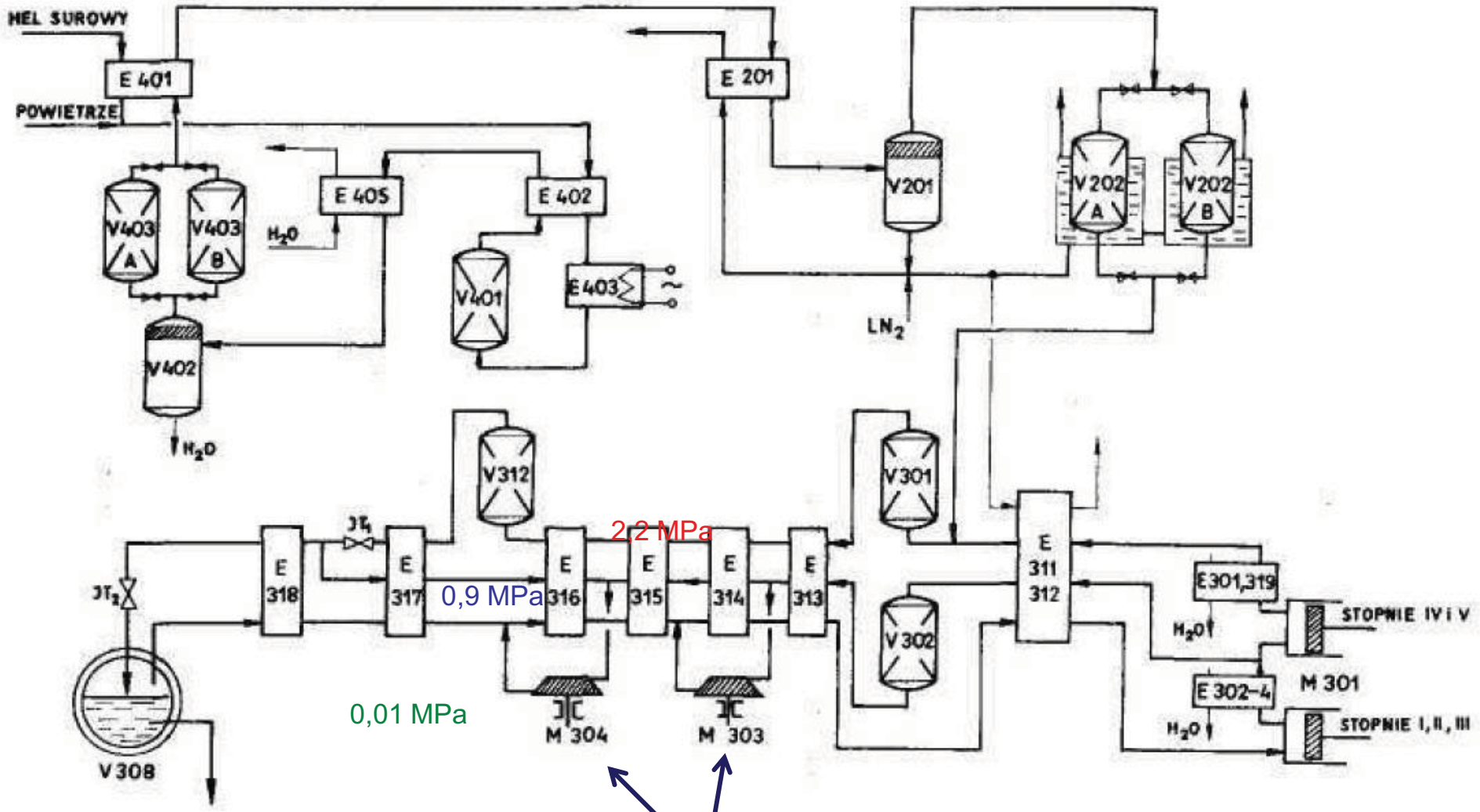

expansion turbines:
rotational speed : 65 000 rpm and 90 000 rpm
gas lubricated bearings

700 l LHe/h

V 308- helium storage tank
120 m^3 = 15 000 kg

T = 4.2 K

Helium liquefaction and storage - flow diagram

of KRIO plant in Odolanów

11 000 US galons (41 800 l)
~5000 kg

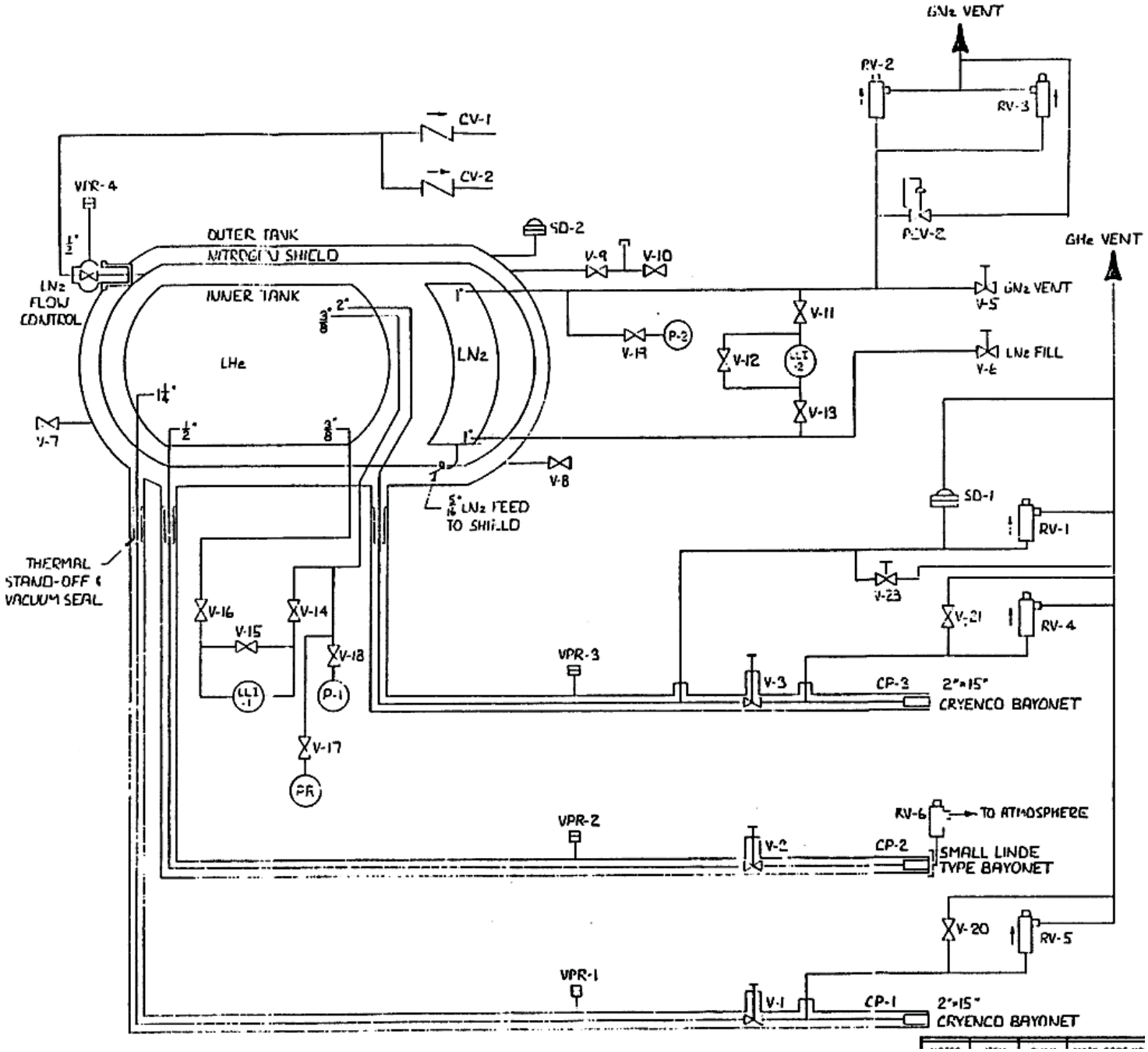

Q~**10 W**

LN_2 ~35 kg/24h

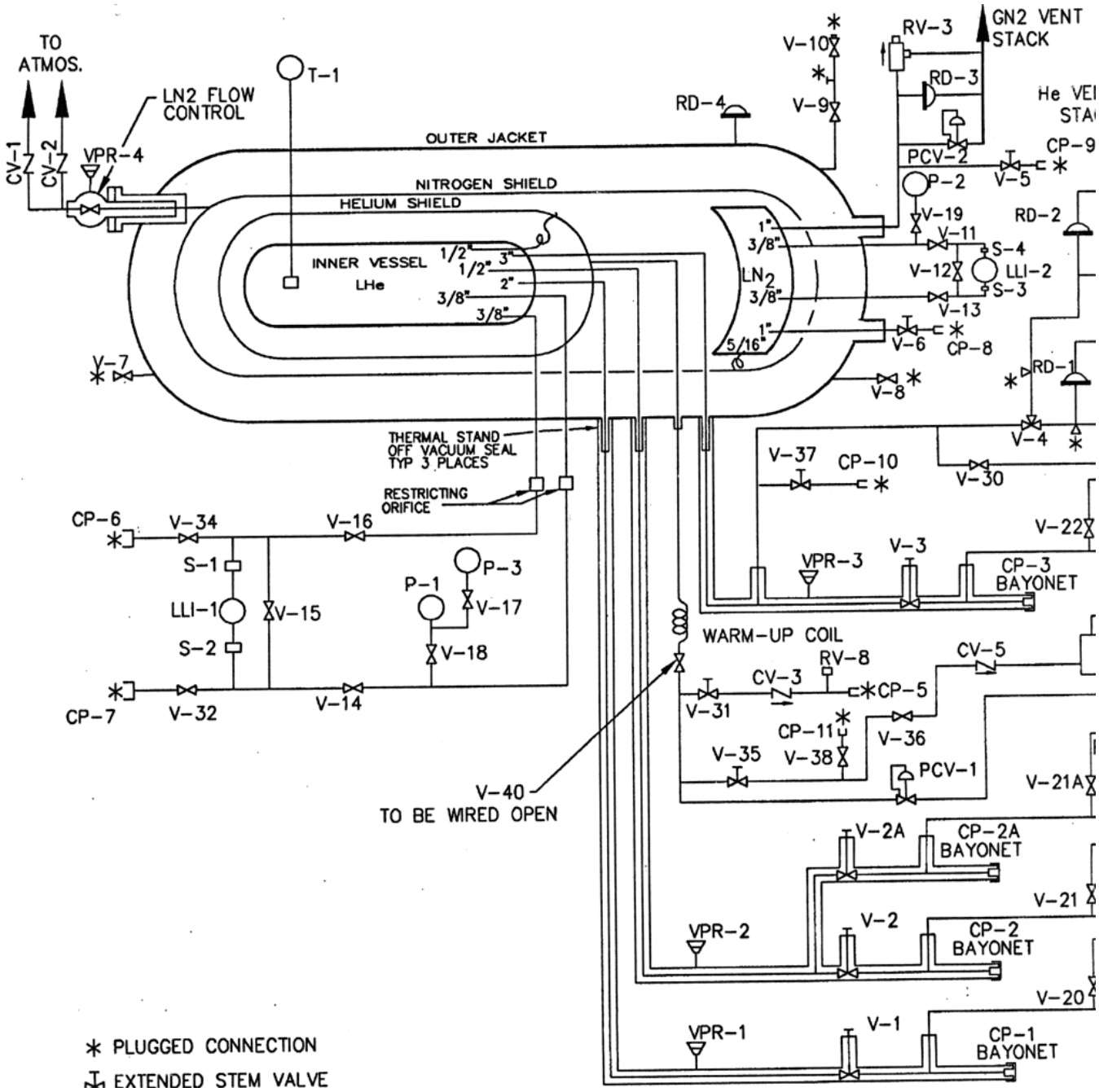

Q**~2,4W**

LN_2 ~30 kg/24h


ALGU-061023-0
FXX-4278
MASSE BRUTE MAX.
MAX. GROSS WT.
KG. 24.721
LB. 54500
TARE
TARE WT.
KG. 17.382
LB. 38.320
22
1983
968 AQY 78
60 70 80

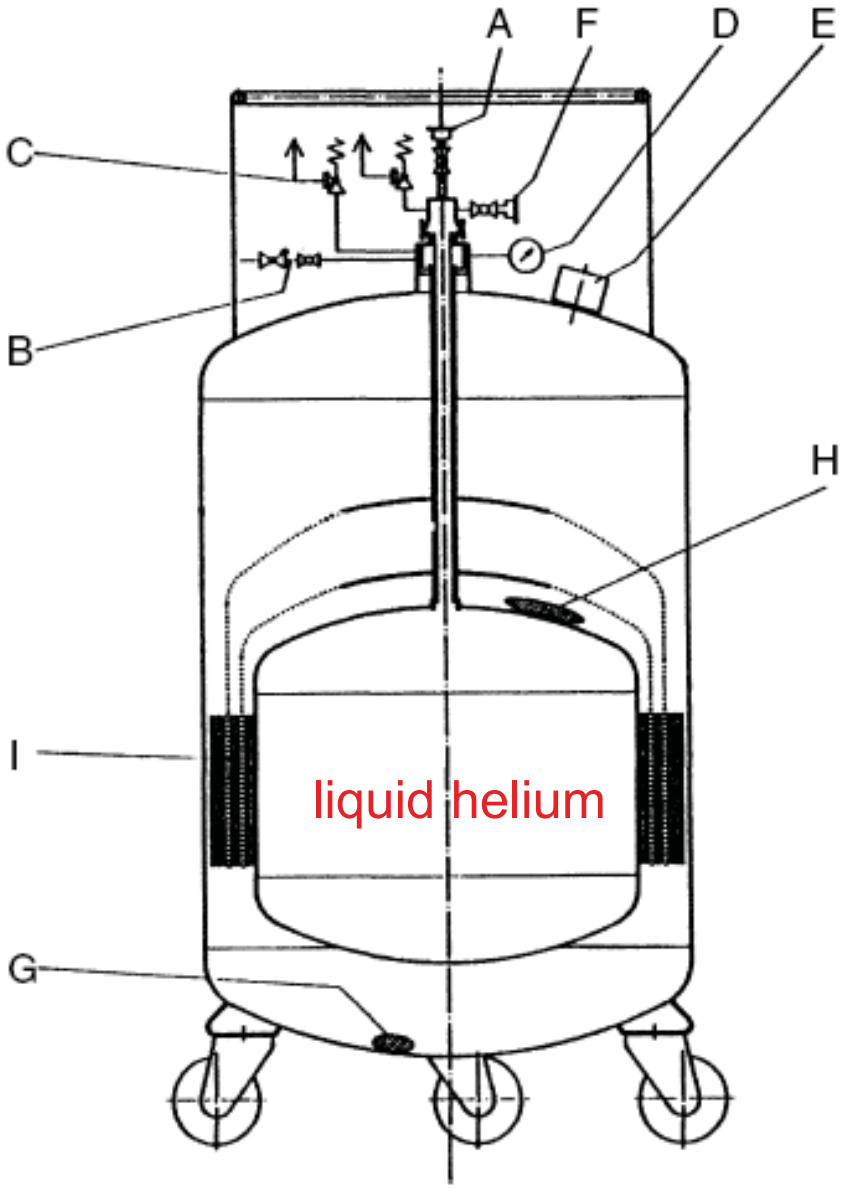

Commercial storage vessel for liquid ^4He

(*A: connection for transfer tube, B: overflow valve, C: safety valve, D: manometer, E: vacuum and safety valves, F:* gas valve, *G: getter material, H: adsorbent material to maintain and improve the* vacuum, *I : superinsulation only partly shown)*

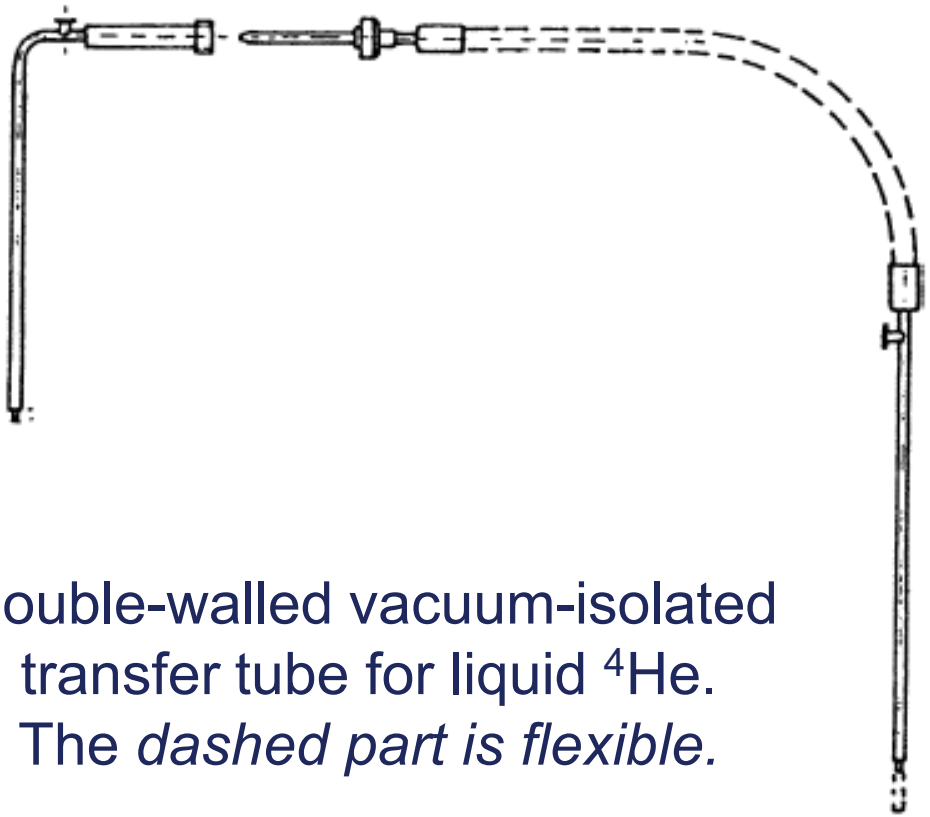

Double-walled vacuum-isolated transfer tube for liquid ^{4}He. The *dashed part is flexible.*

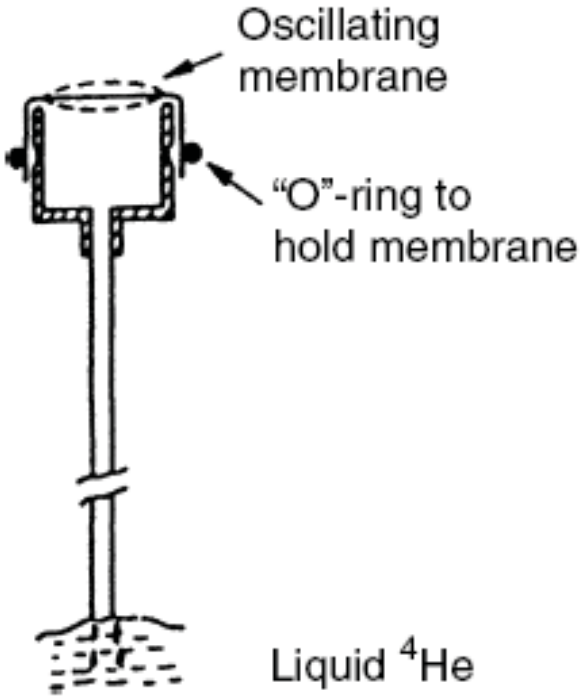

Acoustic level detector for liquid ^{4}He

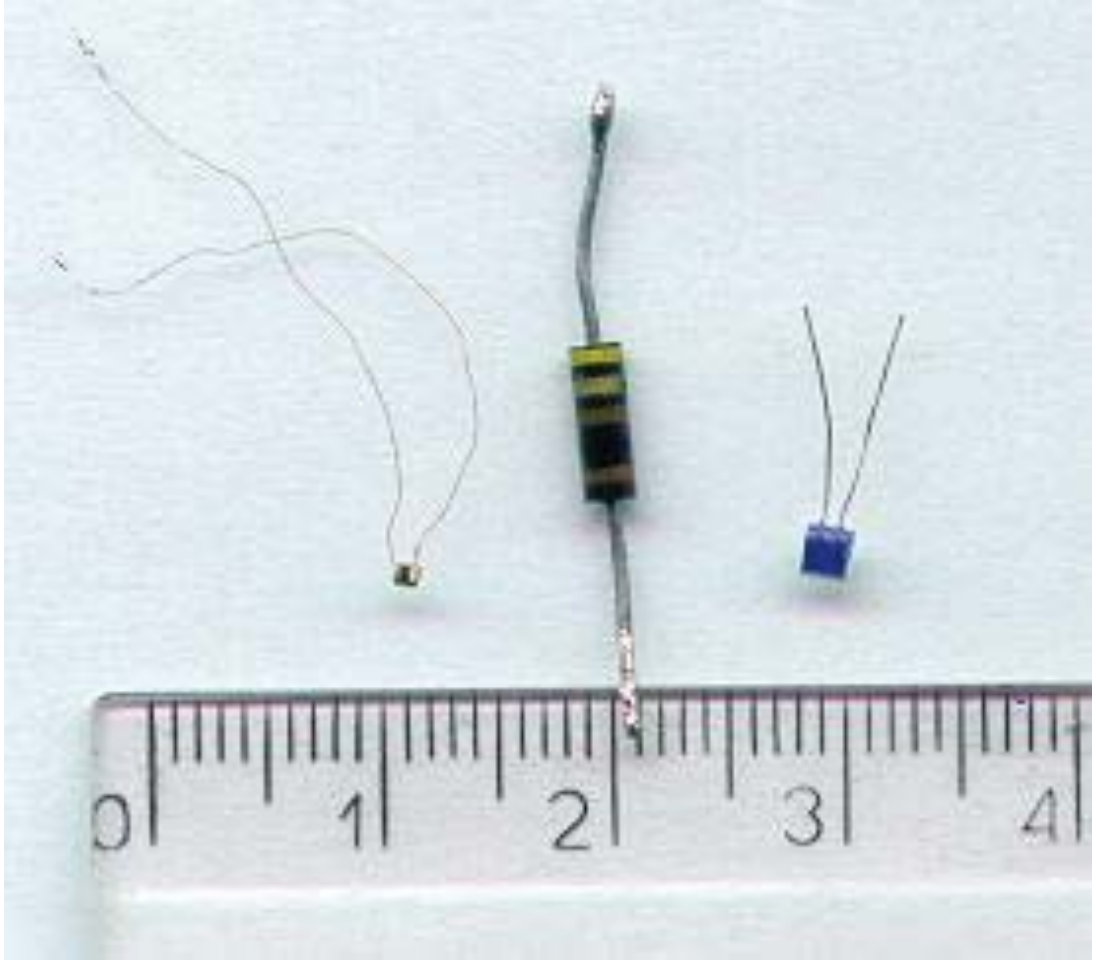

Low Temperature Thermometry:

Cernox CX 1030 BC Lake Shore,

resistor of Allen Bradley,

platinum thermometer PT-1000.

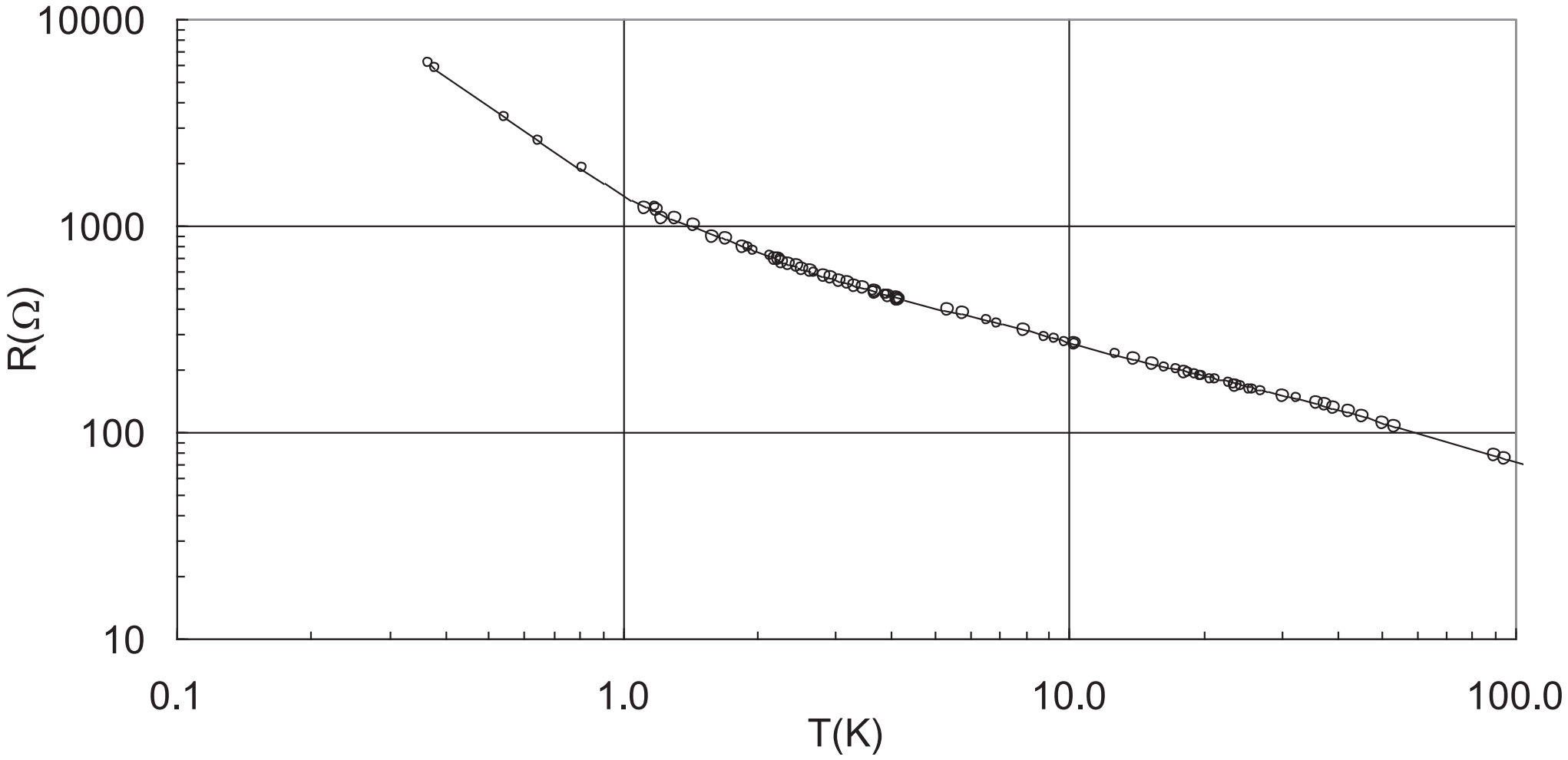

Cernox CX1030 BC - Lake Shore.

Basic Atomic and Nuclear Properties of Helium

- The electronic structure of helium is the simplest many-body system of all atoms. With two electrons completely filling the *K shell* ($1s^2$) *it has a spherical* shape and thus no permanent electric dipole moment.

- Helium has the smallest known atomic polarizability of $\alpha = 0.1232\ cm^3\ mol^{-1}$ *and only a very weak* diamagnetic susceptibility $\chi_d = -1.9 \times 10^{-6}\ cm^3\ mol^{-1}$.

- *With an atomic* radius of only *31pm* it is the smallest atom.

- It has the highest ionization energy of about *24.6 eV*.

- The liquid of both stable isotopes is colorless and since their index of refraction is very close to unity, they are very difficult to see.

- Because of their nuclear spin $I = 1/2$, ^{3}*He atoms are fermions and obey Fermi–Dirac statistics, whereas* ^{4}He atoms are bosons with nuclear spin $I = 0$.

Van der Waals Bond of Helium

- The polarizability of helium atoms is small and the binding force is very weak.

- *Lennard–Jones potential:*

$$\phi(r) = 4\varepsilon \left[\left(\frac{\sigma}{r}\right)^{12} - \left(\frac{\sigma}{r}\right)^{6} \right]$$

with the characteristic parameters *ε and σ. For both helium isotopes we* have ε/k_B = *10.2K and* σ = *2.56Å.*

•The potential energy is obtained by integrating *Lennard–Jones potential:*

$$E_{\mathrm{pot}} = \frac{1}{2} \int_0^\infty \phi(r)\, 4\pi r^2 n(r)\, \mathrm{d}r \,,$$

taking into account the radial density function *n(r). The difference in the* potential energy of liquid and solid helium originates from the difference in *n(r) of the two phases.*

- In addition to the very weak binding forces between helium atoms, there is a reduction of the binding by the zero-point motion.

- The ground-state energy (zero-point energy) of a particle with mass *m in such a cage is given by:*

$$E_0 = \frac{h^2}{8\,ma^2}\,, \qquad \textit{or} \qquad E_0 = \frac{3\hbar^2\pi^2}{2mV^{2/3}}\,.$$

- where $a = (V_m/N_0)^{1/3}$ is the radius of the sphere to which the atoms are confined, and N_0 *is Avogadro's number,* 6.022×10^{23} *atoms* mol^{-1}.

- From this result, we can directly see that the zero-point energy for atoms with a small mass like helium is large and that it increases with decreasing molar volume V_m.

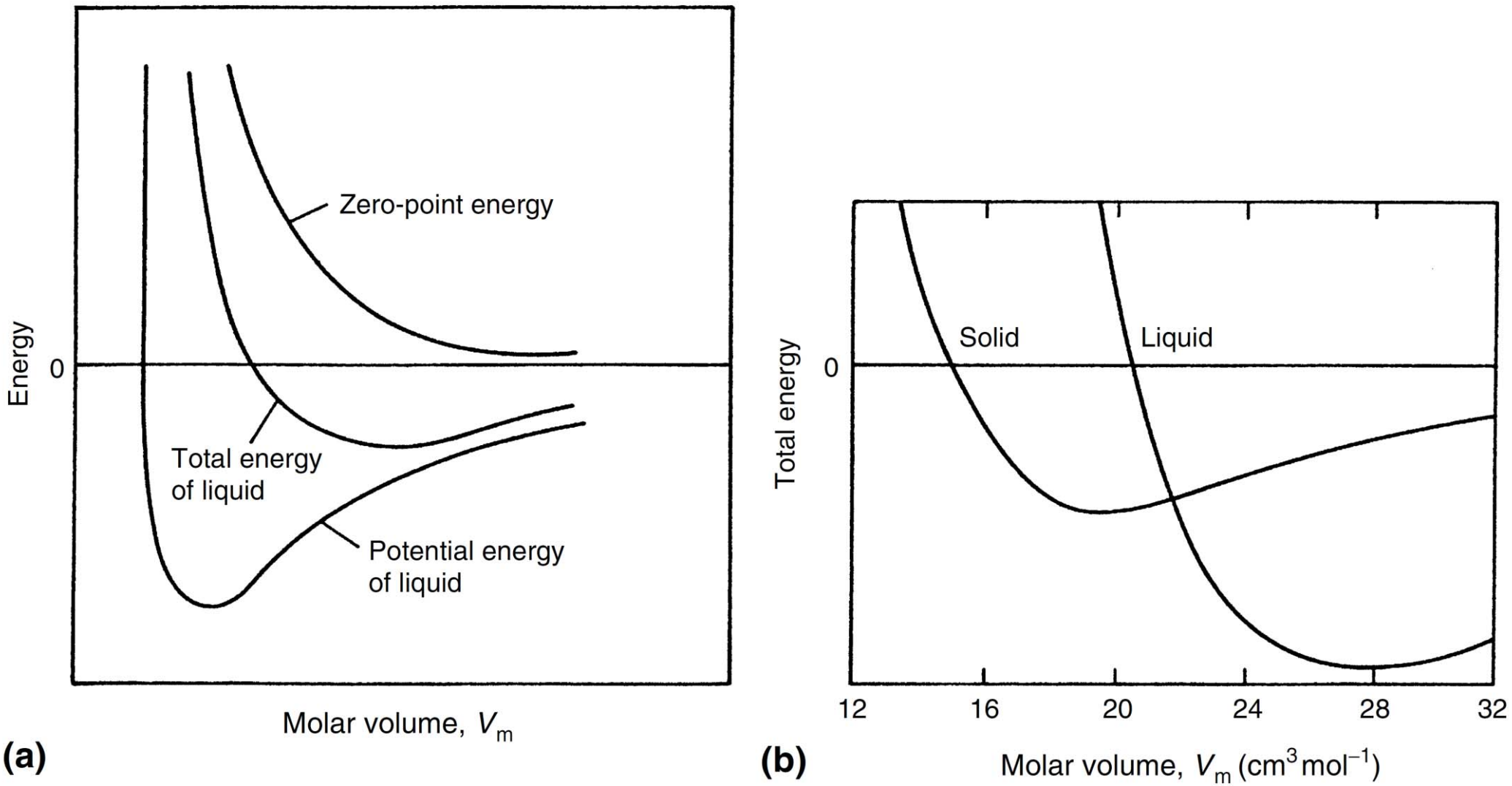

Fig. 2.5. (**a**) Zero-point and potential energies of liquid ^{4}He as a function of molar volume. The total energy is the sum of these two energies. (**b**) Illustration of why the liquid state is the stable one for helium at saturated vapour pressure even at $T = 0\,\mathrm{K}$

- Because of the strong influence of quantum effects on their properties, the helium liquids are called quantum liquids. In general, this term is used for any liquid whose kinetic (or zero-point) energy is larger than its potential (or binding) energy.

- To distinguish these liquids from classical liquids one introduces a quantum parameter $\lambda = E_{kin}/E_{pot}$. *These parameters* λ *for* some cryoliquids are:

liquid:	Xe	Kr	Ar	N_2	Ne	H_2	^{4}He	^{3}He
λ:	0.06	0.10	0.19	0.23	0.59	1.73	2.64	3.05

indicating that hydrogen and the helium isotopes are quantum liquids in this sense.

Table 1.1. Some important material parameters of ^{3}He and ^{4}He. After [12, 13]

	^{3}He	^{4}He
boiling temperature at normal pressure T_b (K)	3.19	4.21
critical temperature T_c (K)	3.32	5.19
critical pressure p_c (bar)	1.16	2.29
density for $T \to 0$ ϱ_0 ($\mathrm{g\,cm^{-3}}$)	0.076	0.145
density at boiling point ϱ_b ($\mathrm{g\,cm^{-3}}$)	0.055	0.125

Density of Helium

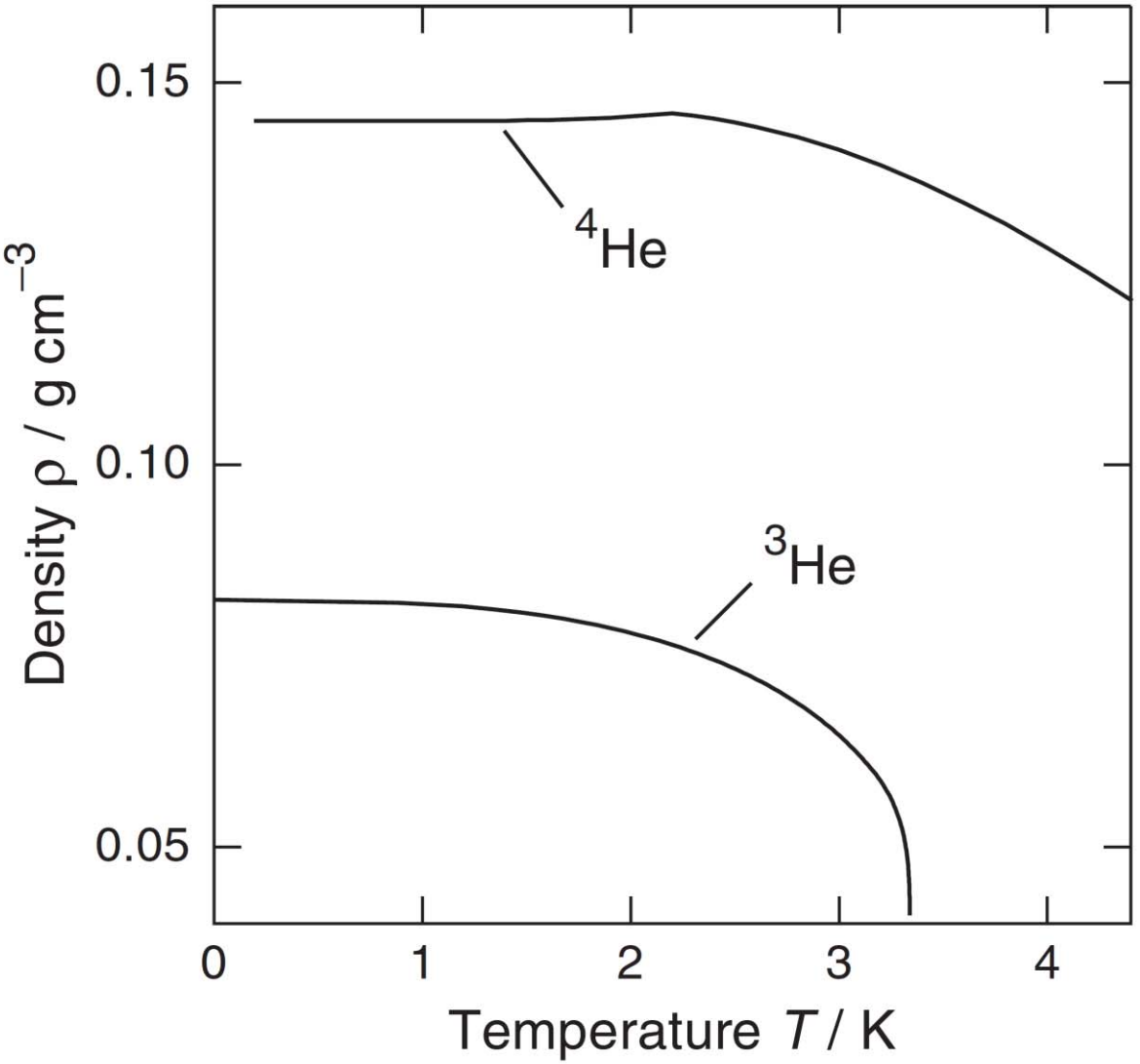

Latent Heat of Helium

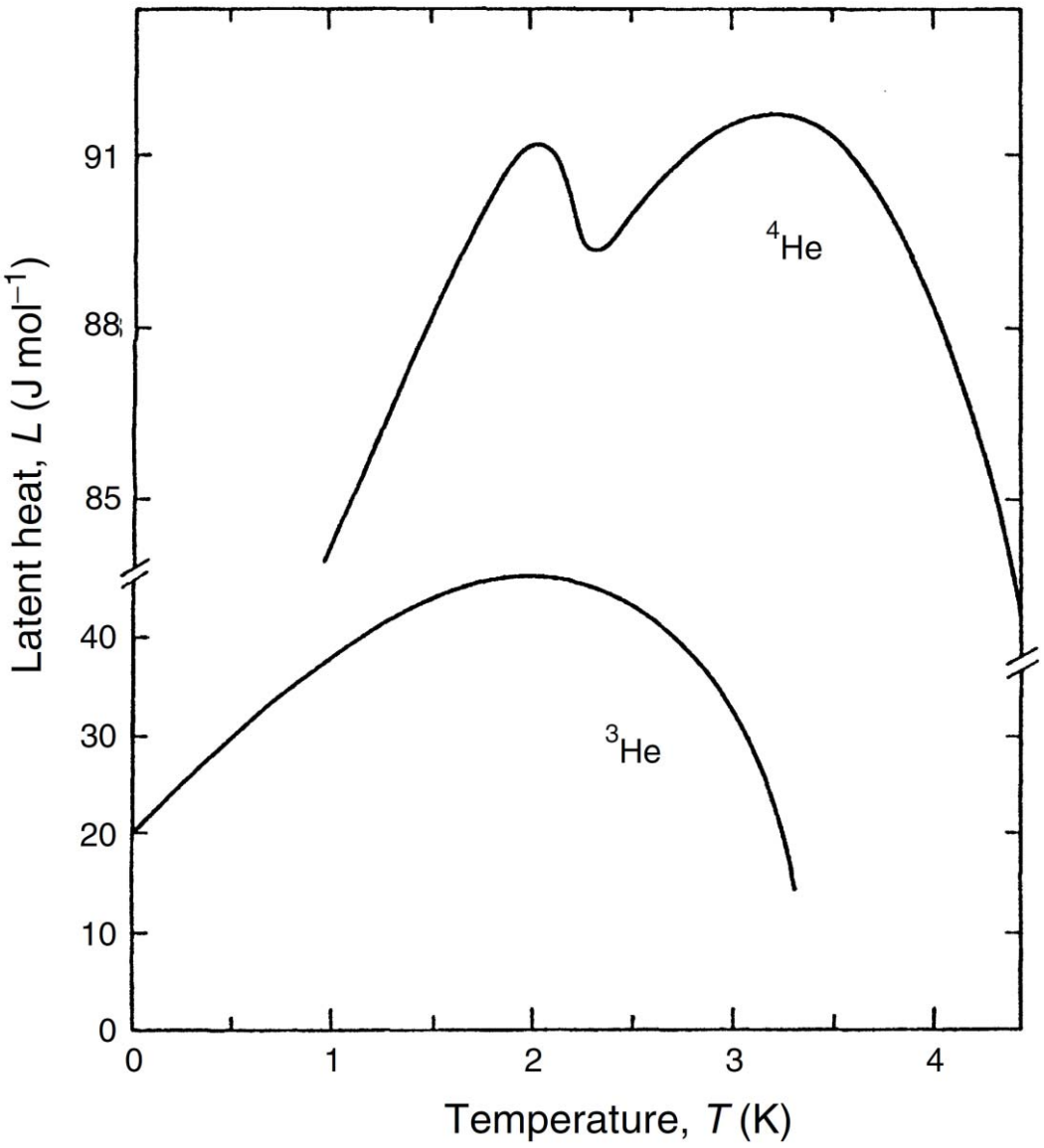

Table 2.1. Properties of some liquids (T_b is the boiling point at $P = 1\,\mathrm{bar}$, T_m the melting point at $P = 1\,\mathrm{bar}$, $T_\mathrm{tr}(P_\mathrm{tr})$ the triple-point temperature (pressure), $T_\mathrm{c}(P_\mathrm{c})$ the critical temperature (pressure), and L the latent heat of evaporation at T_b). The data have mostly been taken from [2.3–2.5, 2.17]

subst.	T_b (K)	T_m (K)	T_tr (K)	P_tr (bar)	T_c (K)	P_c (bar)	lat. heat, L ($\mathrm{kJ\,l^{-1}}$)	vol% in air
H_2O	373.15	273.15	273.16	0.06*	647.3	220	2,252	–
Xe	165.1	161.3	161.4	0.82	289.8	58.9	303	0.1×10^{-4}
Kr	119.9	115.8	114.9	0.73	209.4	54.9	279	1.1×10^{-4}
O_2	90.1	54.4	54.36	0.015	154.6	50.4	243	20.9
Ar	87.2	83.8	83.81	0.69	150.7	48.6	224	0.93
N_2	77.2	63.3	63.15	0.13	126.2	34.0	161	78.1
Ne	27.1	24.5	24.56	0.43	44.5	26.8	103	18×10^{-4}
n-D_2	23.7	18.7	18.69	0.17	38.3	16.6	50	–
n-H_2	20.3	14.0	13.95	0.07	33.2	13.2	31.8	0.5×10^{-4}
^{4}He	4.21	–	–	–	5.20	2.28	2.56	5.2×10^{-4}
^{3}He	3.19	–	–	–	3.32	1.15	0.48	–

* The exact value is $P_\mathrm{tr} = 61.1657\,\mathrm{mbar}$

Vapour Pressure of Helium

- The vapour pressure can be calculated, at least to a first approximation, from the Clausius–Clapeyron equation:

$$\left[\frac{\mathrm{d}P}{\mathrm{d}T}\right]_{\mathrm{vap}} = \frac{S_{\mathrm{gas}} - S_{\mathrm{liq}}}{V_{\mathrm{m,gas}} - V_{\mathrm{m,liq}}},$$

- where *S is the entropy and* V_m *the molar volume.* If we take into account that the difference in the entropies of the liquid and gaseous phases is *L/T, that the molar volume of the liquid is much smaller* than the molar volume of the gas, and that in a rough approximation the molar volume of helium gas is given by the ideal gas equation: $V_{gas} \cong RT/P$, then we obtain:

$$\left[\frac{\mathrm{d}P}{\mathrm{d}T}\right]_{\mathrm{vap}} \cong \frac{L(T)P}{RT^2}, \qquad P_{\mathrm{vap}} \propto \mathrm{e}^{-L/RT}$$

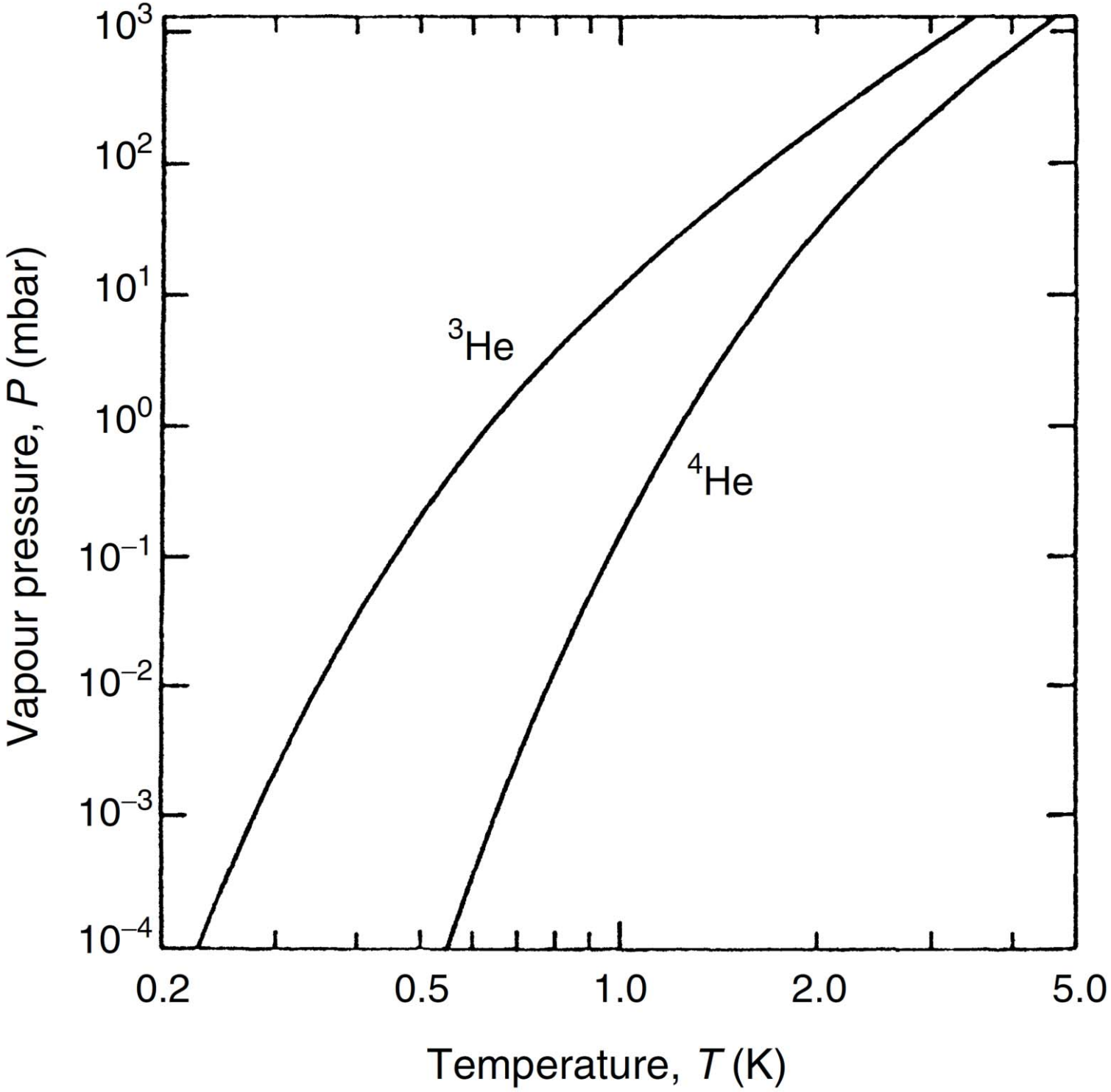
10^3
10^2
10^1
10^0
10^{-1}
10^{-2}
10^{-3}
10^{-4}
Vapour pressure, P (mbar)
^{3}He
^{4}He
0.2
0.5
1.0
2.0
5.0
Temperature, T (K)

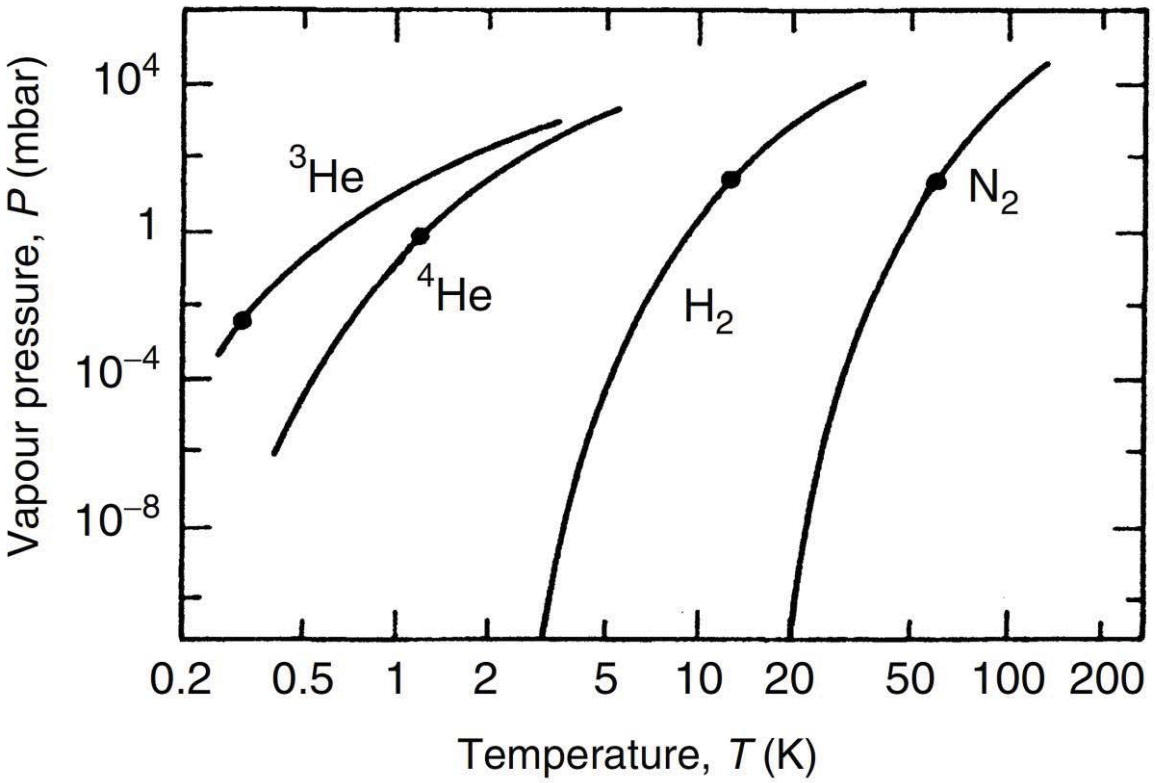

Fig. 2.8. Vapour pressures of various cryoliquids. The dots indicate the practical lower limits for the temperatures which can be obtained by reducing the vapour pressure above these liquids

- One can pump on the vapour above a liquid, for example above a liquid-helium bath, to obtain temperatures below the normal (1 bar) boiling point.

- If one pumps away atoms from the vapour phase, the most energetic ("hottest") atoms will leave the liquid to replenish the vapour. Therefore the mean energy of the liquid will decrease; it will cool.

- For a pumped-on liquid bath where $\dot{n}$ *particles/time are moved to the vapour phase, the cooling power* is given by:

$$\dot{Q} = \dot{n}(H_{\mathrm{liq}} - H_{\mathrm{vap}}) = \dot{n}\dot{L}\,.$$

- Usually a pump with a constant-volume pumping speed d*V/dt* *is used and therefore* the mass flow d*n/dt* *across the liquid–vapour boundary is proportional to the* vapour pressure:

$$\dot{n} \propto P_{\mathrm{vap}}(T)\,,$$

$$\dot{Q} \propto LP_{\mathrm{vap}} \propto \mathrm{e}^{-1/\mathrm{T}}\,.$$

- This last equation demonstrates that the cooling power decreases rapidly with decreasing temperature because the vapour pressure decreases rapidly with decreasing temperature and pumping becomes less and less efficient.

- The practical low-temperature limits determined by experimental parameters are typically about 1.3K for ^{4}He and 0.3K for ^{3}He.

- The temperature dependence of the vapour pressure of liquid helium is well known and can be used for vapour-pressure thermometry.

- By measuring the vapour pressure above a liquid-helium bath (or other liquids at higher temperatures) one can read the temperature from the corresponding vapour pressure table. In fact, the helium-vapour pressure scale represents the low-temperature part of the international temperature scale ITS-90.

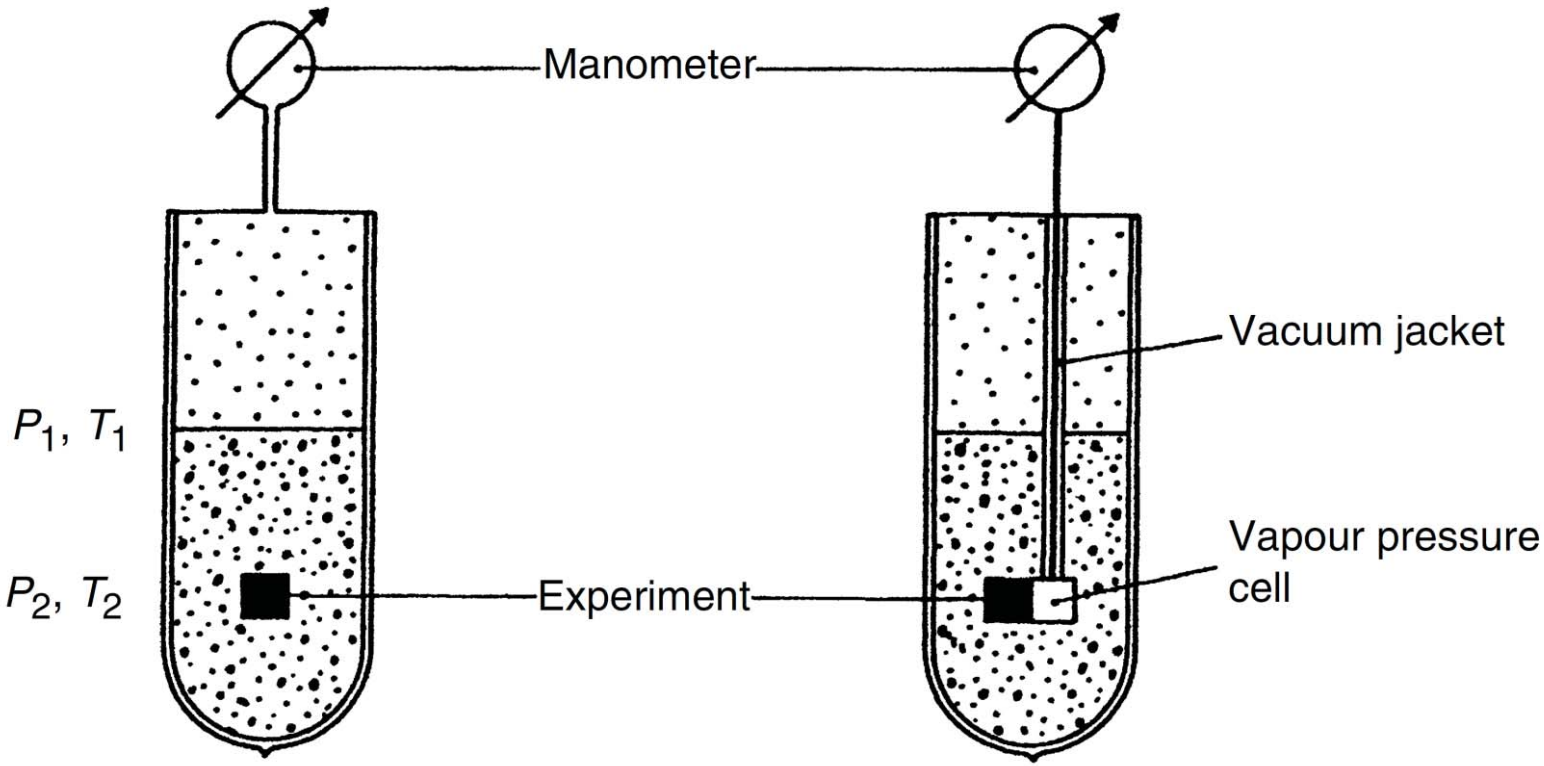

Fig. 12.2. Schematic setups for vapour pressure thermometry. *Left*: The vapour pressure above an evaporating cryoliquid is measured. Substantial temperature differences between the top of the liquid and the experiment can result due to the hydrostatic pressure head and temperature gradients in the liquid, which is usually not a good conductor (except for superfluid helium). *Right*: A small vapour pressure cell is connected to the experiment to avoid these problems. The capillary from this cell to the manometer at room temperature is vacuum jacketed to avoid changes due to a change in height of the cryoliquid

Specific Heat of Helium

- The first measurements of the specific heat of liquid 4He were performed by *Dana and Kamerlingh-Onnes in 1923.*

- They found an abnormal rise of the specific heat around 2K. In the publication of their results in 1926 they decided to leave out these data points, because they feared that this anomaly might have been caused by experimental problems.

- In 1932 *Keesom and Clusius investigated the specific heat of liquid 4He again and observed a* pronounced maximum at about 2.17 K, which they attributed to a phase transition.

- Since the true nature of the phase transition was unclear for a long time, the two phases were distinguished by naming them helium I and helium II, where helium I denotes the liquid phase above the transition.

- The nature of the phase transition at 2.17K can be understood as Bose–Einstein condensation.

specific heat of ^{4}He – the Greek letter λ

lambda point

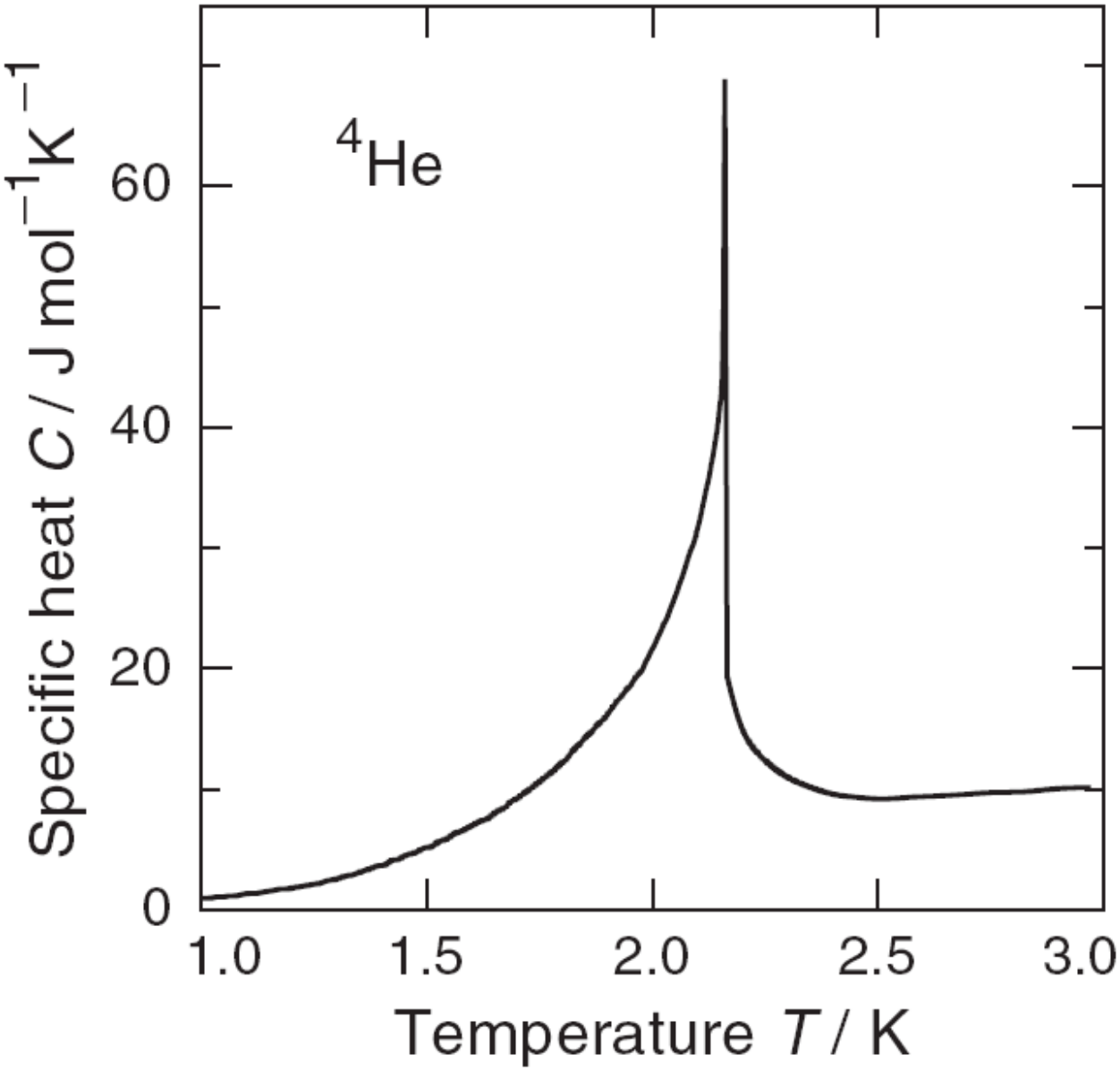

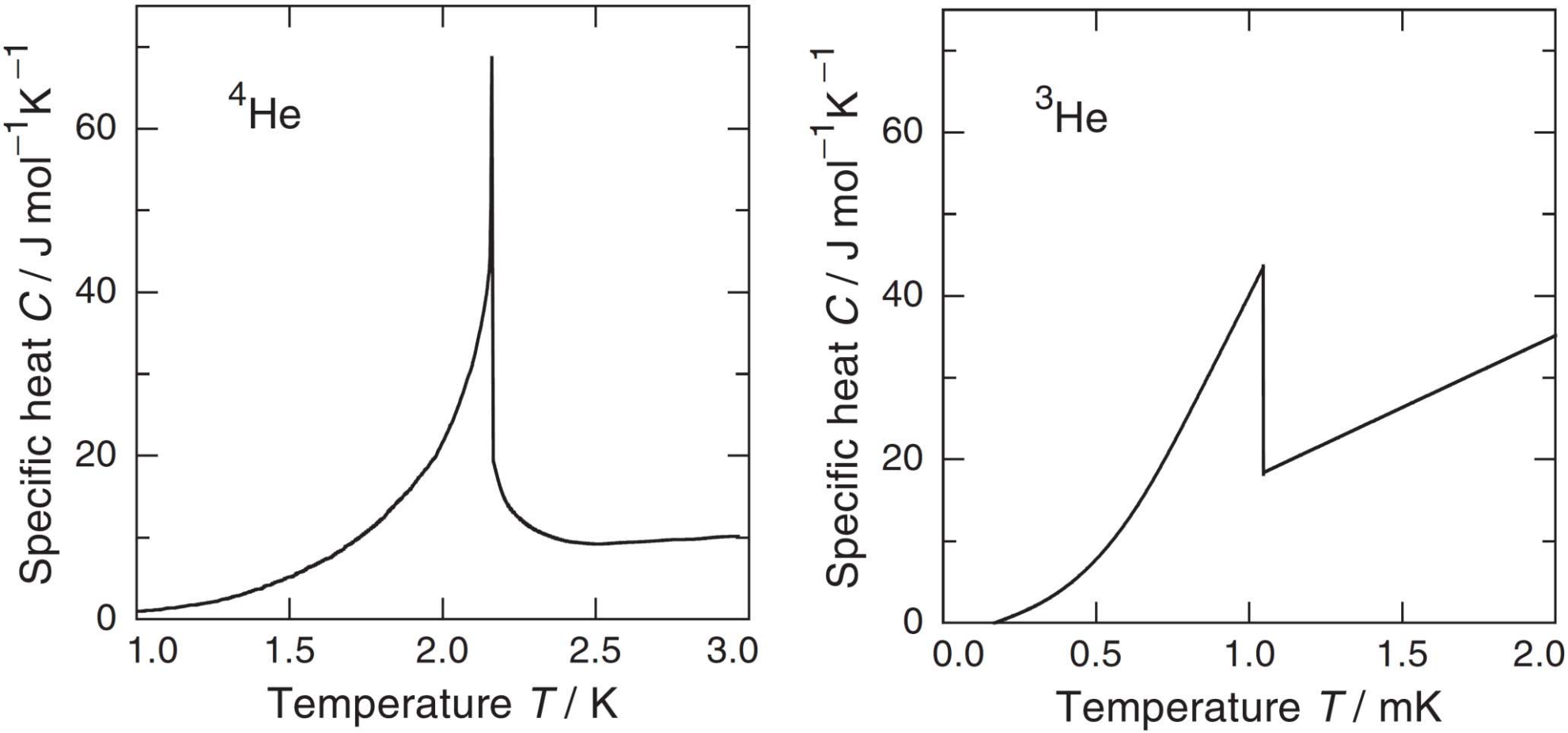

Fig. 1.3. Specific heat of (**a**) ^{4}He [20] and (**b**) ^{3}He [21] in the temperature range where the transition from the normal to the superfluid phase occurs, as a function of temperature

Phase Diagram

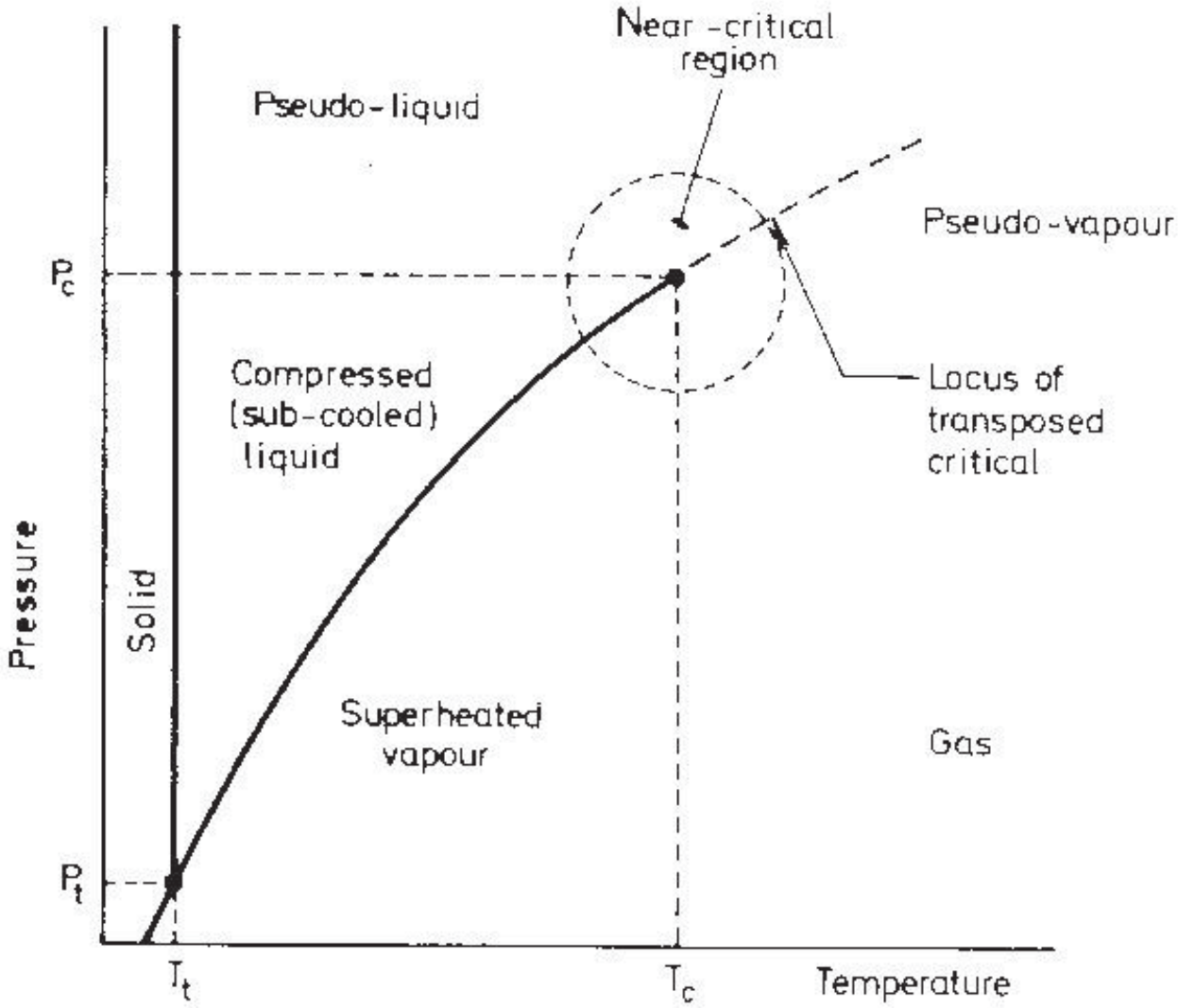

Fig. 2.1 Definition of the various thermodynamic regions.

ciekły azot T_w=77,35K

T_t=63,5 K

Phase diagram of ^{4}He

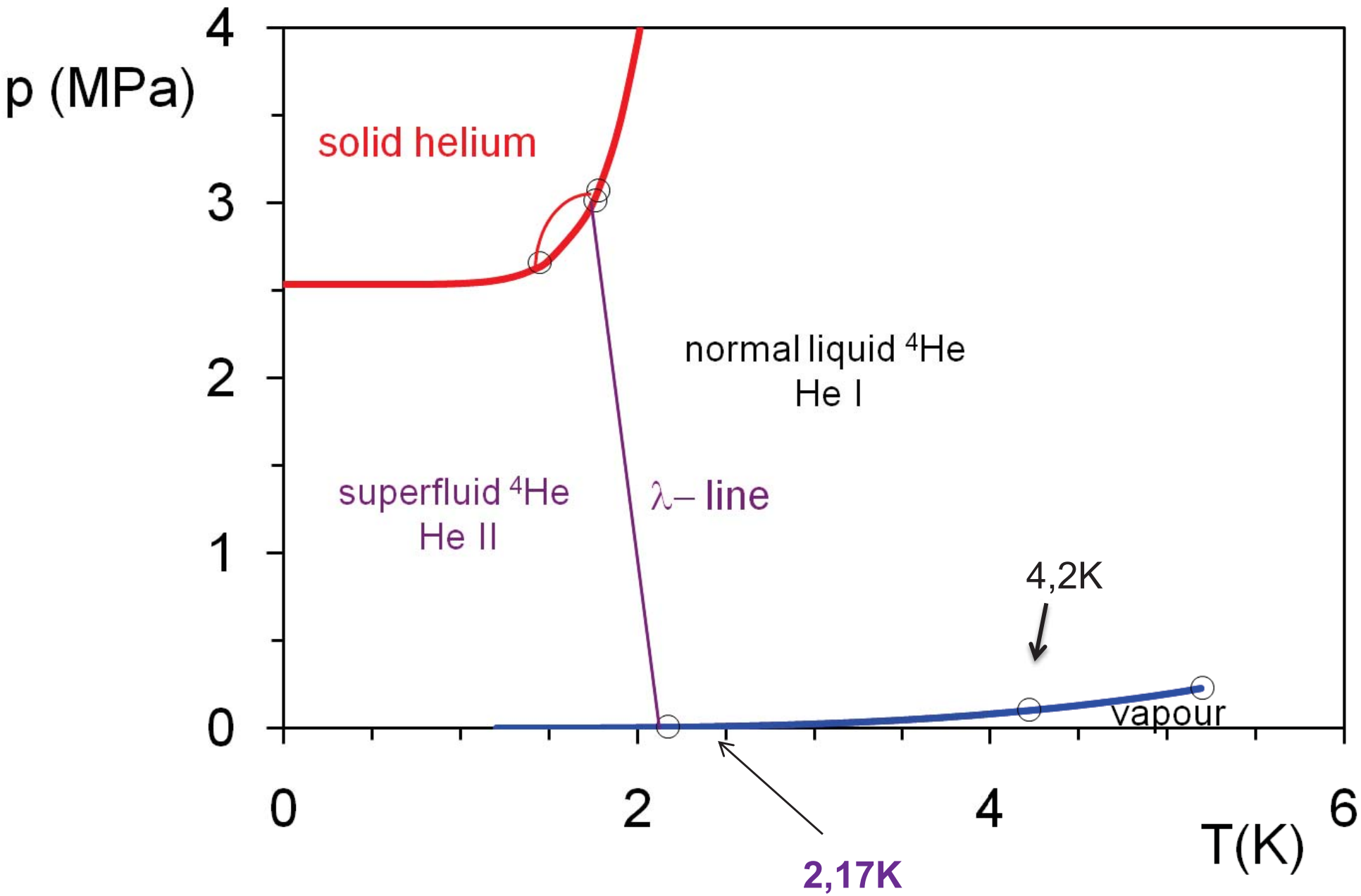

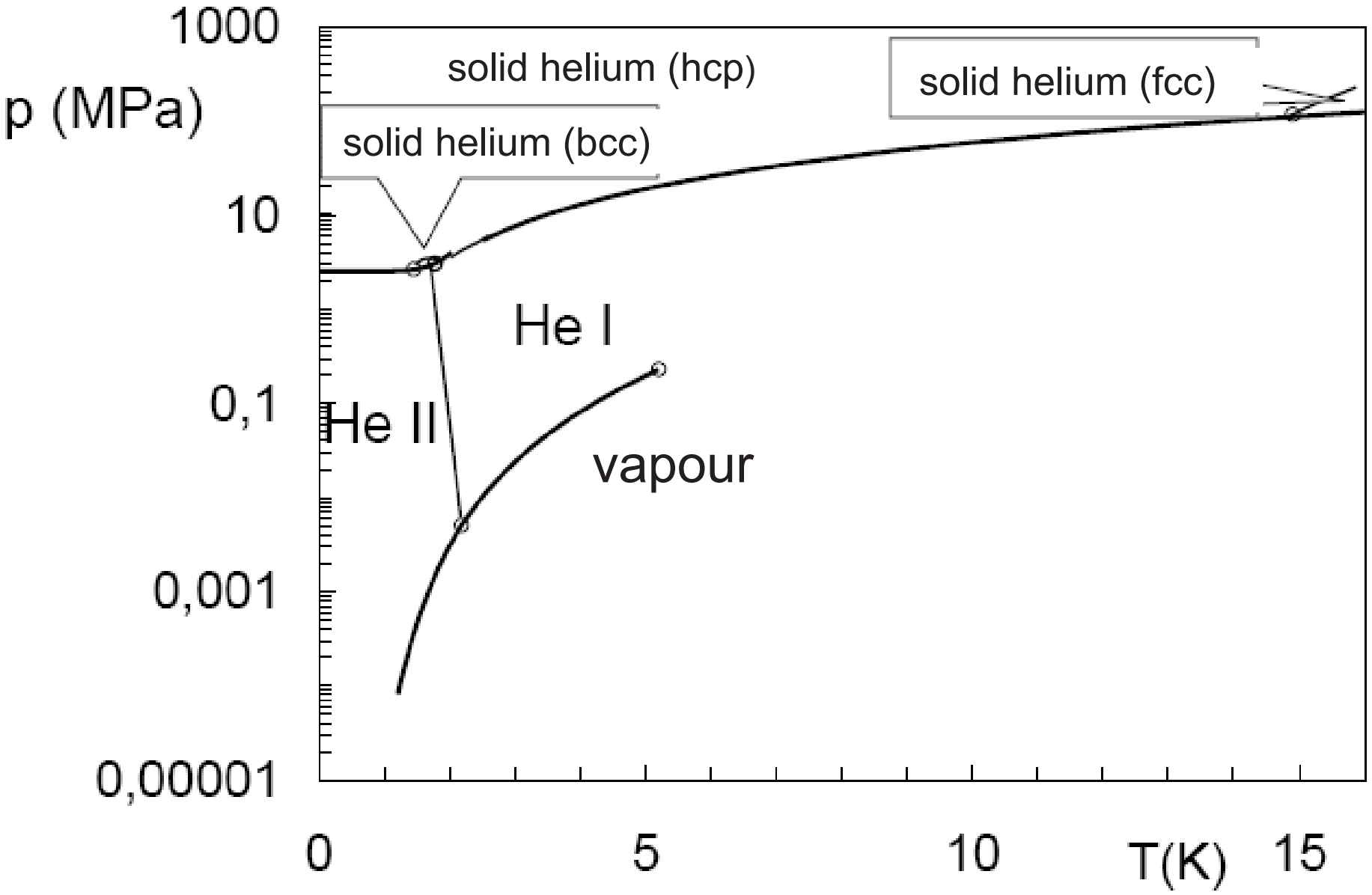

Phase diagram of ^{4}He

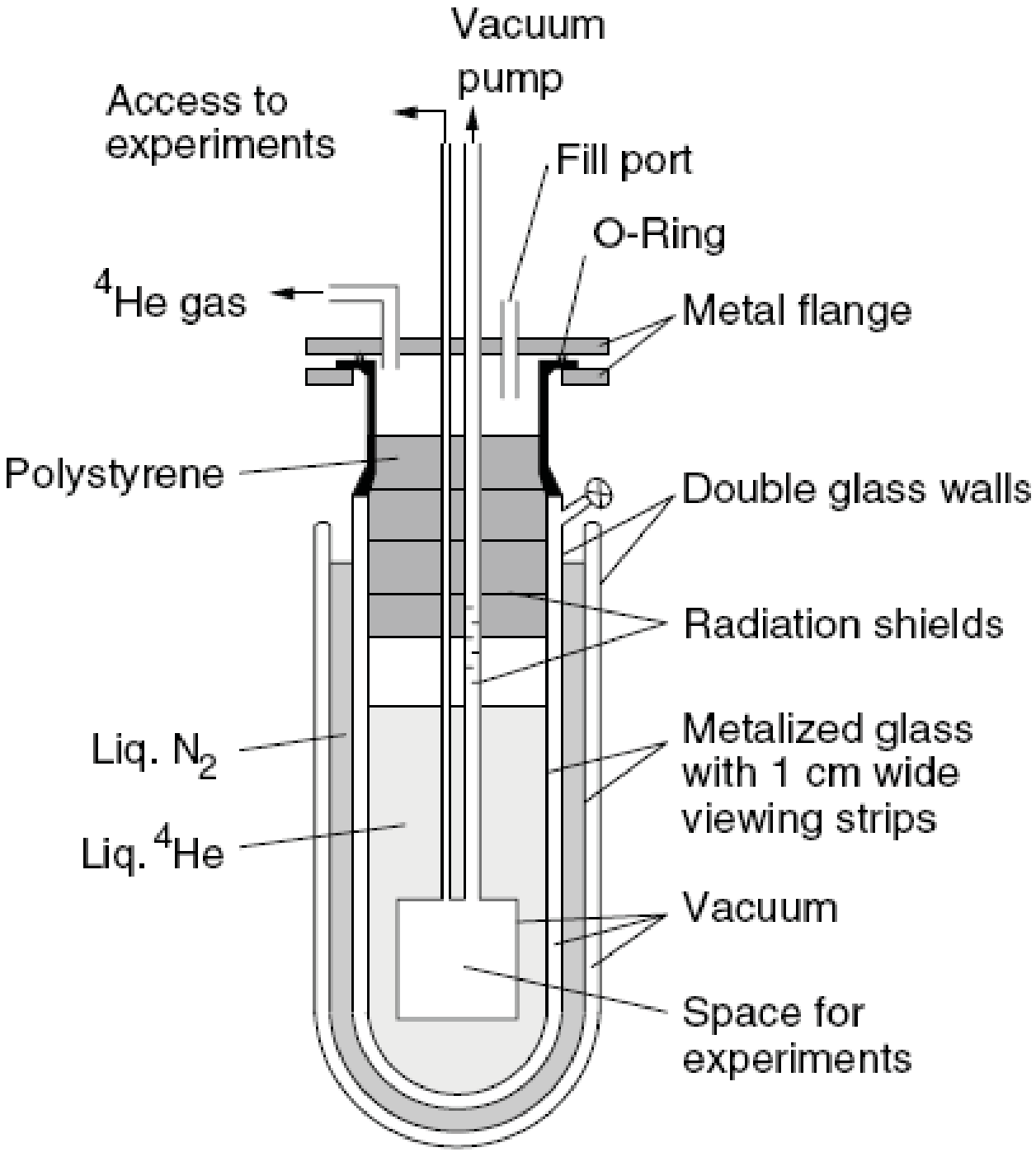
Vacuum
pump
Access to
experiments
Fill port
O-Ring
^{4}He gas
Metal flange
Polystyrene
Double glass walls
Radiation shields
Liq. N_2
Metalized glass
with 1 cm wide
viewing strips
Liq. ^{4}He
Vacuum
Space for
experiments

vacuum
pump

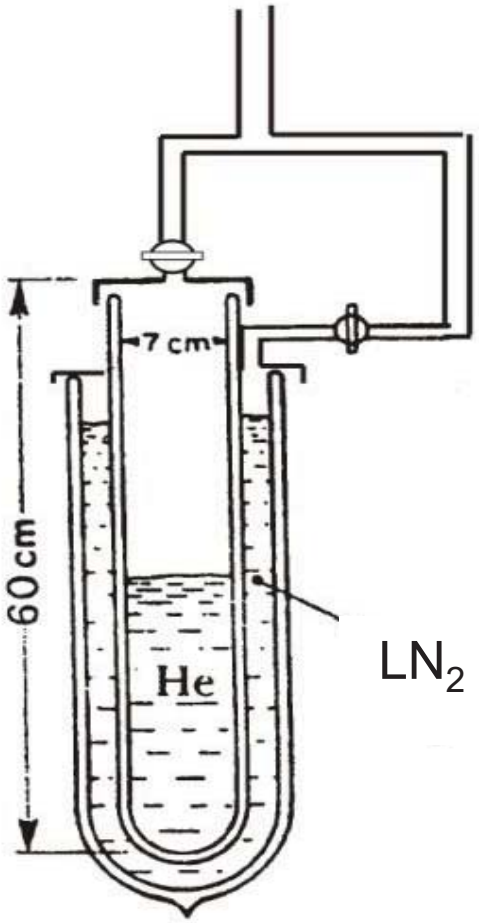

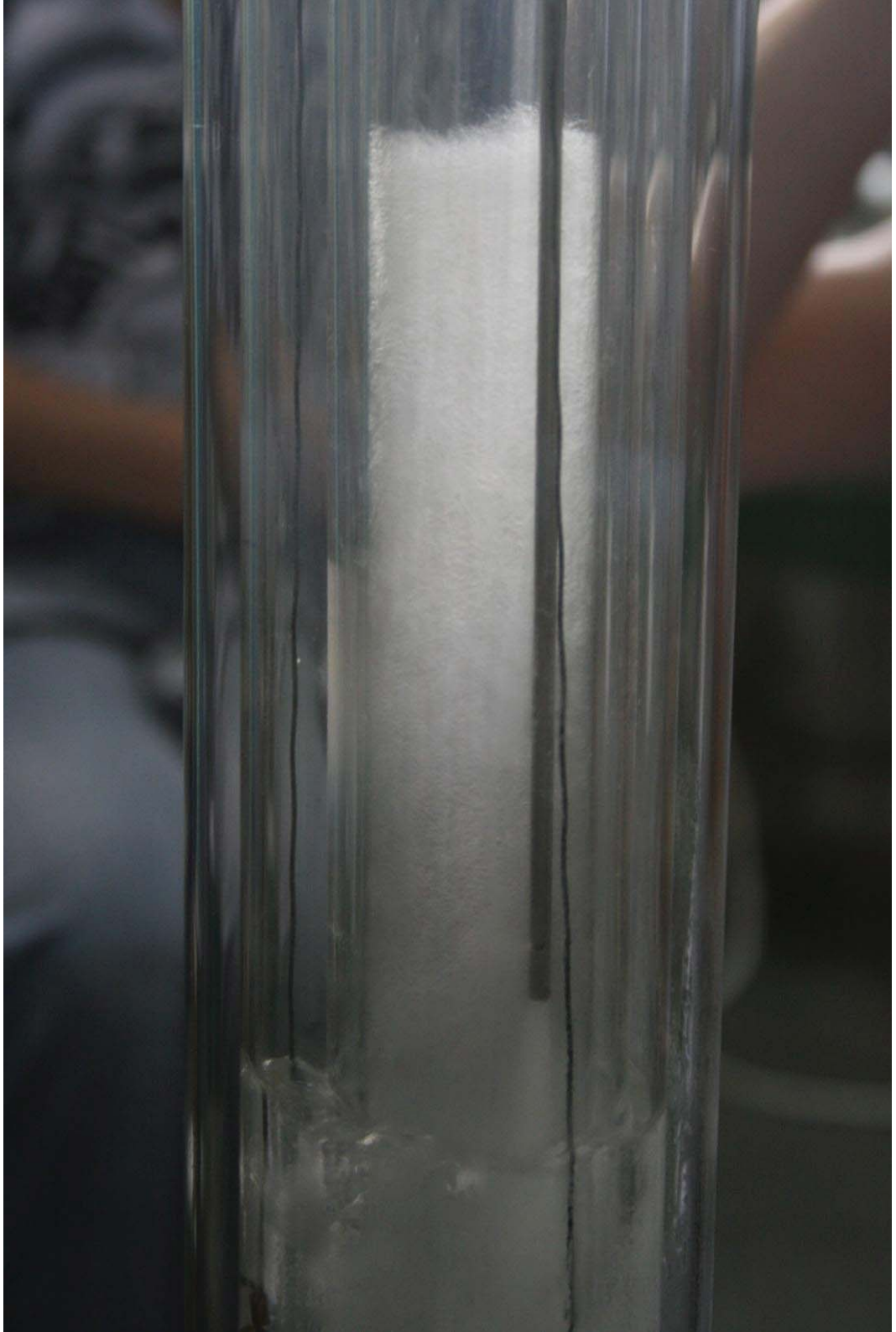

liquid helium

T=4,2K

(-269°C)

Institute of Molecular Physics,
Polish Academy of Sciences,

Division of Low Temperature
Physics in Odolanów

$T > T_\lambda = 2{,}17K$

$T < T_\lambda$

λ- transition **2,17K** (-270,98ºC)

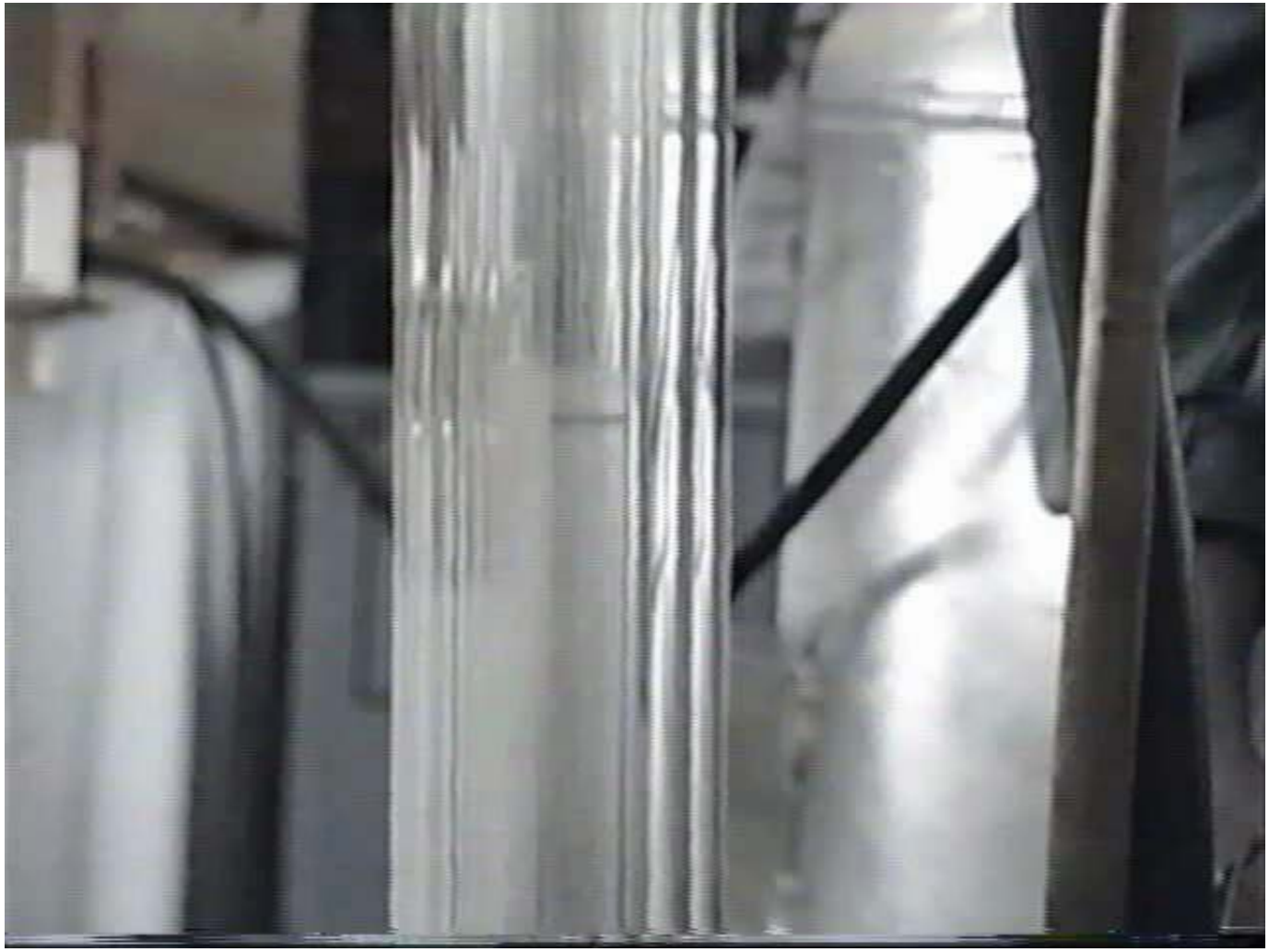

Superfluid ^{4}He – Helium II

Viscosity and Superfluidity

Hagen–Poiseuille law

$$\dot{V} = \frac{\pi r^4}{8} \frac{1}{\eta} \frac{\Delta p}{L},$$

L - denotes the length of the capillary,
r - the radius,
Δp - the pressure drop along the capillary
$\dot{V}$ *- the volume rate of helium* transported through it

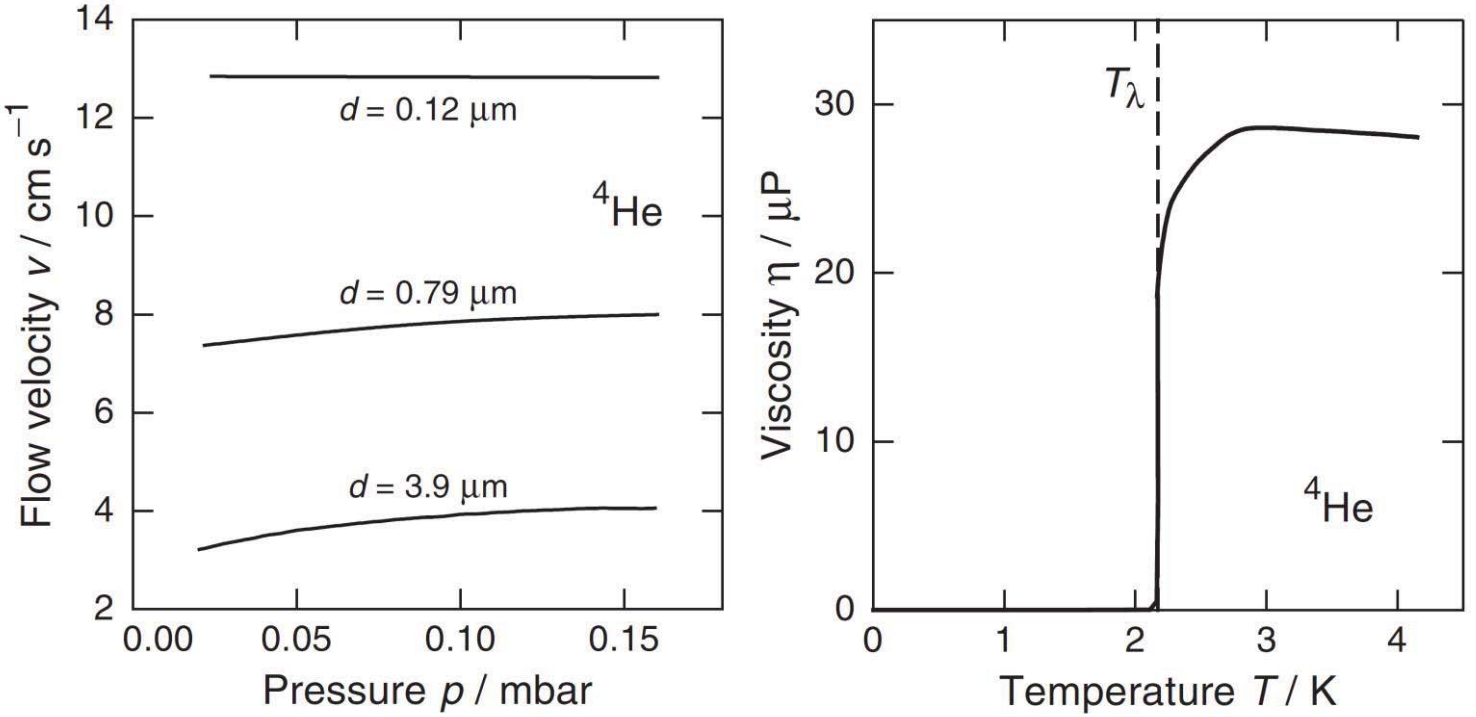

Fig. 2.1. (**a**) Flow velocity of helium II through capillaries with different diameter as a function of the applied pressure [39, 40]. (**b**) Temperature dependence of the viscosity of liquid helium as determined from flow experiments with thin capillaries

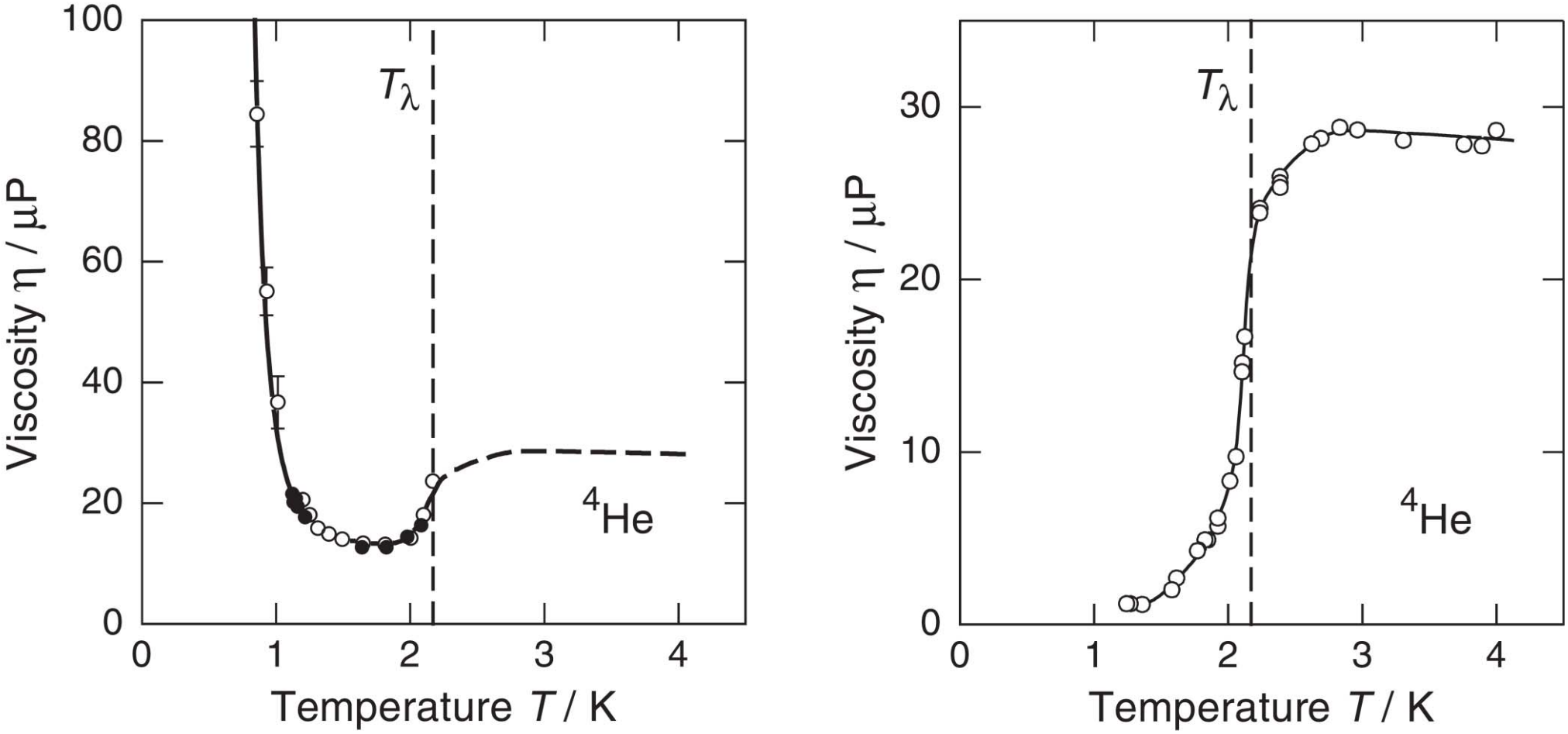

Fig. 2.2. Viscosity of liquid helium as a function of temperature measured (**a**) with a rotary viscosimeter [41, 42] and (**b**) with an oscillating disc [43]

Beaker Experiments

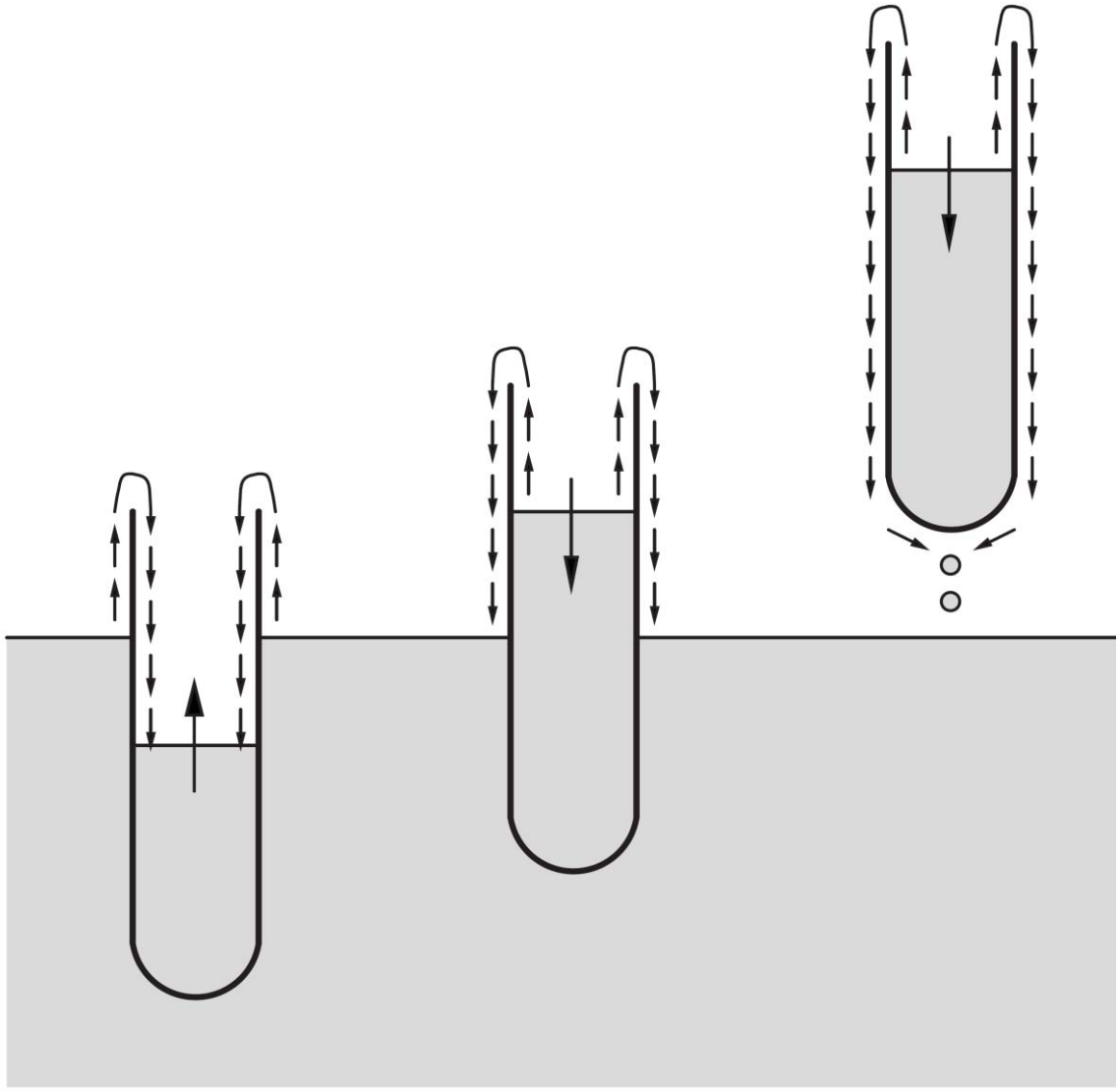

Superfluid helium will flow over the rim into an empty beaker dipped into a bath of helium II until the levels of helium inside and outside the beaker are equal (*left).*

Raising the beaker afterwards causes the helium II to flow back into the bath until equalization of the levels has taken place again (*middle).*

If the beaker is lifted completely out of the bath, helium II will flow over the rim of the beaker and will drop back into the bath until the beaker is empty (*right).*

Thermomechanical Effect

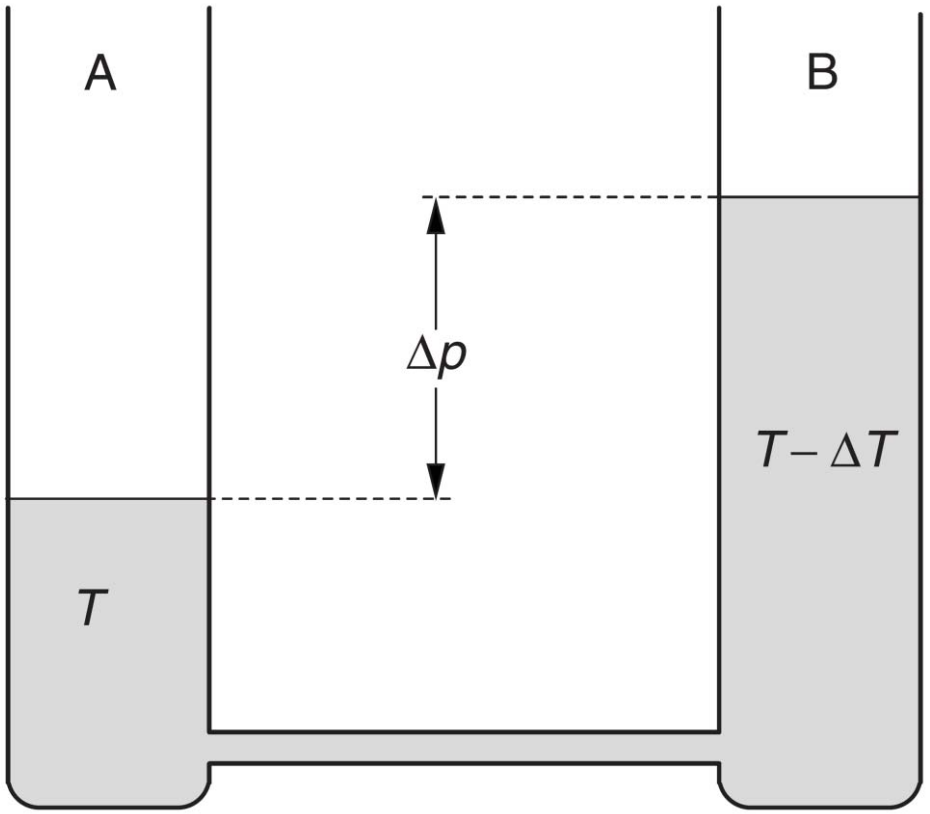

Two vessels (A and B), both containing helium II are connected via a very thin capillary.

Temperature and pressure are equal in both vessels at the beginning of the experiment and thus the helium levels in the two vessels are the same.

Increasing the pressure in A results in a flow of helium towards B. Surprisingly, this causes a difference in temperature in the two vessels. The temperature in B decreases somewhat, whereas it increases in A.

This experiment clearly shows that there is mass flow in helium II associated with the heat flow.

Fountain Effect

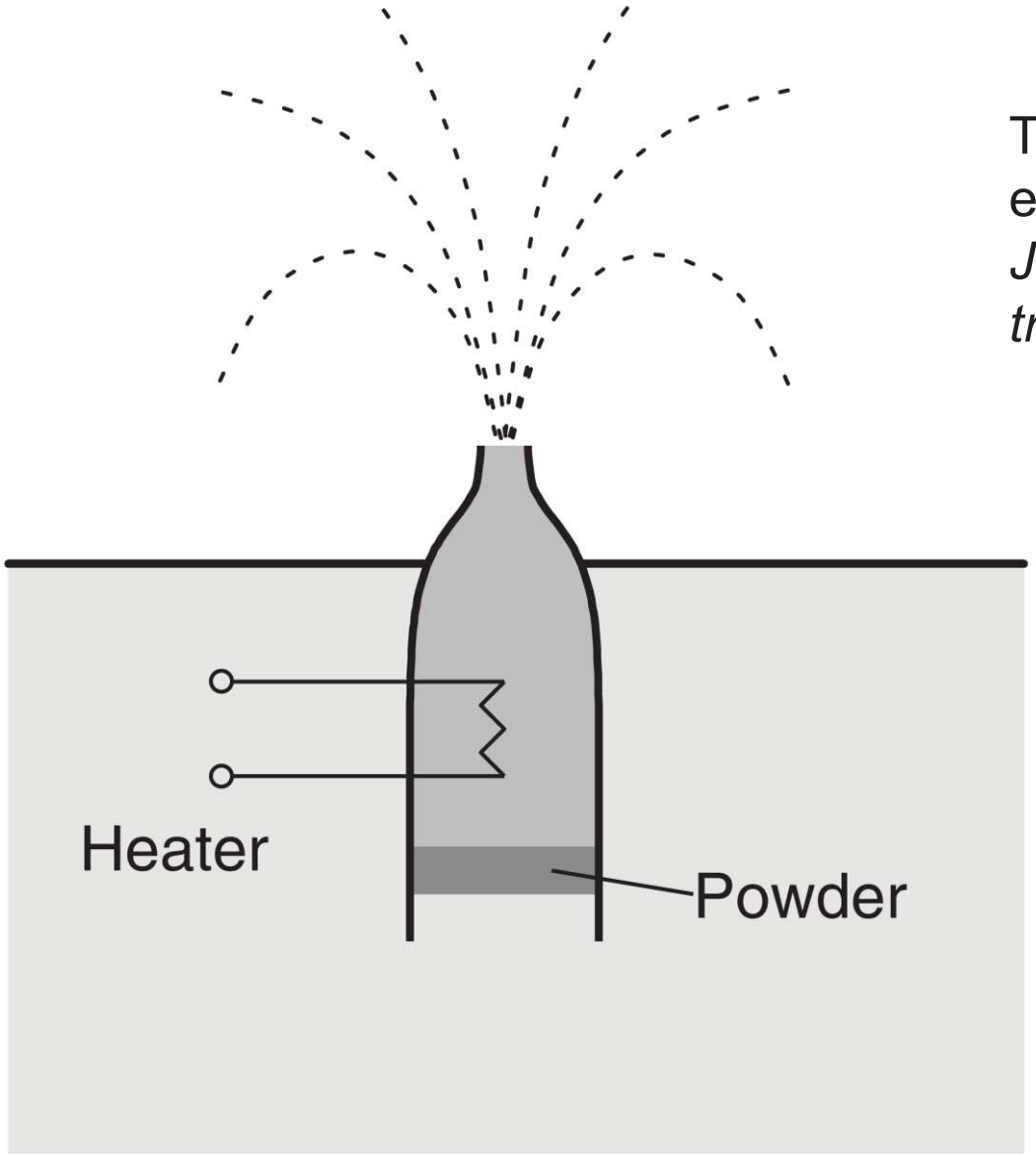

The reversal of the thermomechanical effect was first observed by *Allen and Jones in 1938 in connection with thermal transport* measurements.

Two-Fluid Model

- The basic idea of this concept was first suggested in 1938 by *Tisza, in order to describe* transport phenomena of helium II.
- The density of helium II as the sum of a normal-fluid and a superfluid component:

$$\varrho = \varrho_{\mathrm{n}} + \varrho_{\mathrm{s}} \, ,$$

Table 2.1. Basic assumptions of the two-fluid model

	density	viscosity	entropy
normal-fluid component	ϱ_{n}	$\eta_{\mathrm{n}} = \eta$	$S_{\mathrm{n}} = S$
superfluid component	ϱ_{s}	$\eta_{\mathrm{s}} = 0$	$S_{\mathrm{s}} = 0$

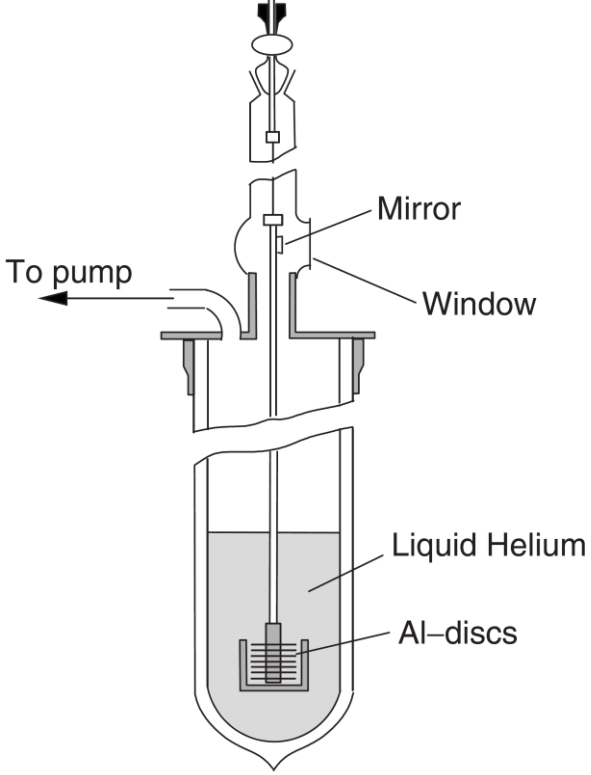

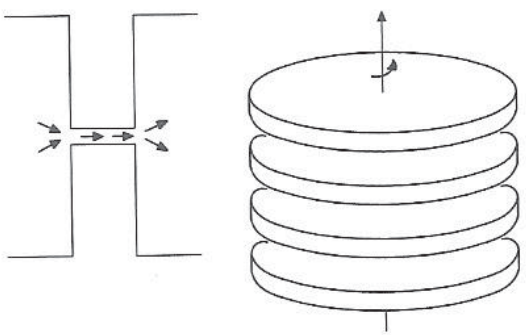

Fig. 2.5 Superfluid properties of He II. (a) Flow through narrow capillaries without resistance due to viscosity. (b) Inertia of a torsional oscillation of a stack of disks.

Fig. 2.12. Schematic drawing of the apparatus used by Andronikashvili to determine the normal-fluid density ϱ_n of helium II

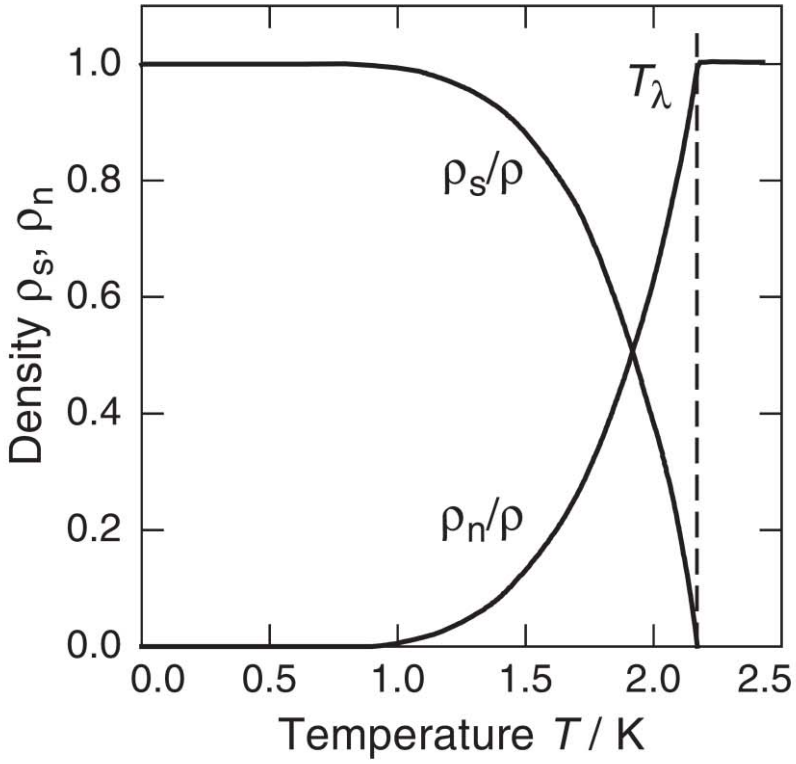

$n_s(T) \approx n - AT^4$ at very low T

$n_s \sim B(T_c - T)^{\upsilon}$ for $T<T_c$

$n_s = 0$ fot $T>T_c$

Fig. 2.11. Density of the superfluid and normal-fluid component in helium II as a function of temperature

Heat Transport

- The thermal conductivity of helium II is more than five orders of magnitude larger than that of helium I.
- The maximum of the heat current density is observed at about 1.8 K.
- The thermal conductivity Λ *would not be constant* but would diverge for small temperature gradients as $\Lambda \propto |grad\ T|^{-2/3}$.

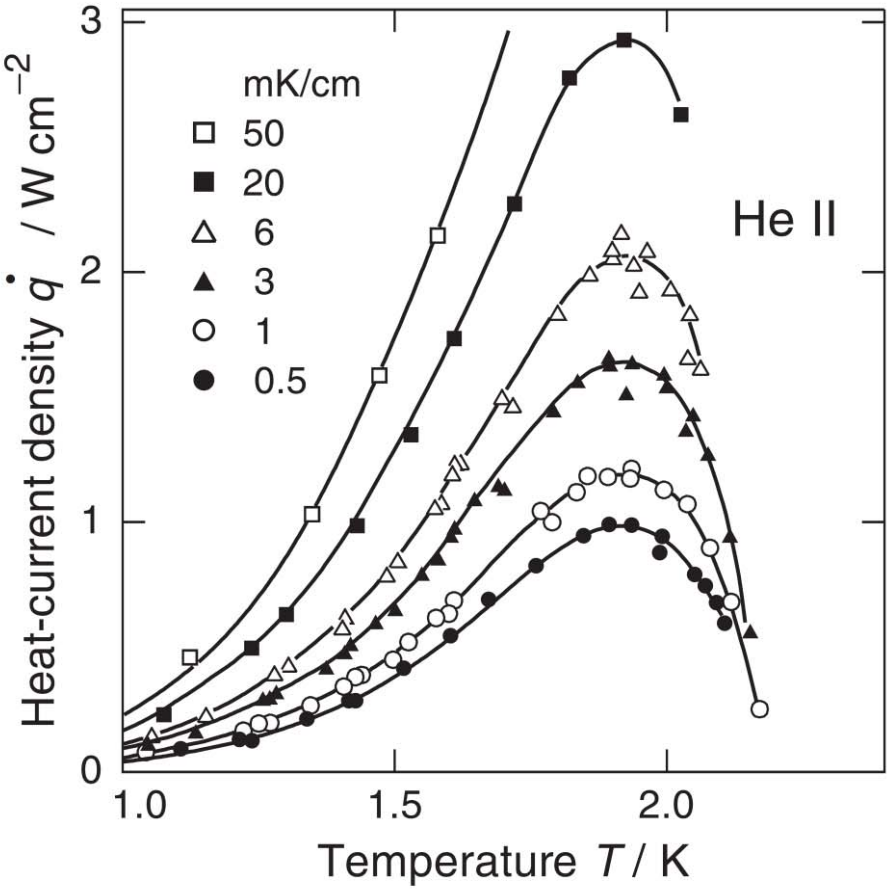

Fig. 2.8. Heat flow in helium II as a function of temperature for different temperature gradients along various capillaries with diameters between 0.3 mm and 1.5 mm [50]

Bose–Einstein condensation in Helium II

- For $T \rightarrow 0$ *the condensate* concentration is only about 13%.
- The pair-correlation function below T_λ *can be* written as:

$$g(r) - 1 = (1 - n_0)^2 \left[g^*(r) - 1 \right] ,$$

- where n_0 *denotes the condensate density and* $g^*(r)$ *the pair-correlation function* of the noncondensate atoms which, in practice, can be taken as being $g(r)$ at a temperature just above T_λ.

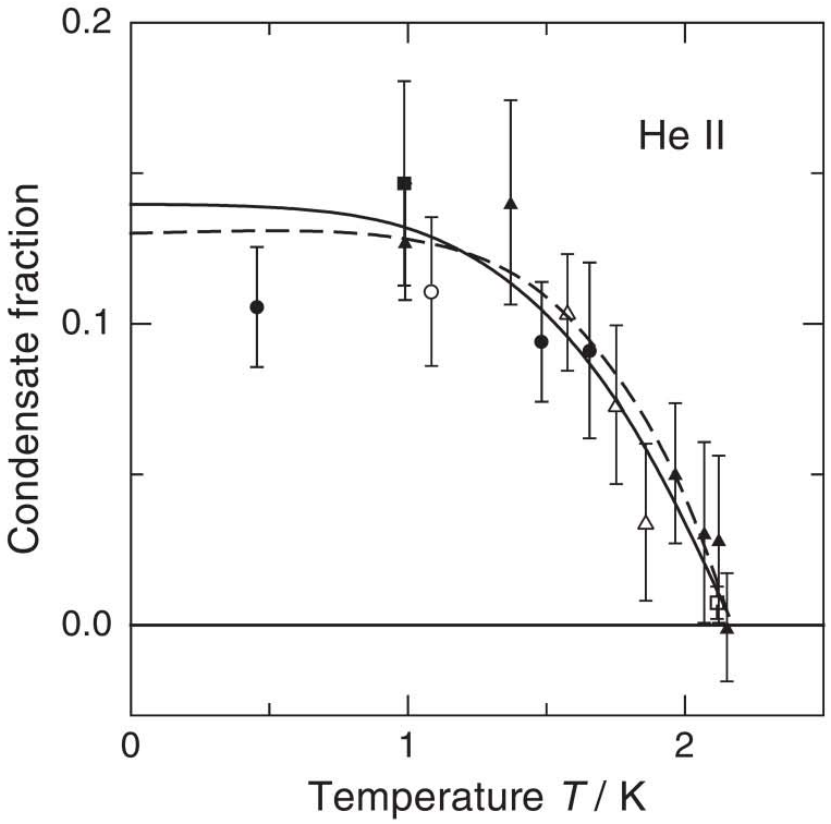

Fig. 2.33. Condensate concentration in helium II as a function of temperature. The experimental data are from X-ray scattering [77], neutron scattering [78–80] and measurements of the surface tension (*dashed curve*) [81]. The *solid line* represents an empirical fit of the data

Phonons and Rotons

For an ideal gas the energy of atoms is given by $E = p^2/2m$. *In such a* system, superfluidity cannot occur, because momentum transfer is allowed at infinitely small velocities. *Landau therefore proposed in 1941 that only collective* excitations exist in superfluid helium and that single-particle excitations are suppressed.

He assumed two kinds of collective excitations, longitudinal phonons with a linear dispersion and so-called *rotons that require* a minimum excitation energy *Δr.*

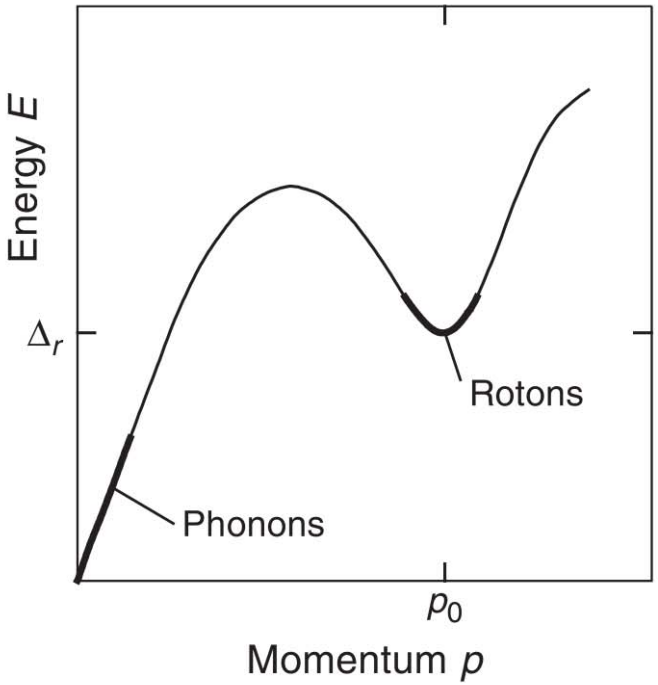

$$E = \Delta_{\mathrm{r}} + \frac{(p - p_0)^2}{2m^*}$$

Fig. 2.40. Dispersion curve of helium II, after a suggestion of Landau in 1947

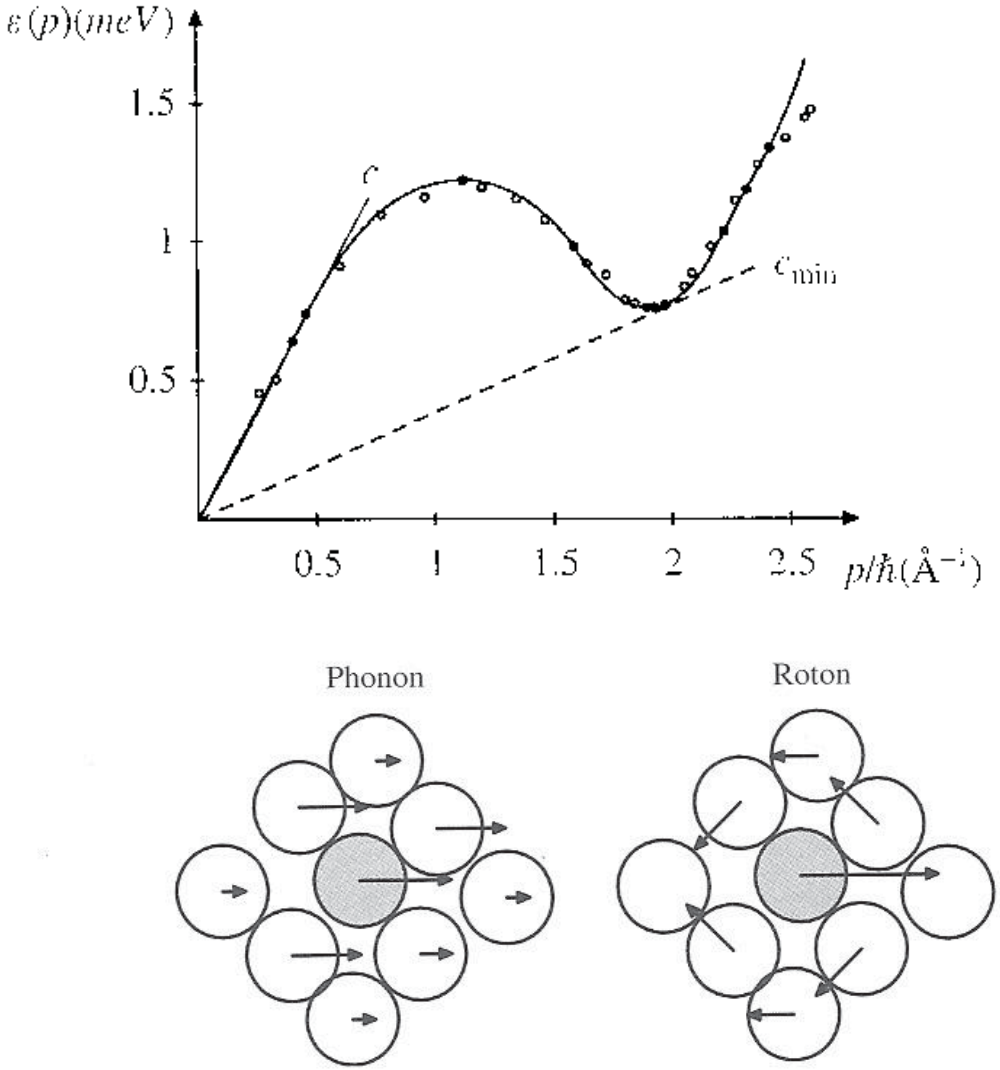

Fig. 2.17 Physical interpretation of the phonon and roton parts of the quasiparticle spectrum. The phonon motion corresponds to de Broglie wavelengths, $p = h/\lambda$ greater than a single atomic size, and leads to coupled motion of groups of atoms moving together, rather like a phonon in a solid. The roton corresponds to de Broglie wavelengths of order the interparticle separation. It corresponds to a central particle moving forward, while the close packed neighbors must move out of the way in a circular motion. Feynman notes that this combination of linear and circular motion has some nice similarity to a moving smoke-ring.

first sound $c \approx 238\ ms^{-1}$

second sound $c_s = c/\sqrt{3}$

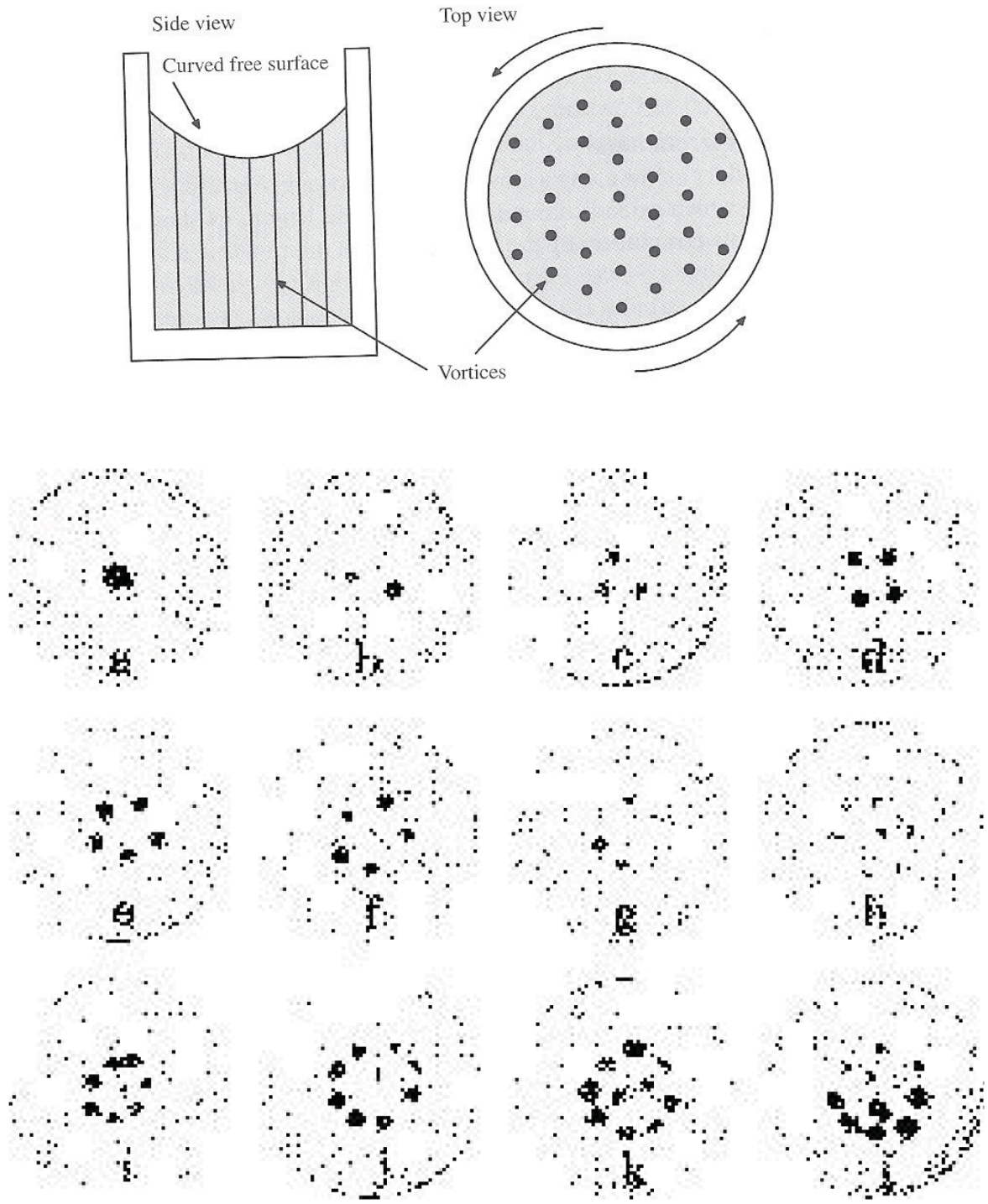

Fig. 2.38. Visualization of quantized vortices in rotating helium II of 0.1 K [93, 94]

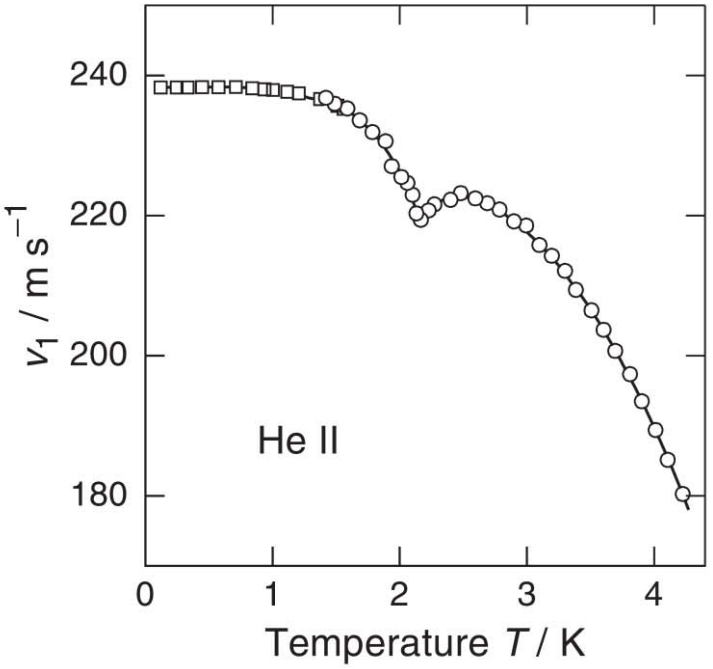

Fig. 2.20. Velocity of first sound in liquid helium as a function of temperature [62, 63]

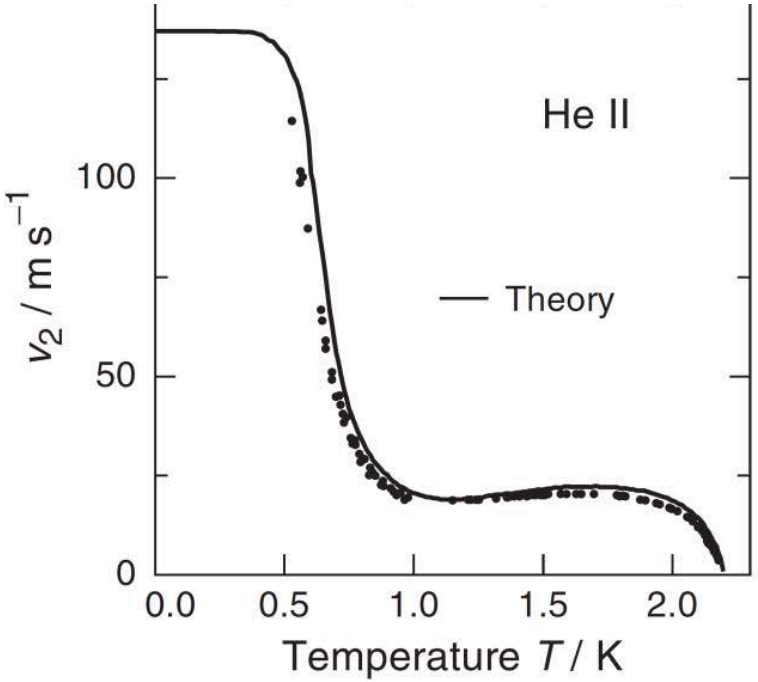

Fig. 2.21. Velocity of second sound in helium II as a function of temperature [53, 64]. The *solid line* shows the result of a calculation with (2.43) (after [65])

Second Sound of Helium II

- Temperature waves, which propagate with a characteristic velocity, was named *second sound.*
- The first experimental observation of second sound was made by *Peshkov in 1944*

$$v_2 = \sqrt{\frac{\varrho_\mathrm{s}}{\varrho_\mathrm{n}} S^2 \left(\frac{\partial T}{\partial S}\right)_\varrho} = \sqrt{\frac{\varrho_\mathrm{s}}{\varrho_\mathrm{n}} \frac{T S^2}{C_p}}$$

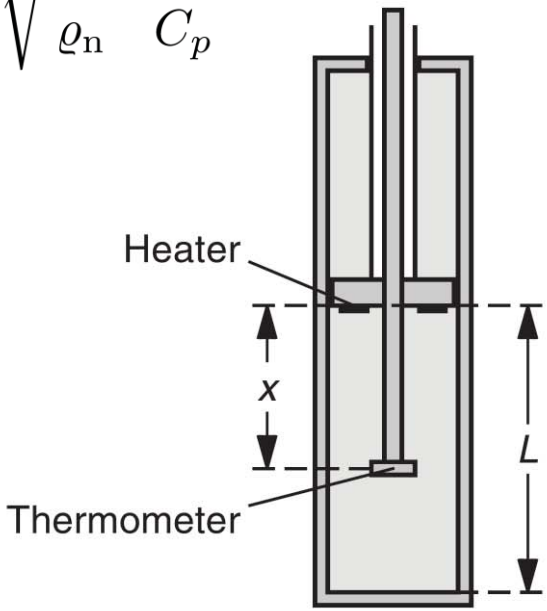

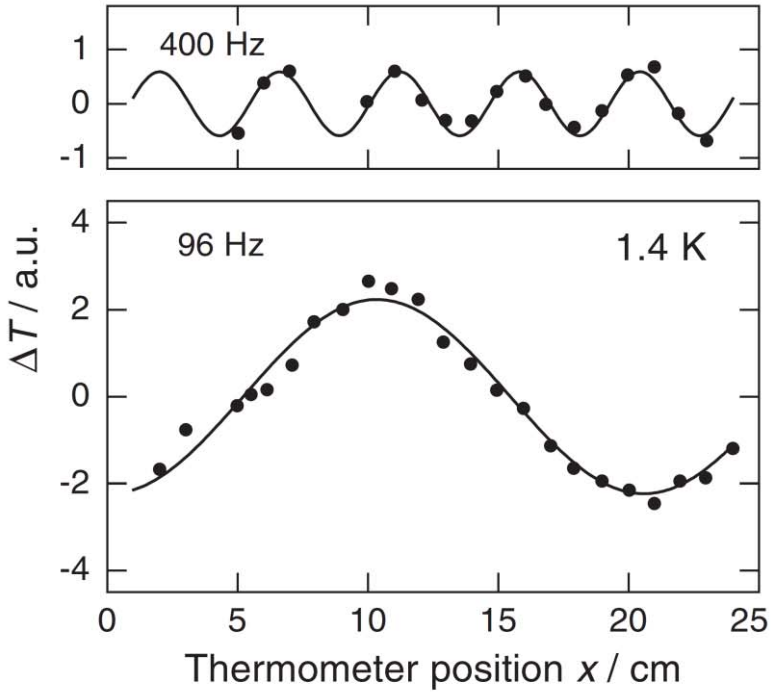

Fig. 2.10. (**a**) Schematic drawing of the apparatus used by Peshkov for the generation and detection of standing temperature waves in helium II. (**b**) Temperature of superfluid helium as a function of the thermometer position obtained at two different resonator modes [53]

Third Sound

- Propagating surface waves on thin helium films are called *third sound.*
- *Such* waves can be produced by local periodic heating of helium II films in the audio-frequency range. The heating causes oscillations of the film thickness, which then propagate as a surface wave on the film.
- Under most experimental conditions, the wavelength is much larger than the film thickness ($\Lambda >> d$) *and thus helium can only move parallel to the substrate* ($v_y = v_z = 0$). *The motion of the normal-fluid component is strongly* damped due to its viscous friction.

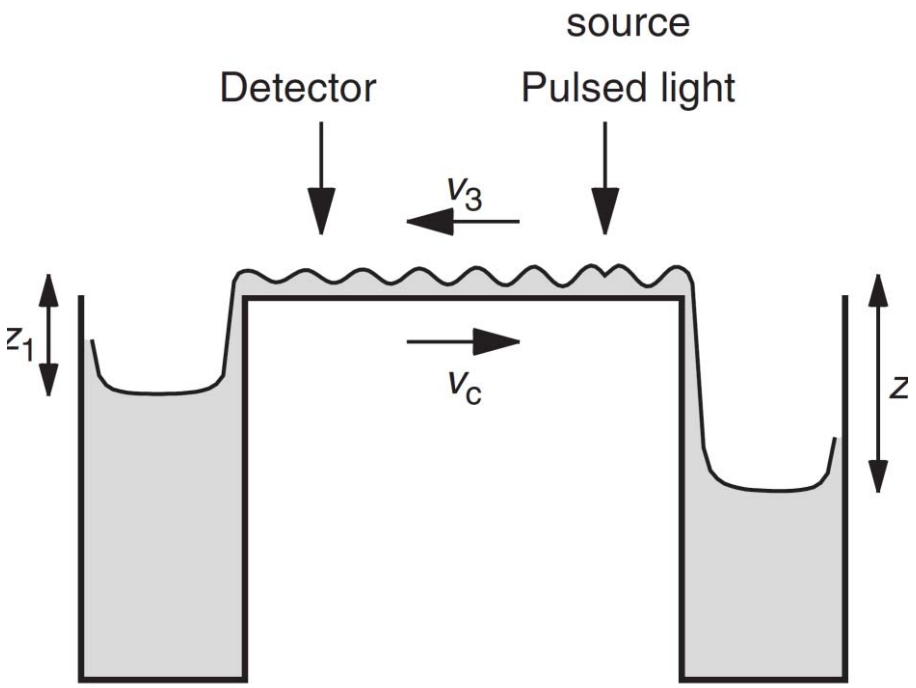

$$v_3^2 \approx \frac{\varrho_s}{\varrho} 3gz \left(1 + \frac{TS}{L}\right)$$

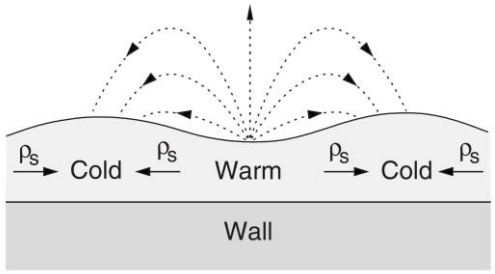

Fig. 2.23. Schematic illustration of the evaporation and condensation effect accompanying the propagation of third sound in superfluid helium films

Fourth Sound

- Compression waves propagating inside fine pores or small slits are called *fourth sound.*
- *As already mentioned, such geometrical restrictions are called* superleaks if the normal component is immobile due to its finite viscosity. Since only the superfluid component is moving under these conditions, a compression wave is not just an oscillation of the density, but also of pressure, temperature, entropy and the relative density of the superfluid component ρ_s/ρ.

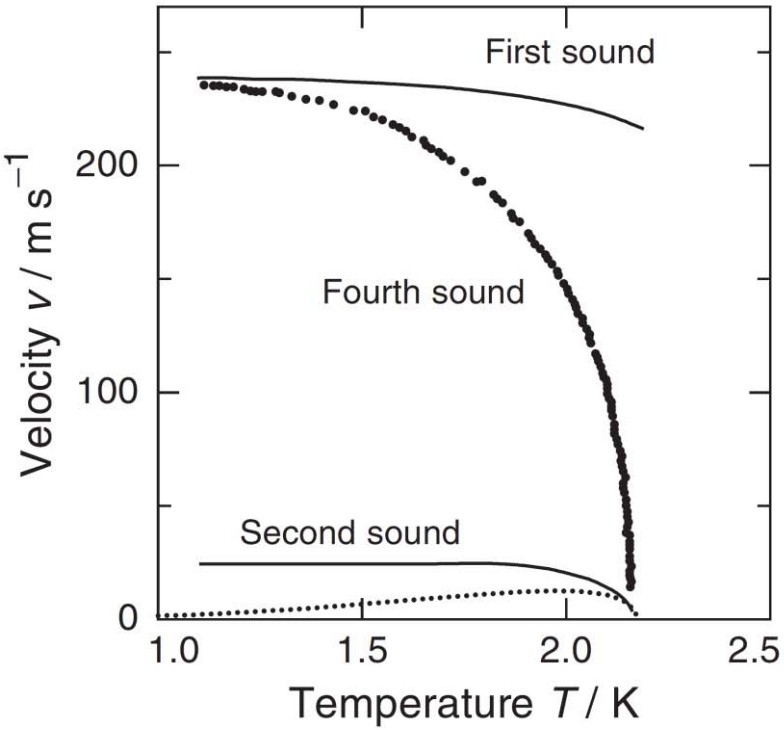

$$v_4 \approx \sqrt{\frac{\varrho_\mathrm{s}}{\varrho}\, v_1^2 + \frac{\varrho_\mathrm{n}}{\varrho}\, v_2^2}$$

Fig. 2.27. Temperature dependence of the velocity of fourth sound in helium II in comparison with first and second sound [72]. Fifth sound is indicated by the *dotted line* [70]

Fifth sound

- The contribution of second sound in

$$v_4 \approx \sqrt{\frac{\varrho_\mathrm{s}}{\varrho}\, v_1^2 + \frac{\varrho_\mathrm{n}}{\varrho}\, v_2^2}$$

  dominates near the lambda point. Under certain experimental conditions only this contribution is observed and is often referred to as *fifth sound.*

- The velocity of *fifth sound* is therefore given by:

$$v_5 = \sqrt{\left(\varrho_\mathrm{n}/\varrho\right)}\, v_2 .$$

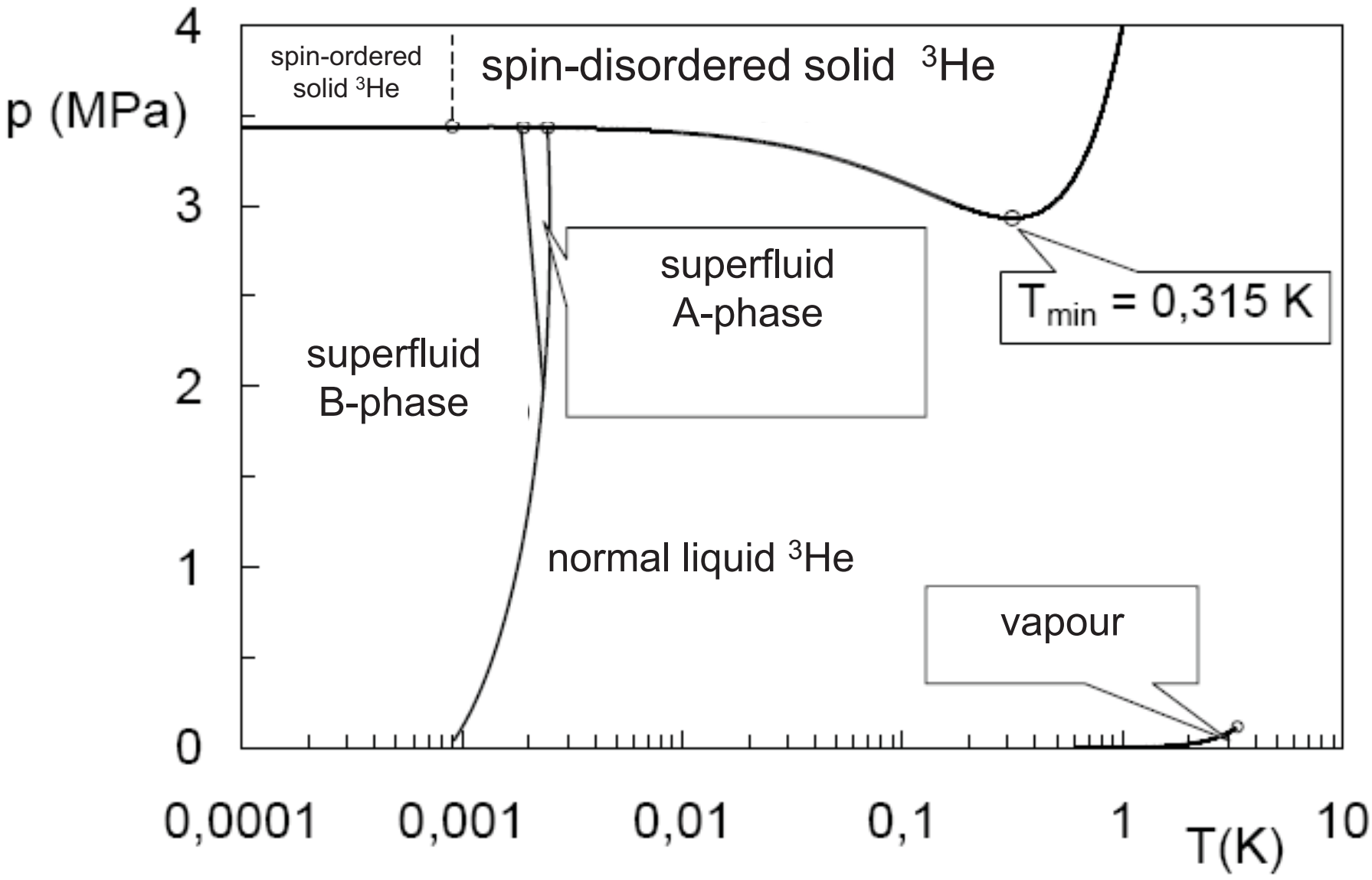

Phase diagram of ^{3}He

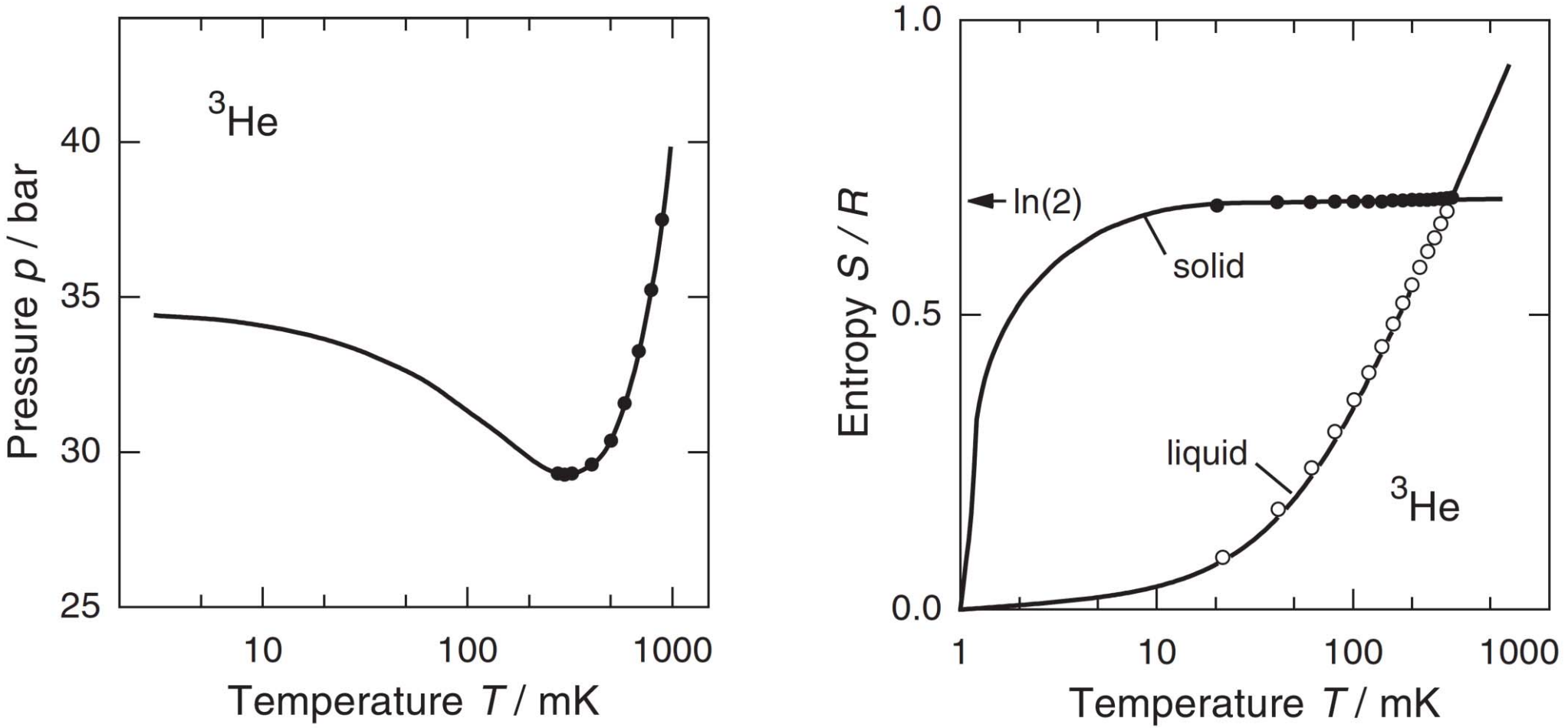

Fig. 1.7. (**a**) Melting curve of ^{3}He. The *solid line* and the points are from different measurements [27–29]. (**b**) Reduced entropy S/R of liquid and solid ^{3}He as a function of temperature. The *solid lines* represent the expected curves for the two phases. *Open* and *closed circles* mark experimental data [30]

- This amazing phenomenon is not caused by an anomaly of the phonon spectrum, as was the case for 4He, because phonons are not the relevant degrees of freedom in 3He at such low temperatures.

- The essential contribution to the entropy comes from nuclear spins.

- In the liquid, the entropy varies at low temperatures proportional to *T as expected for a Fermi gas.*

- In solid ^{3}He the atoms are strongly localized and the Fermi-gas model is not applicable. At high temperatures the orientation of the localized spins is statistical and their contribution to the entropy is S_s = *Rln 2, where R is the universal gas constant.*

- With decreasing temperatures a transition to an antiparallel arrangement of the spins is found.

- The transition temperature to the antiferromagnetic state is 0.9 mK. At *T = 0.32K,* the temperature at which the minimum occurs, the entropies of liquid and solid 3He are equal.

Superfluidity of ^{3}He

Douglas Dean **Osheroff**

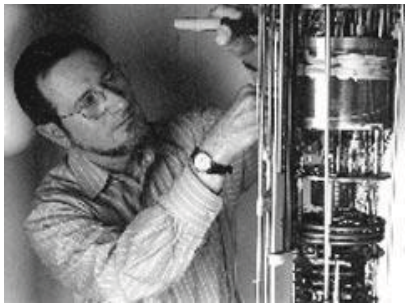

Robert Coleman **Richardson**

David Morries **Lee**

Nobel Prize 1996

BOOKS

2007

Frank Pobell

Matter and Methods at Low Temperatures

Third, Revised and Expanded Edition

With 234 Figures, 28 Tables, and 81 Problems

Springer

2005

Christian Enss Siegfried Hunklinger

Low-Temperature Physics

With 421 Figures

Springer

Thank You!

PGNiG

EMPEX